UNIVERSITY OF CALIFORNIA, SAN DIEGO

Potential Vorticity Dynamics and Models of Zonal Flow Formation

A dissertation submitted in partial satisfaction of the
requirements for the degree
Doctor of Philosophy

in

Physics

by

Pei-Chun Hsu

Committee in charge:

Professor Datrick H. Diamond, Chair
Professor Michael L. Norman
Professor Clifford M. Surko
Professor Sutanu Sarkar
Professor George R. Tynan

2015

The dissertation of Pei-Chun Hsu is approved, and it is acceptable in quality and form for publication on microfilm and electronically:

_____

_____

_____

_____

_____
Chair

University of California, San Diego

2015

DEDICATION

To my father, my mother, my sister and my brother,
for their love and full support.

TABLE OF CONTENTS

LIST OF FIGURES

LIST OF TABLES

ACKNOWLEDGEMENTS

First I would like to express my sincere gratitude to my thesis advisor Prof. Pat Diamond for his guidance, help, patience, encouragement and valuable suggestions. His insightful understanding of physics and his dedication to science research has been and will always be an inspiration to me. I am also sincerely grateful to Prof. Steve Tobias for his guidance and patience during my visit at the University of Leeds and for his continuous support and encouragement.

I would like to thank my officemates Lei Zhao, Chris Lee, Yusuke Kosuga, and Zhibin Guo for their company, support and encouragement. I cherish all the time we spent together discussing physics, figuring out problems (both research and live), helping and encouraging each other. I would also like to thank Stephanie Conover for her help with administrative issues and for many encouraging chats.

I would like to express my gratitude and love to my dear friends Guillermo Blando, Gail Field, Martin Field, Shin-Yi Lin, Silvia Yen, Shenshen Wang, Betty Crisman, and Kilhyun Bang. They are like my family here. They shared good and bad times, laughs and tears with me. Their love and friendship has supported me through the difficult times these years.

Finally and most importantly, I would like to express my everlasting love and deepest gratitude to my father Wen-Rui, my mother Ru-Jin, my sister Pei-Hsuan, my brother Shang-Huan, and the rest of my family. Their love and support is why I am who I am today, and why I was able to get this far.

Chapter 2 is a reprint of material appearing in Pei-Chun Hsu and P. H. Diamond, Phys. Plasmas, **22**, 032314 (2015) and Pei-Chun Hsu, P. H. Diamond, and S. M. Tobias *Phys. Rev. E*, **91**, 053024, (2015).The dissertation author was the primary investigator and author of this article.

Chapter 3 is a reprint of material appearing in Pei-Chun Hsu and P. H. Diamond, *Phys. Plasmas*, **22**, 032314 (2015). The dissertation author was the primary investigator and author of this article.

Chapter 4 is a reprint of material appearing in Pei-Chun Hsu and P. H. Diamond, *Phys. Plasmas*, **22**, 022306, (2015). The dissertation author was the primary investigator and author of this article.

VITA

2004	B. S. in Physics, National Tsing Hua University, Taiwan
2004-2005	Teaching Assistant, National Tsing Hua University, Taiwan
2006	M. S. in Astronomy, National Tsing Hua University, Taiwan
2006-2007	Research Assistant, Academia Sinica, Taiwan
2007-2009	Teaching Assistant, University of California, San Diego
2009-2015	Research Assistant, University of California, San Diego
2015	Ph. D. in Physics, University of California, San Diego

PUBLICATIONS

Pei-Chun Hsu, P. H. Diamond, and S. M. Tobias, "Mean field theory in minimum enstrophy relaxation", *Phys. Rev. E*, 91, 053024, 2015

Pei-Chun Hsu and P. H. Diamond, "On Calculating the Potential Vorticity Flux", *Phys. Plasmas*, 22, 032314, 2015

Pei-Chun Hsu and P. H. Diamond, "Zonal flow formation in the presence of ambient mean shear", *Phys. Plasmas*, 22, 022306, 2015

P. H. Diamond, Y. Kosuga, Z.B. Guo, O.D. Gurcan, G. Dif-Pradalier and P.-C. Hsu, "A New Theory of Mixing Scale Selection: What Determines the Avalanche Scale?", 25th IAEA Fusion Energy Conference, 13-18 October 2014, St. Petersburg, Russian Federation, Paper IAEA-CN-TH/P7-7, 2014

P. H. Diamond, Y. Kosuga, O.D. Gurcan, T.S. Hahm, C.J. McDevitt, N. Fedorczak, W. Wang, H. Jhang, J.M. Kwon, S. Ku, G. Dif-Pradalier, J. Abiteboul, Y. Sarazin, L. Wang, J. Rice, W.H. Ko, Y.J. Shi, K. Ida, W. Solomon, R. Singh, S.H. Ko, S. Yi, T. Rhee, P.-C. Hsu and C.S. Chang, "On the Physics of Intrinsic Torque and Momentum Transport Bifurcations in Toroidal Plasmas", 24th IAEA Fusion Energy Conference, 8-13 October 2012, San Diego, CA, Paper IAEA-CN-197/OV/P-03, 28, 2012

ABSTRACT OF THE DISSERTATION

Potential Vorticity Dynamics and Models of Zonal Flow Formation

by

Pei-Chun Hsu

Doctor of Philosophy in Physics

University of California, San Diego, 2015

Professor Datrick H. Diamond, Chair

We describe the general theory of anisotropic flow formation in quasi two-dimensional turbulence from the perspective on the potential vorticity (PV) transport in real space. The aim is to calculate the vorticity or PV flux. In Chapter 2, the general structure of PV flux is deduced non-perturbatively using two relaxation models: the first is a mean field theory for the dynamics of minimum enstrophy relaxation based on the requirement that the mean flux of PV dissipates total potential enstrophy but conserves total fluid kinetic energy. The analyses show that the structure of PV flux has the form of a sum of a positive definite hyper-viscous and a negative or positive viscous flux of PV. Turbulence spreading is shown to be related to PV mixing via the link of turbulence energy flux to PV flux. In the relaxed state, the ratio of the PV gradient to zonal flow velocity is homogenized.

This structure of the relaxed state is consistent with PV staircases. The homogenized quantity sets a constraint on the amplitudes of PV and zonal flow in the relaxed state.

The second relaxation model is derived from a joint reflection symmetry principle, which constrains the PV flux driven by the deviation from the self-organized state. The form of PV flux contains a nonlinear convective term in addition to viscous and hyper-viscous terms. The nonlinear convective term, however, can be viewed as a generalized diffusion, on account of the gradient-dependent ballistic transport in avalanche-like systems.

For both cases, the detailed transport coefficients can be calculated using perturbation theory in Chapter 3. For a broad turbulence spectrum, a modulational calculation of the PV flux gives both a negative viscosity and a positive hyper-viscosity. For a narrow turbulence spectrum, the result of a parametric instability analysis shows that PV transport is also convective. In both relaxation and perturbative analyses, it is shown that turbulent PV transport is sensitive to flow structure, and the transport coefficients are nonlinear functions of flow shear.

In Chapter 4, the effect of mean shear flows on zonal flow formation is considered in the contexts of plasma drift wave turbulence and quasi-geostrophic turbulence models. The generation of zonal flows by modulational instability in the presence of large-scale mean shear flows is studied using the method of characteristics as applied to the wave kinetic equation. It is shown that mean shear flows reduce the modulational instability growth rate by shortening the coherency time of the wave spectrum with the zonal shear. The scalings of zonal flow growth rate and turbulent vorticity flux with mean shear are determined in the strong shear limit.

Chapter 1

General Introduction

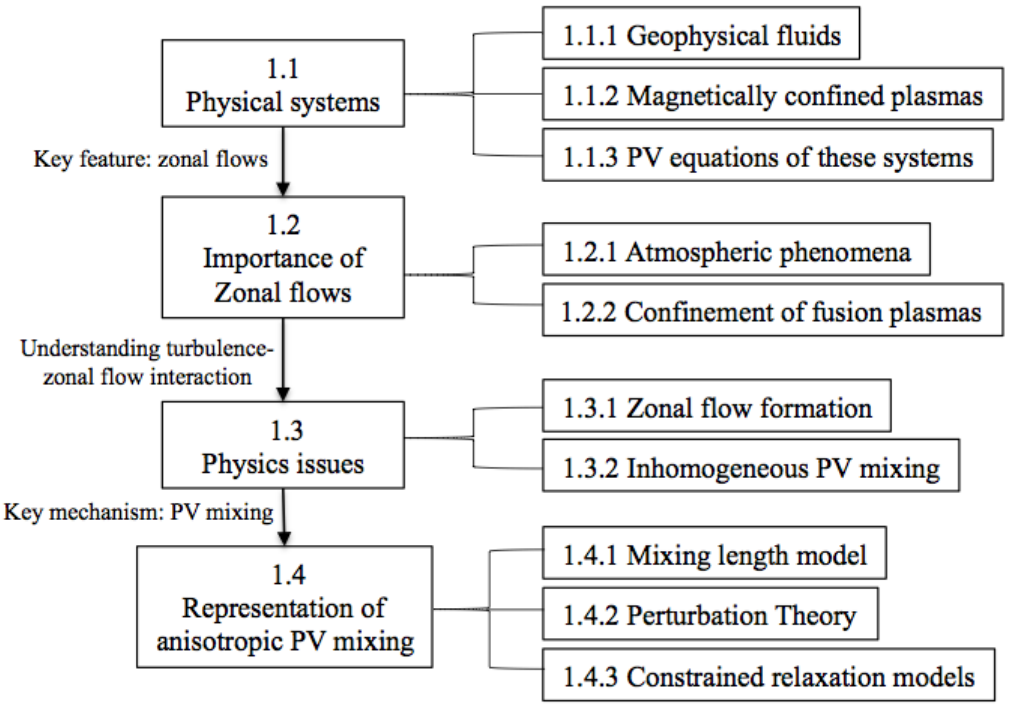

Figure 1.1: Flowchart for Chapter 1.

The overview of this chapter is as follows. We start with an introduction to the physical systems studied: geophysical fluids and plasmas. The main features and problems of these systems are discussed. The focus is on the importance of large-scale, turbulence-generated flows, namely zonal flows. This leads us to

physics issues of zonal flow formation and the dynamics of potential vorticity (PV). The key to the zonal flow-turbulence systems is identified as inhomogeneous PV mixing. The question of how to represent inhomogeneous PV mixing motivates the research presented in this thesis.

1.1 What are the physical systems we study?

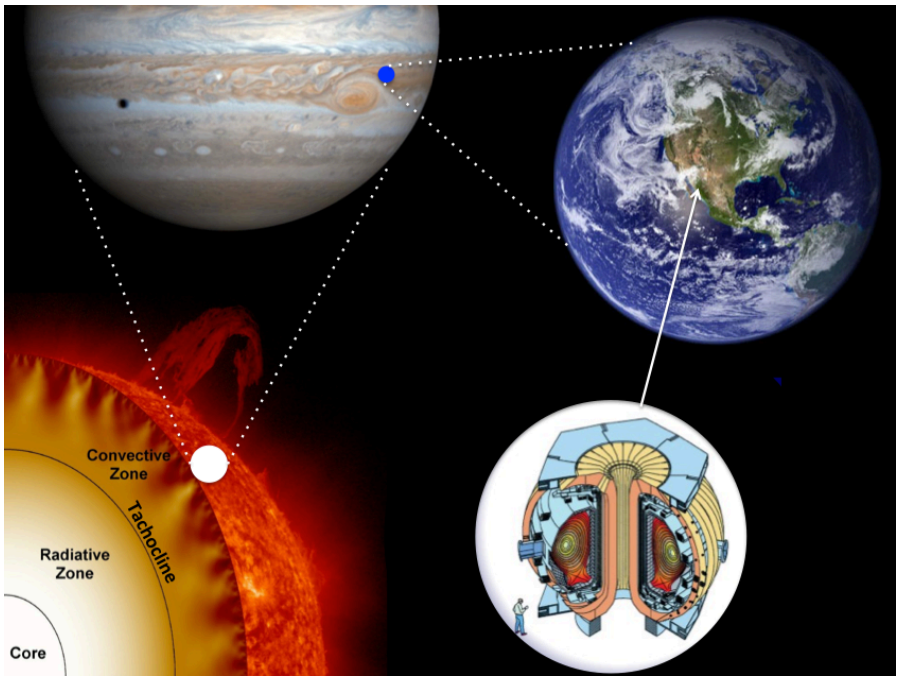

Figure 1.2: The Sun, Jupiter, Earth, and a tokamak. Images from NASA and schematic from General Atomics.

The physical systems we are motivated to study include geophysical fluids like Earth's atmosphere and Jovian atmosphere, the solar tachocline, and plasmas in magnetic confinement fusion devices like tokamaks (Figure 1.2). Even though the sizes of a star, a planet, and a fusion device are different by many orders of magnitude, these systems are all quasi two-dimensionalized due to fast rotation, strong stratification, or fast electron motion along magnetic field lines (Table 1.1), and these systems each have the common element of low effective Rossby number. By effective Rossby number I am referring to the ratio of characteristic vorticity

(convective velocity scale divided by length scale) to effective background vorticity (planetary rotation frequency in geophysical fluids or ion cyclotron frequency ω_{ci} in magnetically confined plasmas). Table 1.1 lists and compares the key parameters of planetary atmospheres, the tachocline, and tokamaks. Researchers have found great similarities in the fundamental dynamics of large-scale flows in these seemingly unrelated systems. A wide class of phenomena in geophysical fluids and magnetically confined plasmas can be understood in terms of the dynamics of vorticity or potential vorticity (PV). In this thesis we focus on one of the ubiquitous phenomena: large-scale, turbulence-generated shear flows, namely zonal flows. Before proceeding to introduce the dynamics of PV transport and zonal flow formation, let me first briefly introduce the physical systems we study.

Table 1.1: Comparison of planetary atmospheres, the solar tachocline, and tokamaks.

	atmosphere	tachocline	tokamak
Leading anisotropy	rotation $\boldsymbol{\Omega}$	stratification buoyancy freq. N_b	guiding field $\boldsymbol{B}_0$
Cause of quasi two-dimensionality	$\Omega \gg U/L$ $\rightarrow R_0 \ll 1$	$N_b \gg U/L$ $\rightarrow R_i \gg 1$	cyclotron motion, fast electron motion along field lines
Eff. Rossby # $R_0 \equiv U/\Omega_{\text{eff}} L$	$\Omega_{\text{eff}} = 2\Omega\sin\theta$ $R_0 \ll 1$	$\Omega_{\text{eff}} = 2\Omega_{\text{Sun}}\sin\theta$ $R_0 \sim 0.1 - 1$	$(\boldsymbol{v} = \boldsymbol{E} \times \boldsymbol{B})$ $\Omega_{\text{eff}} = \omega_{ci}$ $R_0 \ll 1$
Eff. Reynolds # $R_e \equiv UL/\nu$	$R_e \gg 1$	$R_e \gg 1 (\sim 10^{10})$	$R_e \sim 10 - 100$

1.1.1 Geophysical fluids

Geophysical fluids include the Earth's atmosphere, ocean, and interior, lava flows, and planetary atmospheres. The importance of the Earth's atmosphere and the ocean to human beings needs no explanation. The atmosphere is where

we live in; the ocean covers 71 percent of the Earth's surface and contains 97 percent of the planet's water . The phenomena of the atmosphere and the ocean, such as weather, waves, large scale atmospheric and oceanic circulations, water circulation, jets, etc., have fascinated humans for centuries. Even though the motion of some phenomena is complex, scientists have developed simplified models, especially for the dynamics of large-scale flows. Geophysical fluid dynamics (GFD) is the study of fundamental principles for large-scale geophysical flows without considering overwhelming details of small scales.

Charney [5] was one of the first who used scaling laws to develop reduced models of large-scale midlatitude atmospheric circulation. He used an approximation (later called quasi-geostrophic model) to filter out lengths of atmospheric waves that are not important in meteorology. In Charney's letter to Thompson in February of 1947, he wrote: "We might say that the atmosphere is a musical instrument on which one can play many tunes. High notes are sound waves, low notes are long inertial waves, and nature is a musician of the Beethoven than the Chopin type. He much prefers the low notes and only occasionally plats arpeggios in the treble and then only with a light hand. The oceans and the continents are the elephants in Saint-Saëns' animal suite, marching in a slow cumbrous rhythm, one step every day or so. Of course, there are overtones: sound waves, billow clouds (gravity waves), inertial oscillations, etc, but there are unimportant and are heard only at N.Y.U and M.I.T." Other early pioneers in this field include Hadley (1753), Maury (1855) [6] and Ferrel (1856) [7]. Thanks to countless observations of the Earth's atmosphere and oceans, great progress has been made since than, especially in understanding the nonlinear dynamics.

The atmosphere and the ocean are thin layers of stratified fluids on a rotating sphere. The vertical thickness of the atmosphere or the ocean ($H \sim 1-10$ km) is much smaller than the radius of the Earth ($R_\oplus = 6371$km). So the aspect ratio, the ratio of the vertical length scale H to the horizontal scale L, is very small for motion of synoptic scale ($L \sim 10^2 - 10^3$ km in the atmosphere and $10 - 10^2$ km in the oceans). The small aspect ratio and the strong stratification allow us to approximate the system as a "shallow water" system–a thin layer of constant density

fluid with a free surface in hydrostatic balance. The rotating shallow water model is one of the most useful models in GFD, because the effect of Earth's rotation is considered in a simple framework. The effect of rotation is represented by the Rossby number, which is defined as $R_0 \equiv U/fL$, the ratio of the advective time scale U/L (where U is the horizontal velocity scale) to the Coriolis parameter f. When Rossby number is small, the fast motion driven by inertial gravity waves can be neglected. As a result, the motion can be determined by the balance between the Coriolis force and pressure gradient, called geostrophic motion.

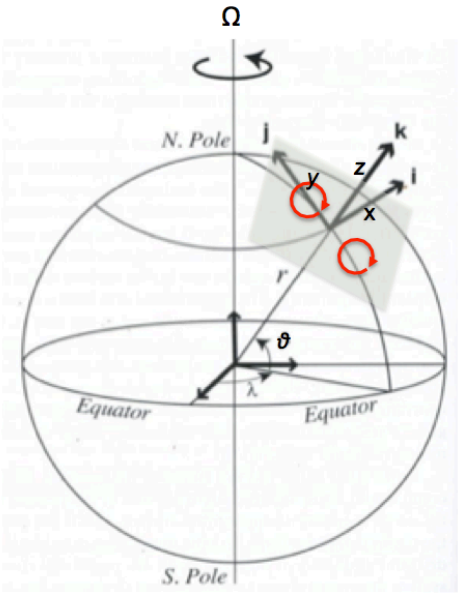

Figure 1.3: A tangent plane on a rotating sphere. β-plane is the simplest tangent plane which takes into account of the variation of Coriolis force with latitude. Coordinates are: the x-axis in the eastward direction, y-axis in the northward direction and z-axis in the vertical direction. Kelvin's theorem states that a circulation around a closed curve moving with the fluid remains constant with time.

The temporal evolution of geostrophic motion is is described by the quasi-geostrophic equations, which are widely used for theoretical studies of geophysical flows. Note that since quasi-geostrophic flows are in near-geostrophic balance, the Rossby number is assumed small. The quasi-geostrophic vorticity equation will be discussed later in 1.1.3, together with the model equation for magnetically confined plasma turbulence. The GFD equations are more conveniently described

using Cartesian coordinates than spherical coordinates. For phenomena on a scale smaller than the global scale, the geometric effects of the Earth's sphericity is not central, and so "a piece of shell" at a certain latitude θ_0 can be approximated as a plane tangent to the surface of the Earth (Figure 1.3). The latitudinal displacement on the plane, y, is approximately equal to $R_\oplus(\theta - \theta_0)$. The simplest tangent plane is the f-plane, in which the Coriolis parameter $f = 2\Omega\sin\theta$ is a constant, where $\mathbf{\Omega}$ is the angular velocity of the Earth. However, the variation of Coriolis force is the most important dynamical effect of sphericity in GFD. Therefore, in this thesis we use the β-plane, in which the variation of Coriolis effect with latitude is approximated as $f = f_0 + \beta y$, where $\beta = \partial f/\partial y = (2\Omega\cos\theta_0)/R_\oplus$.

Kelvin's circulation theorem is a fundamental conservation law for inviscid barotropic fluids. Imagine a patch of fluid elements with area A displaced from one point to the other (Figure 1.3). Kelvin's theorem states that the circulation around the loop of area A that consists continuously of the same fluid elements is conserved, for flows governed by Euler's equation:

$$\frac{d}{dt}\int_A (\nabla \times \boldsymbol{v} + 2\mathbf{\Omega}) \cdot \hat{z} dS = 0. \tag{1.1}$$

We can see that Kelvin's theorem conserves the sum of vorticity ω and planetary vorticity $2\Omega\sin\theta$, i.e., conservation of PV in two-dimensional quasi-geostrophic systems. As we will see later, the dynamics of PV is central to flow formation in quasi-geostrophic fluids. The vorticity $\omega = \hat{z} \cdot (\nabla \times \boldsymbol{v})$ evolves as

$$\frac{d\omega}{dt} = -2\Omega\cos\theta\frac{d\theta}{dt} = -\beta v_y. \tag{1.2}$$

For geostrophic flow, the velocity is determined by the balance between the Coriolis force and pressure gradient $\boldsymbol{v} = -\nabla P \times \hat{z}/2\Omega$, and so the vorticity is given by $\omega = \nabla^2 P/2\Omega$. Note that the pressure P in geostrophic is equivalent to stream function ψ in this case, since $(v_x, v_y) = (-\partial_y P, \partial_x P)$. The vorticity equation then becomes

$$\frac{d\nabla^2\psi}{dt} = -\beta\partial_x\psi. \tag{1.3}$$

This β-plane vorticity equation gives the simplest representations of the large scale dynamics in quasi-geostrophic systems (low frequency and low effective Rossby

number.) The linear wave in quasi-geostrophic fluids is called Rossby wave. It's dispersion relationship in β-plane is given by the β-plane equation: $\omega_k = -\beta k_x / k_\perp^2$, where $k_\perp^2 = k_x^2 + k_y^2$. Note that as a patch of fluid moves along the meridional direction, planetary vorticity $f_0 + \beta y$ varies in $\hat{y}$. As a consequence, the relative vorticity ω of a fluid parcel must change accordingly, in order to conserve PV, and so resulting in the propagation of a Rossby wave (Figure 1.4). Rossby waves are dispersive and "backward", i.e., their latitudinal/radial phase and group velocity are opposite. We will see later that drift waves in magnetically confined plasmas is also dispersive and backward, because their governing vorticity equations have the same form.

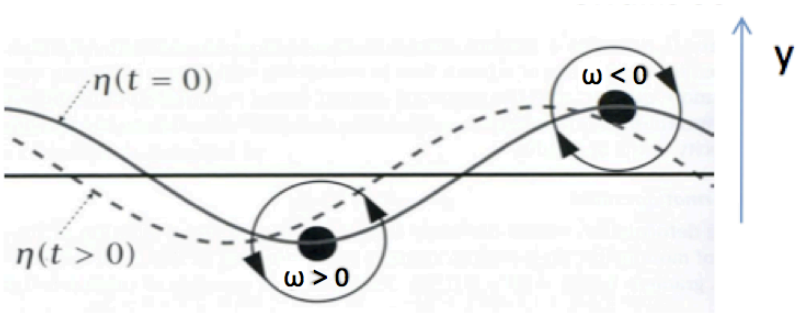

Figure 1.4: Rossby wave (Vallis 2006 [1]). The conservation of $\omega + \beta y$ results in the propagation of Rossby wave.

The quasi-geostrophic equations can be used as the hydrodynamic model equations of the solar tachocline, a thin layer between the solar convection zone and the radiative interior. This transition layer (especially the lower part) is stably stratified, resulting in its quasi two-dimensional nature. The tachocline has strong latitudinal and radial differential rotation, because the angular velocity profile of its two neighbors are totally different: the convection zone has profound latitudinal differential and radial rotation, while the radiation zone has nearly uniform rotation. The tachocline is believed to play a crucial role in the solar magnetic activity associated with global dynamo. It is still unclear why the tachocline is so thin– less than 5% of the solar radius. To answer this question one must understand the momentum transport in the tachocline. The tachocline is stably stratified (Richardson number $\sim 10^3$ in lower tachocline), rotationally influenced (Rossby

number $\sim 0.1-1$), and strongly turbulent (Reynolds number $\sim 10^5$). Thus, quasi-geostrophic equations are suitable equations for hydrodynamic models of turbulent transport in the tachocline.

1.1.2 Magnetically confined plasmas

Nuclear fusion is the process that the Sun and other stars generate energy at their cores. It is also one of the most promising options for generating large amounts of carbon-free energy here on Earth in the future. Magnetic confinement fusion devices, like tokamaks and stellarators, use strong magnetic fields to confine plasmas so that the plasmas can achieve the temperature and pressure necessary for fusion to take place. The challenge is to confine the hot plasmas for a long enough time so that the energy produced by fusion reactions is larger than the energy put into heating up the fuel. The condition for which a fusion reaction release more energy than the input energy is known as ignition. Ignition can be achieved when the Lawson criterion is satisfied. The idea of the Lawson criterion is to have 1) high enough ion temperature T_i so that nuclei with large kinetic energies are able to overcome the Coulomb barrier; 2) sufficient ion density n_i so that the reaction rate is reasonably high; 3) sufficient confinement time τ_E, i.e., that the energy lost rate of the system is small enough so that the reaction is sustainable. The Lawson criterion of a magnetically confined, deuterium-tritium plasma is given by $n_i \tau_E T_i > 3\times 10^{21} \mathrm{m}^{-3}\mathrm{s\,keV}$. The Lawson criterion can be written in terms of magnetic field as $\beta_t B^2 \tau_E > 6 \times 10^{21} (\mu_0 k_B) \mathrm{m}^{-3}\mathrm{s\,keV}$, for a given plasma beta $\beta_t = \frac{n k_B T}{B^2/(2\mu_0)}$. We can see increasing the strength of the magnetic field helps to reach ignition.

The Lawson criterion clearly points out the crucial role of plasma confinement. Since plasmas in toroidal magnetic devices are hotter and denser in the core than the edge, the gradients of temperature and density naturally drive "outward" transport of heat and particles. The classical cross-field transport mechanism is collisional diffusion. However, the observed transport in the experiments is significantly higher than that would be expected on the basis of classical considerations, even in the absence of macroscopic instabilities. This so-called "anomalous" trans-

port is due to turbulence, which is ubiquitous in magnetically confined plasmas and can effectively transport heat across confining field lines. Therefore, turbulent transport has been a major issue for the development of fusion reactors, and understanding the physics of turbulent transport has been a key scientific challenge. Turbulence in magnetically confined plasmas consists of instabilities and collective oscillations. There are many collective modes, but what dominates the transport are the lowest frequency modes. In particular, drift wave turbulence can explain the observed anomalous transport level and so is widely accepted as the main contributor to turbulent transport. A comparison between drift wave turbulence and quasi-geostrophic turbulence is shown in Table 1.2. A comparison of the linear waves in these two systems–drift wave and Rossby wave–is shown in Table 1.3.

Table 1.2: Comparison of quasi-geostrophic and drift-wave turbulence.

	quasi-geostrophic	drift-wave
force	Coriolis	Lorentz
velocity	geostrophic	$\boldsymbol{E} \times \boldsymbol{B}$
linear waves	Rossby waves	drift waves
conserved PV	$q = \nabla^2\psi + \beta y$	$q = n - \nabla^2\phi$
inhomogeneity	β	$\nabla n, \nabla T$
turbulence	usually strongly driven	not far from marginal
Reynolds number	$R >> 1$	$R \sim 10 - 10^2$
zonal flows	jets, zonal bands	$n = 0$ electrostatic fluctuations $\rightarrow$ sheared $\boldsymbol{E} \times \boldsymbol{B}$ flows
role of zonal flows	transport barriers	L-H transition, ITB

Drift waves are driven by the inhomogeneity of the plasma, one of the most universal configurations of fusion plasmas. In the presence of density gradient ∇n, electrons react much faster (along the field lines) than ions to the density perturbations $\tilde{n}$, due to low electron inertia. Thus, positive potentials $\phi > 0$

and the electric field ($\boldsymbol{E} = -\nabla\phi$) develop in the regions with positive density perturbations $\tilde{n} > 0$. The corresponding electric field then causes the $\boldsymbol{E} \times \boldsymbol{B}$ drift, which results in a propagation of the density perturbations in the direction of $\nabla n \times \boldsymbol{B}$. In the case of adiabatic electrons $\tilde{n}/n_0 = e\phi/T_e$–i.e., electrons respond to the parallel perturbations instantaneously–the cross phase between the density perturbation and electrostatic potential goes to zero $\langle \tilde{n} v_r \rangle = 0$, and there will be no net transport. The electron response can be non-adiabatic $\tilde{n}/n_0 = (1 - i\delta)e\phi/T_e$ due to various dissipative mechanisms. In this case, the potential perturbation fall behind the density perturbation. This in turn amplifies density perturbations, so drift wave modes become unstable. Similar to the quasi-geostrophic system, drift wave turbulence is anisotropic; the turbulent transport is quasi two-dimensional in the sense that it mainly occurs in the poloidal plane. The reason is that plasma fluctuations have very small along-field components compared with the cross-field components, because of strong guiding magnetic fields.

Table 1.3: Comparison of Rossby wave and drift wave.

	Rossby wave	drift wave
equation variable	variable fluid depth	electrostatic potential ϕ
background	average depth H	mean density n_0
dispersion relation	$\omega_k = -\frac{\beta k_x}{k_\perp^2 + L_D^{-2}}$	$\omega_k = -\frac{\beta k_x}{k_\perp^2 + \rho_s^{-2}}$
symmetry breaking	$\beta = \partial_y f$	$\beta = \partial_r \ln n_0$
characteristic scale	$L_D = \frac{\sqrt{gH}}{f} \approx 10^6 m$	$\rho_s = \frac{1}{\omega_{ci}}\sqrt{\frac{T_e}{m_i}} \approx 10^{-3} m$
fast frequency of the system	$f \approx 10^{-2} s^{-1}$	$\omega_{ci} \approx 10^8 s^{-1}$
period	≈ 5 days	$\approx 10^{-3} s$
wavelength	$\approx 10^6$ m	$\approx 10^{-3} m$

The theoretical studies of drift wave instabilities were initially focused on a perturbation analysis of weak turbulence theory. However, strong electrostatic turbulence was diagnosed in the late 1970s. In turbulent fusion plasmas, modes

grow and interact with one another, and the non-linearity becomes important. The nonlinear coupling can cause wide spreading of frequency and wave numbers in drift wave turbulence spectra. The Hasegawa-Wakatani (H-W) [8] system is the simplest nontrivial drift wave system which takes into account non-linearity and relates the transport of PV to the energetics of the system by, including resistivity. The HW system is a coupled set of equations for the plasma density and electrostatic potential:

$$\begin{aligned} \frac{d\nabla^2\phi}{dt} &= -D_{||}\nabla_{||}^2(\phi - n) + \nu\nabla^2\nabla^2\phi, \\ \frac{dn}{dt} &= -D_{||}\nabla_{||}^2(\phi - n) + D_0\nabla^2 n, \end{aligned} \tag{1.4}$$

with ν kinetic viscosity, D_0 diffusivity, and $D_{||} = T_e/\eta n_0 \omega_{ci} e^2$, where η is the electron resistivity and n_0 equilibrium density. The variables in equation (1.4) are normalized as $x/\rho_s \to x$, $\omega_{ci}t \to t$, $e\phi/T_e \to \phi$, and $\tilde{n}/n_0 \to n$, where ρ_s is the ion gyroradius at electron temperature and ω_{ci} the ion cyclotron frequency. The PV in H-W system, $n - \nabla^2\phi$, is locally advected and is conserved in the inviscid limit. The H-W system has two limits with respect to $D_{||}k_{||}^2/\omega$, which describes the parallel electron response. In the hydrodynamic limit $D_{||}k_{||}^2/\omega = 0$, the vorticity and density equations are decoupled. Vorticity is determined by the 2D Navier-Stokes equation, and the density fluctuation is passively advected by the flow obtained from the NS equation. In the adiabatic limit $D_{||}k_{||}^2/\omega \to \infty$, the electrons become adiabatic $n \approx \phi$, and the equations reduce to the Hasegawa-Mima (H-M) equation [9], which we discuss together with the quasi-geostrophic vorticity equation in 1.1.3. The nonlinear coupling of drift-wave turbulence includes the coupling between drift wave modes (finite n) and zonal flows (n=0). Zonal flow plays a crucial role in controlling transport in drift-wave turbulence, because 1) zonal flows can de-correlate eddys and so reduce turbulent transport and 2) turbulent energy can transferred to zonal flow, since zonal flow are driven by drift waves (see section 1.2 for details).

1.1.3 Charney-Hasegawa-Mima equation

The model equations we consider for quasi-geostrophic fluids and drift wave turbulence are the quasi-geostrophic equation [5] and the H-M equation [9]. The 2D quasi-geostrophic equation is given by

$$\frac{\partial}{\partial t}(\nabla^2\psi - L_d^{-2}\psi) + \beta\frac{\partial}{\partial x}\psi + J(\psi, \nabla^2\psi) = 0, \tag{1.5}$$

where ψ is the stream function, L_d is the Rossby deformation radius, x-axis is in the zonal direction, and J is the Jacobian operator. The H-M equation for drift wave turbulence is given by

$$\frac{1}{\omega_{ci}}\frac{\partial}{\partial t}(\nabla^2\phi - \rho_s^{-2}\phi) - \frac{1}{L_n}\frac{\partial}{\partial y}\phi + \frac{\rho_s}{L_n}J(\phi, \nabla^2\phi) = 0, \tag{1.6}$$

where ϕ is the normalized electrostatic potential, L_n is the density gradient scale length, and y-axis is in the poloidal direction. The quasi-geostrophic equation and the H-M equation have the same structure. Both equations express material conservation of potential vorticity (PV) in the inviscid limit. The PV in geostrophic fluids is $q = \nabla^2\psi - L_d^{-2}\psi + \beta y$, the sum of absolute vorticity and effective planetary vorticity, while the PV in drift-wave turbulence is $q = \nabla^2\phi - \rho_s^{-2}\phi + L_n^{-1}x$, i.e., polarization charge, or ion vorticity due to $\boldsymbol{E} \times \boldsymbol{B}$ drift, plus plasma density fluctuation, which is equivalent to potential fluctuation in H-M model. Thus, the Charney-Hasegawa-Mima equation conserves, in addition to total kinetic energy, potential enstrophy (squared PV).

We use GFD notation and equation (1.5) for the rest of the thesis, so the y-axis is in the direction of inhomogeneity, i.e., the radial direction in plasma or the meridional direction in GFD, and the x-axis is in the direction of symmetry, i.e., the poloidal direction in plasma or the longitudinal direction in GFD. For turbulence with scales much smaller than L_d or ρ_s, PV is $\nabla^2\psi + \beta y$ ($\beta = \frac{\partial}{\partial y}\ln n_0$ for drift wave turbulence). The flux of PV is simply the flux of vorticity, and the dispersion relation of the linear waves (drift waves in plasma or Rossby waves in GFD) is $\omega_k = -\beta k_x/k^2$, where $k^2 = k_\perp^2 = k_x^2 + k_y^2$.

1.2 Why are jets and zonal flows important in quasi-geostrophic and drift wave turbulence?

1.2.1 Atmospheric phenomena

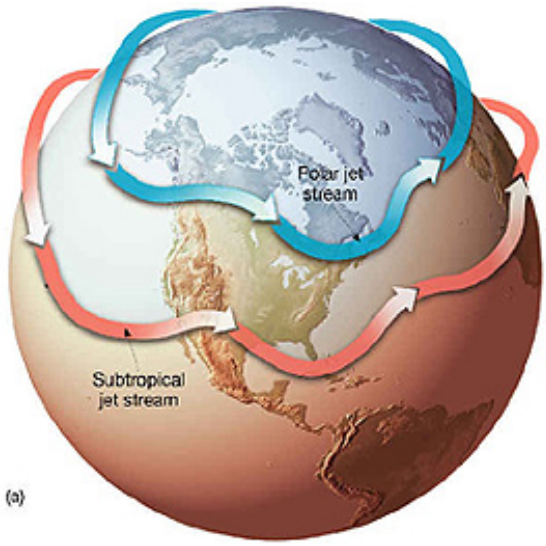

Figure 1.5: Typical Locations of Jet Streams Across North America. Image from NASA.

Zonal jets and zonally symmetric band-like shear flows, hereafter zonal flows, are ubiquitous atmospheric phenomena. The jet stream in the Earth's atmosphere (Figure 1.5), and belts and zones in the Jovian atmosphere (Figure 1.2 and 1.7) are well-known examples of zonal flows. There are two classes of jet stream on Earth: the mid-latitude eddy-driven jet stream and the subtropical thermally-driven jet stream. The former, also called sub polar jets, are driven by baroclinic eddies in the midlatitudes. The formation of such jets can be explained by momentum convergence of Rossby wave turbulence, as shown in Figure 1.6. When Rossby waves are excited in a finite region, the condition of wave radiation requires outgoing wave energy flux from the excitation region, i.e., outgoing group velocity. Since $\omega_k = -\beta k_x/k^2$, the meridional energy density flux $v_{gy}(\nabla\psi_k)^2 = 2\beta k_x k_y k^{-2}|\psi_k|^2$ is in the opposite direction to the meridional eddy zonal-momentum flux, i.e., Reynolds stress $\langle\tilde{v_x}\tilde{v_y}\rangle = -k_x k_y|\tilde{\psi_k}^2|$. Thus, energy divergence directly results in

momentum convergence. Note that this picture is meaningful when the excitation region is localized relative to the dissipation region. Rossby wave turbulence in the mid-latitude are predominantly excited by baroclinic instabilities. Thus, eddy-driven jets in the mid-latitudes are more evident in baroclinic zones over the Western Atlantic and Pacific ocean.

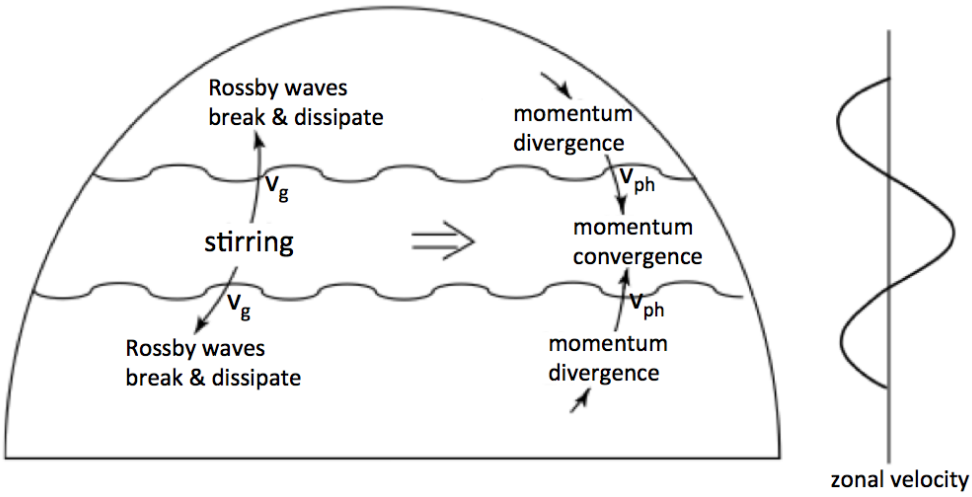

Figure 1.6: Generation of zonal flow on a β plane or on a rotating sphere (Vallis 2006 [1]). "Stirring in mid-latitudes (by baroclinic eddies) generates Rossby waves that propagate away from the disturbance. Momentum converges in the region of stirring, producing eastwardd flow there and weaker westward flow in the flanks."

Zonal flows and other large-scale atmospheric motions are one of the most active areas of GFD research. Understanding the physics of zonal flows and their influence on the atmospheric and ocean circulations, climate, and the ecosystem is of great practical interest. It can help meteorologists to improve the weather forecasting (e.g., [10]). Moreover, the "ozone hole" problem is closely related to the interplay between the flow motions and the chemicals in the ozone layer (e.g. [11]). To have a complete understanding of large-scale atmospheric motions, one should also consider the effects of small scale motions, convection, boundary conditions (like interaction with the ocean and land), etc. The study of the whole picture is beyond the scope of this thesis. I will focus primarily on the dynamics for large-scale flow formation and it's interplay with small-scale fluctuations in this thesis.

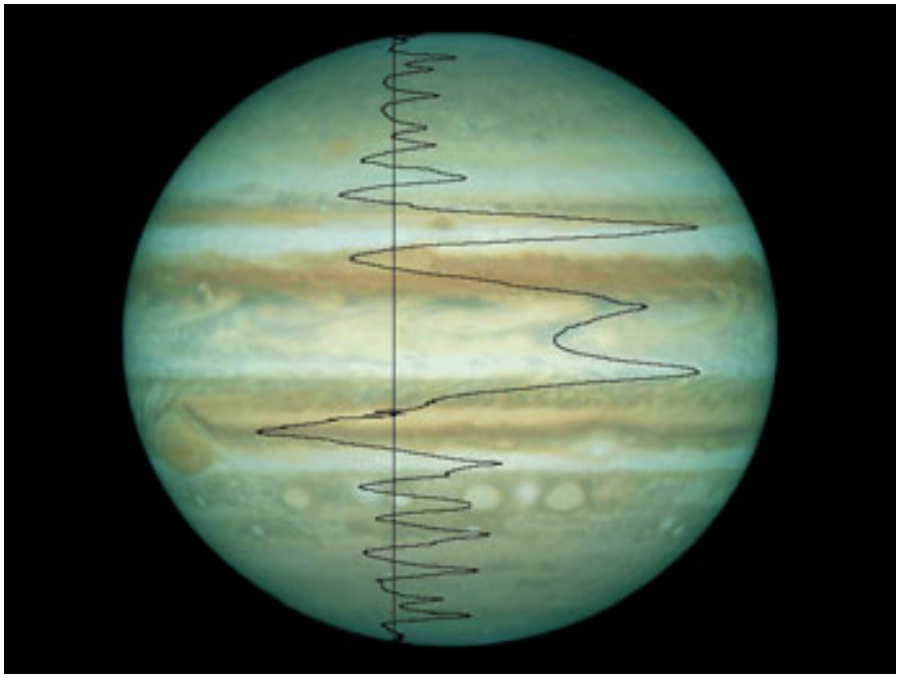

Figure 1.7: The speed measurements of Jovian zonal flows have been added to the image of Jupiter. The vertical black line indicates zero speed. The highest velocities exceed 150m/s. Image from NASA.

Zonal flows are also commonly observed in the atmospheres of other planets. Jupiter's banded flow structure is one of the most spectacular display of fluid mechanics. The pattern of striped bands parallel to the equator with various colors was first observed by R. Hook nearly 350 years ago [12]. The banded structure, consisting a series of zones and belts across the planet, are in the weather layer of Jovian atmosphere. The weather layer is a thin, stably stratified surface spherical layer above the convectively unstable interior. The light zones and dark belts are above upward and downward parts of convective currents, and so correspond to high-pressure and low-pressure regions in Jupiter's atmosphere. Underlying the bands is a stable pattern of eastward and westward wind flows, namely Jupiters zonal flows. The eastward equatorial zonal flow has similar speed as the Earth's jet stream ($\sim 10^2$m/s). Outside the equatorial region, the speed of alternating zonal flows diminishes toward the pole (Figure 1.7). Contrary to the Earth's zonal flows, Jovian zonal flows have persisted without major changes. The latitudes of maximum and minimum zonal velocities have remained remarkably constant since

the first observations from Voyager in 1979.

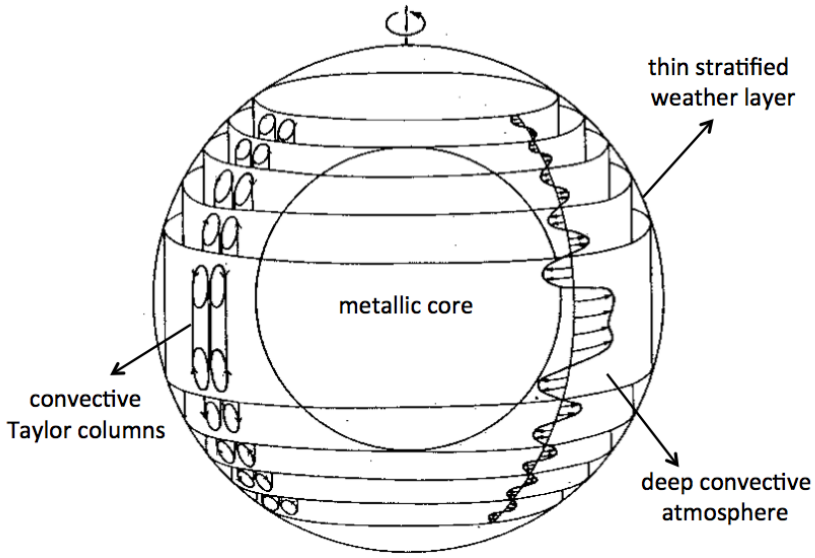

Figure 1.8: Deep layer model of Jovian zonal flows (Busse 1976 [2]). A schematic drawing of the interior of Jupiter is shown. Taylor columns are formed in the deep convective layer of the atmosphere. Northern and southern projections of the Taylor columns onto the weather layer are shown. Zonal flows are driven by coherent modulational (tilting) instability of an array of convective Taylor columns.

The origin of Jovian zonal flows is not fully understood. There are two main theoretical scenarios. In the first scenario (see e.g., [13]), zonal flows form in a shallow-water β-plane system. The zonal flows are driven by small scale turbulence, which is maintained by convection in the underlying atmosphere, where the convection is ultimately driven by the temperature gradient. In a two-dimensional turbulent system, energy inverse cascades from small scales to large scales. In the presence of anisotropic effect (β effect), banded zonal flows are formed instead of large-scale round vortices. In the second scenario (first proposed by Busse in 1976 [2]), zonal flows are coupled with their energy source–the underlying deep convective atmosphere. Because of small Rossby number, fluid flows tend to form columnar cells aligned with the rotation axis, based on the Taylor-Proudman theorem. The formation of zonal flows occurs via coherent instability of an array of these Taylor columnar vortices (Figure 1.8) in the convective interior. As for numerical studies, numerical shell models have been able to generate zonal flows

pattern in agreement with the observation. However, the Ekman numbers (the ratio of viscous forces to Coriolis forces) explored in the numerical models are many orders of magnitude larger than the reality.

Table 1.4: Comparison between shallow and deep models.

shallow shell	deep convection layer
imposed turbulence on a thin weather layer	quasi-geostrophic convection
inverse cascade with Rhines mechanism	coherent modulational instability of an array of convection cells
increasing PV with latitude	decreasing PV with latitude

The terrestrial jet stream and Jovian zonal flows have a crucial influence on turbulent mixing and formation of transport barriers. For example, zonal flows of Jupiter have been observed to inhibit the transport of vortex eddies across the flows. Another example is the isolation of the polar vortex, a key player in polar zone loss. The polar night jet effectively blocks mixing between southern polar region from the outside during the winter. Therefore, air with richer ozone from the mid-latitudes cannot be transported into the polar region.

1.2.2 Confinement of fusion plasmas

In toroidal magnetic fusion devices, zonal flows are sheared $\boldsymbol{E}\times\boldsymbol{B}$ flows from disturbances in the electrostatic potential (Figure 1.9). Zonal flows are poloidally symmetric ($n = 0$) and toroidally symmetric ($m = 0$) modes, with finite radial scale (finite k_r). Because of their symmetry, zonal flows do not have radial velocity perturbations, and so do not have access to the free energy source stored in radial gradients (e.g., $\nabla T, \nabla n$). This means zonal flows must be excited by nonlinear processes. Zonal flow are driven by nonlinear interactions between finite-n modes in a spectrum of drift wave turbulence and $n = 0$ zonal flow modes.

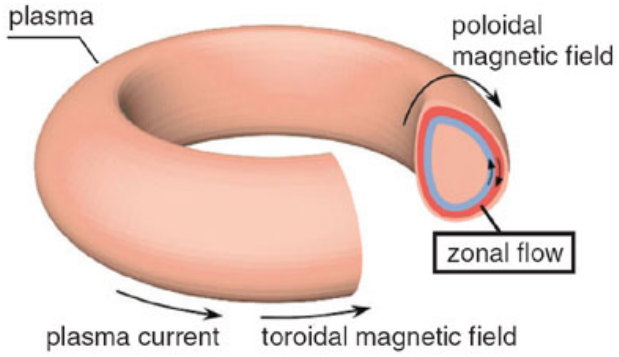

Figure 1.9: Zonal flows in toroidal plasma. The red region and the blue region denote the positive and negative charges, respectively. Illustration from Japan Atomic Energy Agency.

Zonal flows are important for plasma confinement because their shearing acts to regulate drift wave turbulence and transport. A simple thought experiment is as follows: consider a drift wave-packet propagating in zonal flow shear layers. The zonal shearing will randomly tilt the wave-packet and narrow its radial extent, i.e., the mean square radial number k_r will increase. Consequently, the drift wave frequency ($\omega_k = \omega_{*e}/(1 + k_\perp^2 \rho_s^2)$) will decrease. There is a separation in time scales between the low frequency zonal flow and the high frequency drift waves. Thus, the wave action density, the ratio of wave energy density to wave frequency, is conserved, and so drift wave energy will also decrease. Since the total energy of the wave-zonal flow system is conserved, the energy of zonal flows must increase. In other words, since zonal flows are generated by its nonlinear interactions with drift wave turbulence, the energy growth of zonal flow must be transfered from turbulence. Thus zonal flows naturally act to suppress drift wave turbulence and the corresponding transport.

Table 1.5: Characteristics of zonal flow.

$n = 0$ and $k_{\|\|} = 0$
modes of minimal inertia
modes of minimal Landau damping
modes of minimal radial transport

One may wonder what makes zonal flows unique? Speaking of shearing effects, the mean $\boldsymbol{E}\times\boldsymbol{B}$ shear flows are also able to decorrelate eddies and regulate turbulent transport. Speaking of drawing energy from drift waves turbulence, other low-n drift modes can also interact nonlinearly with finite-n modes and grow. First, zonal flows and mean shear flows have an important difference: the driving mechanism. Zonal flows are driven by turbulence, so the intensity of zonal flows must decrease when there is no source of drift wave turbulence. On the other hand, mean $\boldsymbol{E}\times\boldsymbol{B}$ flows are driven by mean pressure gradient, and so can be sustained in the absence of turbulence. Second, zonal flows are special compared with other low-n modes because zonal flows are modes of minimum inertia, minimal Landau damping, and no radial transport (see e.g., [14]). In the H-M equation (1.1.3), the PV of drift waves is $\tilde{\phi}-\rho_s^2\nabla^2\tilde{\phi}=(1+k_\perp^2\rho_s^2)\tilde{\phi}$. Since $n=m=0$ zonal flow modes are not affected by Boltzmann electron response, the PV of zonal flow modes is $k_\perp^2\rho_s^2\tilde{\phi}$, i.e., zonal flow modes have minimum inertia among all the drift modes. Consequently, zonal flows are the "preferential" modes to which to couple energy. Moreover, as we've mentioned, zonal flow cannot tap the energy

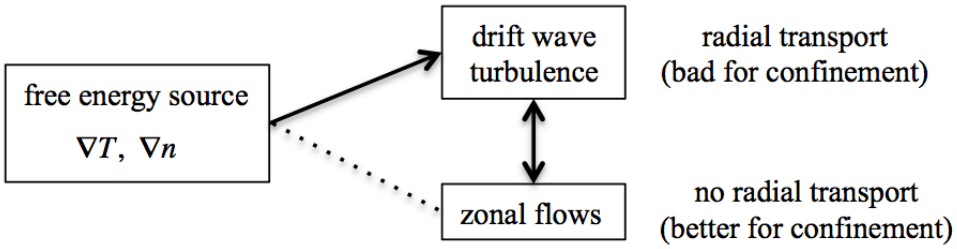

Figure 1.10: Energy channel chart.

stored in radial gradients, and so do not contribute to radial transport. Therefore, energy is "better-confined" when it is stored in zonal flows than in drift wave turbulence. In other words, transferring free energy from the finite-n drift waves to zonal flows gives a benign energy transfer channel for fusion confinement (Figure 1.10). Because of zonal flows' favorable behavior for confinement, the physics of zonal flow-drift wave dynamics have become the subject of intense interest and investigation.

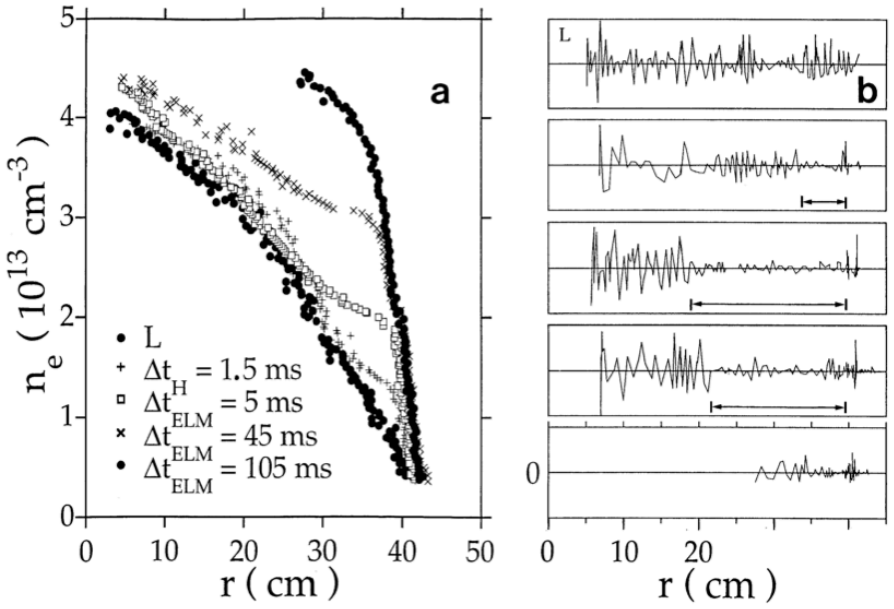

Figure 1.11: Density profiles and fluctuations at five time points during the LH transition in ASDEX (Wagner et al 1991): (a) development of steep density gradient; b) suppression of edge fluctuations.

Due to the effect of decorelating eddies and suppressing turbulence, zonal flows are believed to play an importance role in the development of the low-to-high confinement mode (L-H) transition (see e.g., the review by Connor and Wilson [15]). When the input power is near the H-mode power threshold, an intermediate, oscillatory phase between the L mode and the H mode, called intermediate phase (I-phase), can often be observed. The high confinement mode (H-mode), one possibility of enhanced operation regimes in the next step large fusion devices, is characterized by steep gradients at the edge of the plasma (Figure 1.11 a). During the L-H transition, turbulence in edge plasmas is suppressed significantly (Figure 1.11 b). Correspondingly, the turbulent transport is reduced at the edge, so that in turn can leads to the steepening of edge profiles. The suppression of edge turbulence can be attributed to mean $\boldsymbol{E} \times \boldsymbol{B}$ shear flows and zonal flows. Since zonal flows are modes of minimal effective inertia, zonal flows tend to develop in response to drift wave drive and regulate turbulence and associated transport, allowing the buildup of a steep pressure gradient. As the mean shear driven by

mean pressure gradient grows sufficiently strong, both turbulence and zonal flows are damped at the final stage of the transition. While the shearing by mean flows is coherent over longer times, the shearing of zonal flows has a complex spatial structure (Figure 1.12) and is of limited coherency in time. Observations of time-varying shear radial electric fields at the plasma edge suggests a link between the formation of zonal flows and the development of L-H transitions. It is now believed that mean shear flows and zonal flows both participate in the L-H transition, while each plays a different role. (see e.g., [16, 17, 18, 19]).

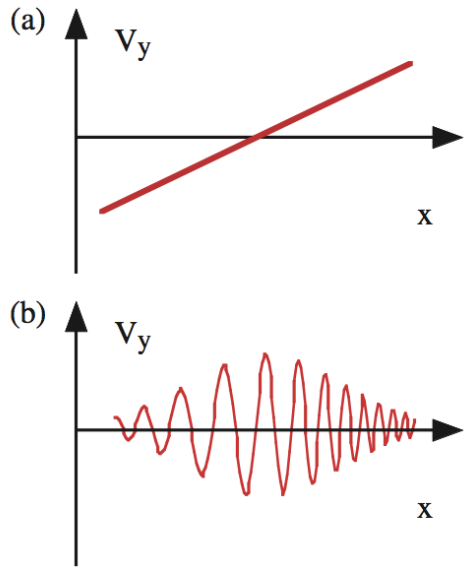

Figure 1.12: Mean shear flow (a) and zonal flow (b) are illustrated (Diamond et al 2005).

1.3 What are the physics issues?

The zonal flow problem is really one of self-organization of large-scale structure in turbulence. The physics of zonal flow dynamics is that of turbulence-zonal flow dynamics, because zonal flow and turbulence are strongly coupled together, forming a feedback loop (Figure 1.13). In fact, the drift wave turbulence is frequently called "drift wave-zonal flow" turbulence. While the focus in this section is primarily on the physics of zonal flow generation, we keep in mind this is just

"half of the loop."

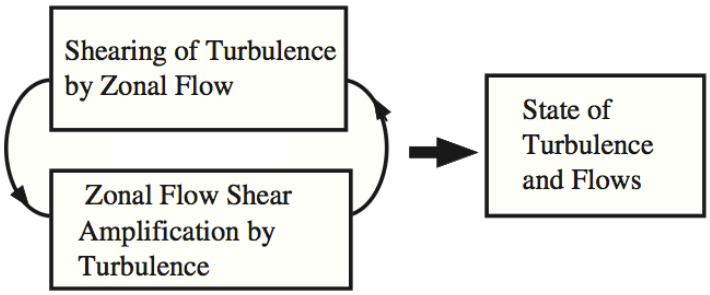

Figure 1.13: Mutual interaction between turbulence and zonal flows (Diamond et al. 05).

1.3.1 Physics of zonal flow formation

Zonal flows are generated by nonlinear interactions between wave turbulence and zonal flow. In wave number space, energy is transferred from small-scale Rossby/drift waves to large-scale zonal flows by nonlinear interactions, which are three-wave (triad) interactions among two high-wave number drift waves and one low-wave number zonal flow excitation, as shown in Figure 1.14 (b).

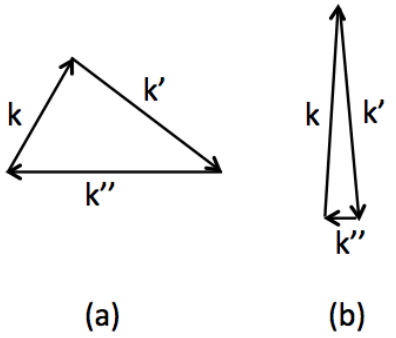

Figure 1.14: Possible triad interactions where $k + k' + k'' = 0$. (a)"local" triads $k \sim k' \sim k''$: the wave-numbers of the three waves are similar. (b) "non-local" triads $k \sim k' >> k''$: one of the wave (zonal flow mode) has wavenumber much smaller than that of the other two waves.

In position space, the energy transfer to zonal flows occurs via Reynolds work. The evolution of zonal flow is determined by source (Reynolds stress) and

sink (frictional damping):

$$\frac{\partial}{\partial t}\langle v_x\rangle = -\frac{\partial}{\partial y}\langle \tilde{v_y}\tilde{v_x}\rangle - \mu\langle v_x\rangle, \tag{1.7}$$

where μ is friction in GFD or collisional drag in plasma. The angle brackets denote the zonal average, and the tilde departure from it. The Reynolds stress is related to vorticity flux by the Taylor identity [20]. The proof of the Taylor identity is as follows: PV and velocity vector in quasi-geostrophic β-plane turbulence are $q = (\nabla^2 - L_d^{-2})\psi + \beta y$ and $(v_x, v_y) = (-\partial\psi/\partial y, \partial\psi/\partial x)$. Therefore, the turbulent PV flux is given by

$$\begin{aligned}\langle \tilde{v_y}\tilde{q}\rangle &= \left\langle \frac{\partial\tilde{\psi}}{\partial x}\left(\frac{\partial^2\tilde{\psi}}{\partial x^2} + \frac{\partial^2\tilde{\psi}}{\partial y^2} - L_d^{-2}\tilde{\psi}\right)\right\rangle \\ &= \left\langle \frac{1}{2}\frac{\partial}{\partial x}\left(\frac{\partial\tilde{\psi}}{\partial x}\right)^2 + \frac{\partial}{\partial y}\left(\frac{\partial\tilde{\psi}}{\partial x}\frac{\partial\tilde{\psi}}{\partial y}\right) - \frac{\partial^2\tilde{\psi}}{\partial y\partial x}\frac{\partial\tilde{\psi}}{\partial y} - \frac{L_d^{-2}}{2}\frac{\partial}{\partial x}\tilde{\psi}^2\right\rangle. \end{aligned} \tag{1.8}$$

The first, third and forth terms on the RHS of equation (1.8) vanish because of zonally periodic boundary conditions. Thus, the PV flux becomes equivalent to the Reynolds force

$$\langle \tilde{v_y}\tilde{q}\rangle = -\frac{\partial}{\partial y}\left\langle \tilde{v}_x\tilde{v}_y\right\rangle, \tag{1.9}$$

and so the zonal flow is driven by turbulent transport of PV [20]

$$\frac{\partial}{\partial t}\langle v_x\rangle = \langle \tilde{v_y}\tilde{q}\rangle - \mu\langle v_x\rangle. \tag{1.10}$$

The Taylor identity clearly links the emergence of zonal flows to the transport of PV by Rossby/drift wave motions. There is no assumption about the fluctuation amplitude. Thus, the Taylor identity tells us that the turbulent PV flux, including any contributions from strongly nonlinear processes like PV mixing and wave breaking, is directly tied to formation of large-scale flows and jets. Since the mixable quantity is PV instead of momentum, there is no reason to suppose that the momentum flux is down-gradient, i.e., the "negative-viscosity" is no longer an enigma. Note that one direction ($\hat{x}$) of symmetry and another direction ($\hat{y}$) of inhomogeneity are essential elements for the validity of the identity. To sum up, the Taylor identity shows that *inhomogeneous PV mixing is the fundamental mechanism of zonal flow formation in a quasi two-dimensional fluid or plasma.*

While the significance of the PV mixing for zonal flow dynamics has been more widely appreciated, the conventional explanation for zonal flow generation has usually been referred to "inverse energy cascade" in two-dimensional turbulence [21] together with the "Rhines mechanism" [22]. Two dimensional turbulence behaviors very differently from three dimensional turbulence (Figure 1.15). In three dimensional turbulence, energy forward cascades to small scales. The cascade pic-

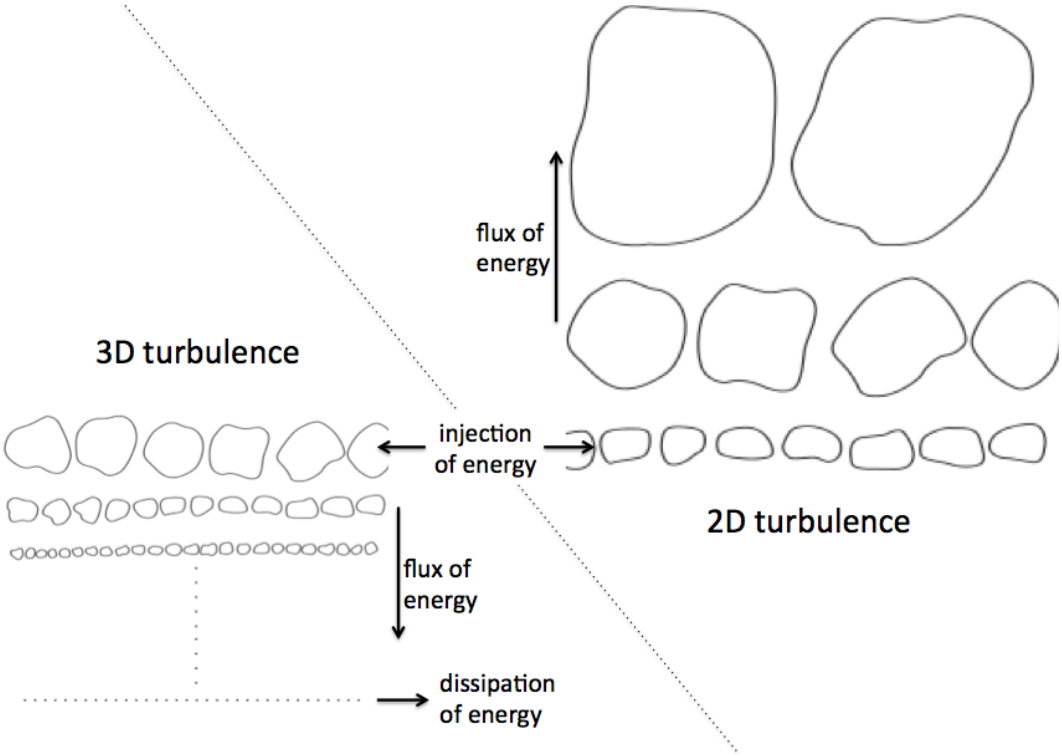

Figure 1.15: Contrast between energy cascades in three-dimensional and two-dimensional turbulence.

ture of three-dimensional turbulence is captured by Lewis Fry Richardson's poem indebted to Jonathan Swift:

Big whirls have little whirls
That feed on their velocity;
Little whirls have lessor whirls,
And so on to viscosity.

The energy cascade in two dimensional turbulence is an opposite extreme (M. E. McIntyre):

Big whirls meet bigger whirls,
And so it tends to go on:
By merging they grow bigger yet,
And bigger yet, and so on...

Two-dimensional turbulence supports two quadratic conserved quantities, namely energy and potential enstrophy, resulting in a forward cascade of enstrophy to small scales and an inverse cascade of energy to large scales. In the limit of small viscosity, the energy is thought to inverse cascade to the largest possible scale–the system size or to wavenumber zero.

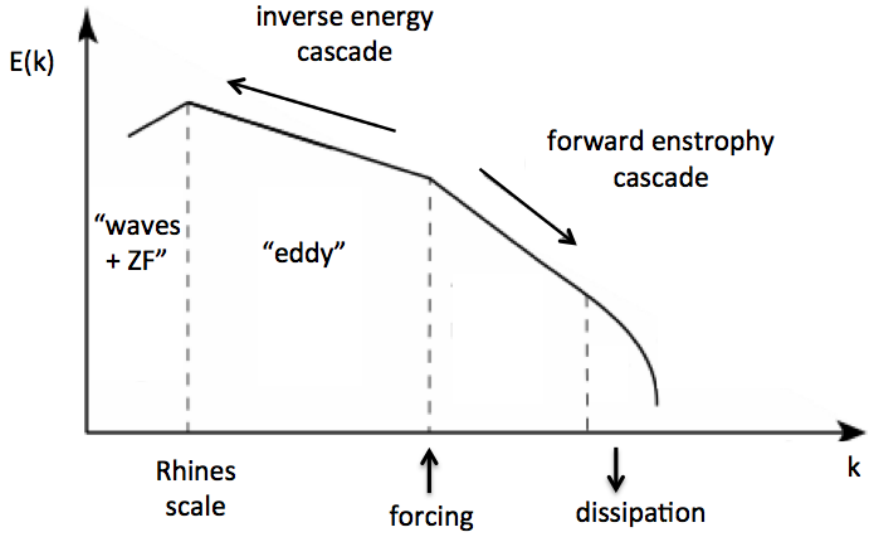

Figure 1.16: Dual cascade and Rhines scale in two-dimensional Rossby/drift wave turbulence.

Instead of eddies with sizes of the system, elongated vortices–zonal flows–are formed in two-dimensional quasi-geostrophic or drift wave turbulence because of the effect of anisotropy (β-effect). In this anisotropic cascade scenario, the size of zonal flows is characterized by the Rhines scale, the cross over scale at which eddy turnover rate and Rossby wave frequency mismatch are comparable (Figure

1.16). Scales larger than the Rhines scale are dominated by Rossby waves, while smaller scales are dominated by eddies. (Note that both eddies and waves can be represented by $\tilde{\psi}_k = \hat{\psi}_k e^{-i\omega t}$. Fluctuations with Im($\omega$) >Re($\omega$) are called eddies; perturbations with Im(ω) <Re(ω) are called waves.) If the external forcing (stirring) is at a scale smaller than Rhines scale, energy will inverse-cascade to larger scales. The inverse cascade is dominated by local triad interactions of Rossby/drift-wave turbulence (see Figure 1.14 (a)). Since Rossby waves are strongly dispersive at large scales (low k), triad interactions are severally inhibited (three wave mismatch). Only the interaction between one $k_x \approx 0$ zonal flow mode and two higher-k Rossby waves are allowed (see Figure 1.14 (b)). Thus, the combination of Rossby wave and turbulence preferentially leads to the formation of zonal flow.

The inverse cascade in quasi two-dimensional turbulent fluid can explain zonal flow generation. However, zonal flows are also observed in systems with no obvious inertial range, so inverse cascade cannot be the cause of zonal flow in this case. The inverse cascade picture is simplistic since zonal flow can be and is driven by Reynolds stresses, which result from vorticity (or potential vorticity) mixing. Such small scale mixing processes depend more upon the forward scattering of fluctuation enstrophy than they do on the inverse cascade. Moreover, the inverse cascade is "local" while zonal flow generation is "non-local" in wave number space: the inverse cascade occurs via nonlinear couplings between waves with similar scales, while zonal flows are generated via nonlinear interactions between small-scale Rossby/drift waves and large-scale zonal flows. Since PV mixing is a more general mechanism for zonal flow formation than inverse cascade, I'll move the focus back to PV mixing.

1.3.2 Inhomogeneous PV mixing in space

The importance of PV mixing in space with respect to zonal flow formation has been demonstrated in the Taylor identity: turbulent flux of PV equals to a Reynolds force, which in turn drives the flow. In plasma community, Diamond and Kim [23] were the first who discussed the vorticity and wave momentum transport and zonal flow formation. The vorticity in magnetically confined plasmas is polar-

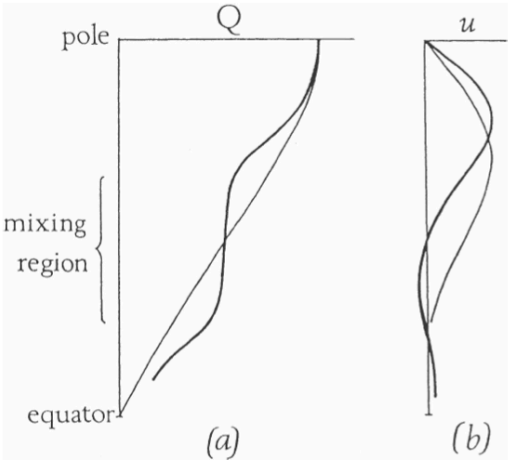

Figure 1.17: Schematic jet-sharpening by inhomogeneous PV mixing (McIntyre 1982). The light and heavy curves are for before and after the mixing event. The velocity curves in (b) are determined by inversion of PV profiles in (a).

ization charge, and the vorticity mixing is due to the guiding center am bipolarity breaking. In GFD community, the physics of PV dynamics and zonal flow formation has been studied ever since Charney derived the quasi-geostrophic equation in 1948. Dritschel and McIntyre [24] have reviewed PV mixing and formation of persistent zonal jets in the Earth's atmosphere and oceans. Figure 1.17 shows a schematic of inhomogeneous PV mixing leading to sharpening of the zonal velocity profile [25]. PV is strongly mixed on the equatorward side of the zonal flow. The mixing of PV reshapes the large-scale PV distribution; it weakens the PV gradient in the mixing region and strengthens the PV gradients in the adjacent regions. The inversion of the change of the PV profile gives the change of the zonal velocity profile. Thus, PV mixing in turn causes changes in the angular momentum distribution. The latitudinal scale of the zonal flow becomes narrower after the mixing, i.e., zonal flow is sharpened.

Dritschel and McIntyre point out that it has been observed in both experiments and numerical simulations that mixing of PV usually results in parallel zonal bands with nearly uniform values of PV. Zonal jets are located around the interfaces of the bands, where PV gradients are steep. In extreme circumstances when the PV gradients evolve steeper and steeper, the meridional profile of PV

resembles a "staircase". The structure of banded patterns accompanying jets is observed in the atmospheres of Jupiter and some other giant gas planets, as well as Earth's atmosphere (though jets are more wavy). PV staircase is an idealized saturated state consisting of perfectly mixed zones separated by sharp PV gradients. The formation of PV staircase can be understood as follows. Considering a system with a monotonic meridional background PV gradient, in the region where PV are irreversibly mixed, waves break and dissipate. The PV gradients are increased in the neighboring regions with no wave breaking. The gradient of PV provides a restoring force for Rossby waves and thus prevents wave breaking and PV mixing. Conversely, the restoring force in mixed regions is weakened, leading to further mixing. This positive feedback mechanism is similar to the Phillips effect (O. M. Phillips 1972), which states that in a system with background buoyancy gradient, the gravity wave elasticity are weakened in the mixing layers, causing further mixing across stratification surfaces. On the other hand, the wave elasticity is strengthened in the interfaces between the mixed layers, inhibiting mixing across the interfaces. The formation of PV staircase can be explained by the PV Phillips effect. In this thesis we provide another way to understand the formation of PV staircase. In our minimum enstrophy model of PV transport, selective decay of potential enstrophy in quasi-2D turbulence naturally results in a relaxed state with the structure similar to the PV staircase.

The alternating jet pattern of coherent structures, the so-called $\boldsymbol{E} \times \boldsymbol{B}$ staircases, is also found in magnetized plasmas [3] (Figure 1.18). "This structure may be defined as a spontaneously formed, self-organizing pattern of quasiregular, long-lived, localized shear flow and stress layers coinciding with similarly long-lived pressure corrugations and interspersed between regions of turbulent avalanching" [26]. The staircase indicates the non-local interaction between widely separated regions in quasi-2D turbulence, and the large-scale, avalanche-like, temporally intermittent transport. Thus, a generalized Fickian diffusion described using local transport coefficients is not adequate to model the turbulent transport. Moreover, the staircase points out the critical role of the scale of inhomogeneity and thus presents a challenge to models of inhomogeneous PV mixing.

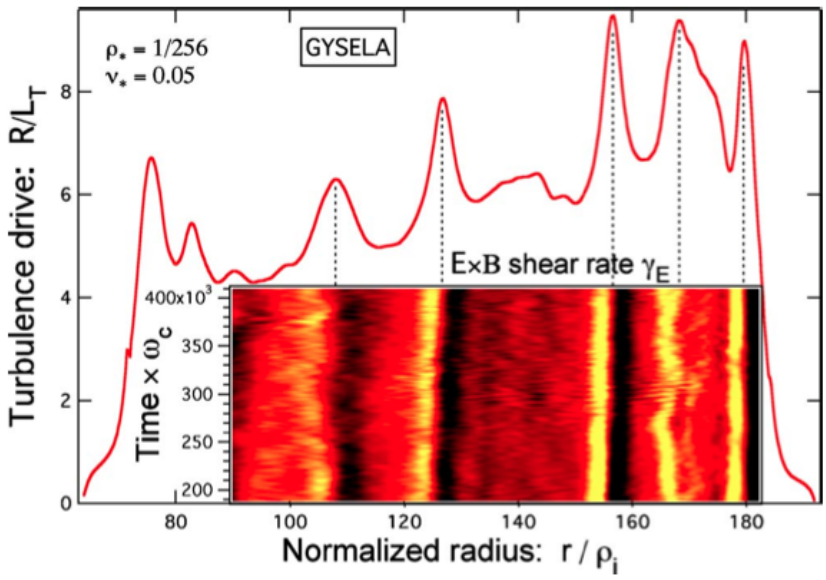

Figure 1.18: Corrugations of the mean temperature profile correlate well with dynamically driven steady-standing $\boldsymbol{E} \times \boldsymbol{B}$ sheared flows which self-organize nonlinearly into a jetlike pattern of coherent structures of alternating sign: the $\boldsymbol{E} \times \boldsymbol{B}$ staircase (Dif-Pradalier et al. 2010 [3]).

PV mixing in a system with one direction of symmetry is the fundamental mechanism of zonal flow formation. The origin of PV mixing is the cross phase between fluctuating velocity $\tilde{v_y}$ and vorticity $\nabla\tilde{\psi}$, which is determined by the microdynamics of the mixing processes (see e.g., [27]). Candidate mixing processes include molecular viscosity, eddy viscosity, Landau resonance, and non-linear Landau damping. Eddy viscosity is an effective viscosity due to nonlinear coupling to small scale by forward cascade of potential enstrophy. Landau resonance here is Rossby/drift wave absorption when $\omega = k_x\langle v_x\rangle$ is satisfied. Non-linear Landau damping here represents nonlinear wave-zonal flow scattering. Again, we note that it is the forward enstrophy caecade which is critical to the mixing processes, not the inverse energy cascade.

In pragmatic terms, understanding vorticity mixing requires determination of the cross phase in the vorticity flux. Thus, the origin of irreversibility in vorticity transport is fundamental to zonal flow formation. Forward potential cascade to small scale dissipation makes the PV mixing processes irreversible. As for the

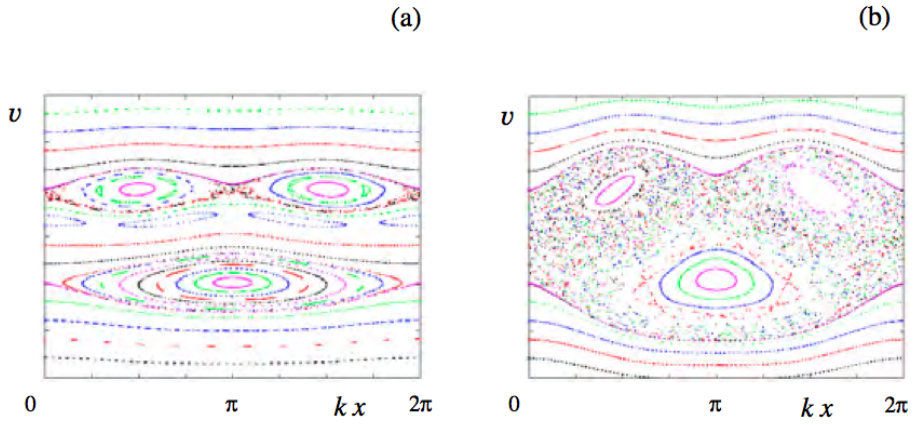

Figure 1.19: "Cateye" islands overlap (Diamond et al 2010 [4]). (a) Particles inside the separatrix (inside the island) are trapped. Particles outside the separatrix circulate. (b) When the distance between two islands is smaller than the separatrix width, the separatrices are destroyed, i.e. islands overlap.Particles can stochastically wander from island to island, so the particle motion becomes stochastic.

case of Landau damping, stochasticity of streamlines provide the key element of irreversibility. The resonance condition for drift wave-packets and zonal flow field in wave kinetic equation is $v_{gy}(\boldsymbol{k}) = \Omega/q_y$: the radial group velocity of wave-packet equals the radial phase velocity of zonal flow. Ω and q_y are the frequency and radial wave number of the zonal flow mode. When the "phase space islands overlap" (Figure 1.19), i.e. wave group-zonal flow resonances overlap, ray trajectories of wave-packets becomes stochastic. This gives a source of irreversibility for zonal flow formation via modulational instability based on wave kinetics. Analogy between phase islands overlap for quasi-linear theory and wave kinetic theory is in table 1.6.

1.4 How to represent anisotropic PV mixing?

Now we know that the key to understanding the physics of zonal flow formation is to understand inhomogeneous PV mixing. So the next question is: how do we represent PV mixing in space? In other words, how do we calculate the spatial

Table 1.6: Analogy between phase islands overlap for quasi-linear theory and wave kinetic theory.

	quasi-linear theory	wave-kinetic theory
particles	resonant particles v	Rossby/drift wave packets v_g
fields	waves ω_k, k	zonal flow shearing field Ω_q, q
resonance condition	$v \approx \omega_k/k$	$v_g \approx \Omega_q/q$
island width	excursion in v due to libration $\Delta v \sim \sqrt{q\phi/m}$	variation of v_g in a trough of large-scale field $(\partial v_g/\partial k)\Delta k$
island separation	distance between adjacent resonance $\Delta(\omega_k/k)$	distance between adjacent resonace $\Delta(\Omega_q/q)$
overlaping condition $\rightarrow$ stochasticity/mixing	$\Delta(\omega_k/k) < \Delta v$	$\Delta(\Omega_q/q) < (\partial v_g/\partial k)\Delta k$

flux of PV? Calculating the spatial PV flux in quasi-two dimensional turbulence is the goal of this thesis. Here we introduce some theoretical approaches.

1.4.1 Mixing length model

Fig. 1.20 illustrates a simple model of PV mixing processes. Because of the material conservation of PV, when a fluid parcel is displaced from y_0 to $y_0 + l$, the change of PV at $y_0 + l$ due to mixing is equal to mixing length l times the negative gradient of mean PV, i.e.

$$\tilde{q} = -l\frac{\partial\langle q\rangle}{\partial y}. \tag{1.11}$$

Thus, PV flux is given by

$$\langle\tilde{v}_y\tilde{q}\rangle = -\langle\tilde{v}_y l\rangle\frac{\partial\langle q\rangle}{\partial y} = -\frac{\langle\tilde{v}_y^2\rangle}{|\delta\omega|}\frac{\partial\langle q\rangle}{\partial y}, \tag{1.12}$$

where $\delta\omega$ is the mixing rate in the mixing length picture. Note that the PV flux in this mixing length picture is down-gradient. The mixing rate originates in the

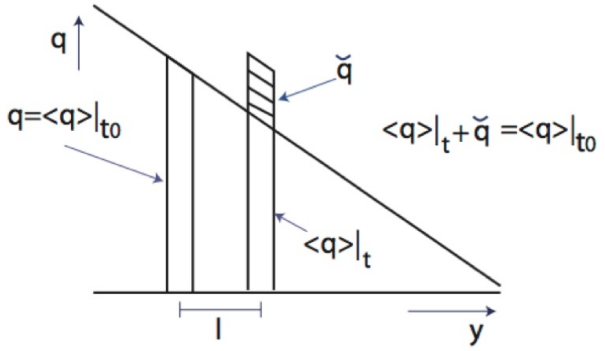

Figure 1.20: Mixing length model.

cross phase in PV flux. It is different from the term "eddy turn over rate" used in turbulent cascade. While turn over rate is determined by local interactions in wavenumber space, mixing rate depends also on non-local couplings. Therefore we expect the mixing rate to be a function of shear flow, turbulent amplitude, and damping parameters. In this thesis we study the mixing rate and the physical mechanism of mixing, by deriving the cross phase in the PV flux. Note that the mixing of PV is different from the conventional mixing of passive scalars. PV is an active scalar, so the change of PV in the mixing process modifies the turbulent velocity field, which determines the dynamics of PV.

1.4.2 Perturbation theory

Most of the wave-zonal flow problems are approached by perturbation theory, or more precisely, by studying the stability of an ensemble of ambient turbulence to a perturbation flow. The test zonal flow interacts with a spectrum of Rossby/drift wave fluctuations, or, an ensemble of wave-packets. Each wave-packet has a frequency ω_k and a finite self-correlation time $\delta\omega_k^{-1}$. The frequency of the zonal flow Ω_q is much smaller than ω_k, i.e., there is a time-scale separation between the zonal flow and the waves. The idea of modulational instability analysis is to derive a mean field evolution equation of the seed zonal flow in the presence of wave stresses, and at the same time consider the response of the wave spectrum to the seed zonal flow.

Wave action density is useful for computing the response of the primary wave spectrum to the test shear because it is conserved along the wave-packet trajectories [28]. This adiabatic conservation is due to the time scale separation between wave-packets and the zonal flow. The wave action density in quasi-geostrophic β-plane turbulence is given by

$$N_k = \frac{E_k}{\omega_k} = \frac{k^2|\tilde{\psi}_k|^2}{-\beta k_x/(k^2)}, \tag{1.13}$$

where $E_k = |\nabla\tilde{\psi}_k|^2$ is the kinetic energy density. The wave action density is proportional to the potential enstrophy density $|\nabla^2\tilde{\psi}|^2 = k^4|\tilde{\psi}_k|^2$ by a factor of βk_x. Since k_x does not change under zonal shear flows, the factor is a constant. As a result, the wave action density can be renormalized to the potential enstrophy density (N_k is redefined as $k^4|\tilde{\psi}_k|^2$). In drift wave turbulence, the wave action density $N_k = (1 + k_\perp^2\rho_s^2)^2|\tilde{\phi}_k|^2/\omega_{*e}$ also equals to the enstrophy density times a constant (in k_r) factor ω_{*e}.

The driving force of the zonal flow–the Reynolds force–is linked to the N_k:

$$-\frac{\partial}{\partial y}\langle\tilde{v_y}\tilde{v_x}\rangle = \frac{\partial}{\partial y}\int d^2k k_x k_y|\tilde{\psi}_k|^2 = \frac{\partial}{\partial y}\int d^2k\frac{k_x k_y}{k^4}N_k. \tag{1.14}$$

The modulation induced in N_k by the seed zonal flow $\delta\langle v_x\rangle$ produces a "modulational" Reynolds stress, which in turn drives the seed flow:

$$\frac{\partial}{\partial t}\delta\langle v_x\rangle = \frac{\partial}{\partial y}\int d^2k\frac{k_x k_y}{k^4}\frac{\partial N_k}{\partial\delta\langle v_x\rangle}\delta\langle v_x\rangle \tag{1.15}$$

To calculate the modulational response of N_k, we use the wave kinetic equation

$$\frac{\partial N_k}{\partial t} + (v_g + \delta\langle v_x\rangle)\cdot\nabla N_k - \frac{\partial}{\partial\boldsymbol{x}}(\omega_k + k_x\delta\langle v_x\rangle)\cdot\frac{\partial N_k}{\partial\boldsymbol{k}} = \gamma_k N_k - \frac{\delta\omega}{N_0}N_k^2, \tag{1.16}$$

where v_g is the group velocity of wave-packets, γ_k the linear growth rate, $\delta\omega_k$ nonlinear self-decorrelation rate via wave-wave interaction, and N_0 the equilibrium enstrophy spectrum. The linear growth rate is equal to the self-decorrelation rate at equilibrium, so we assume $\gamma_k \cong \delta\omega_k$ near equilibrium $N = N_0 + \tilde{N}$, where $\tilde{N} = \frac{\partial N_k}{\partial\delta\langle v_x\rangle}\delta\langle v_x\rangle << N_0$. The modulational enstrophy is then determined by the linearized wave kinetic equation

$$\frac{\partial\tilde{N_k}}{\partial t} + v_{gy}\frac{\partial}{\partial y}\tilde{N_k} + \delta\omega_k\tilde{N_k} = \frac{\partial(k_x\delta\langle v_x\rangle)}{\partial y}\frac{\partial N_0}{\partial k_y}. \tag{1.17}$$

Assuming small perturbations $(\tilde{N_k}, \delta\langle v_x\rangle) \sim e^{-i\Omega_{\boldsymbol{q}}t+iq_y y}$, where q_y is the meridional/radial wave number of the zonal flow, the modulation of $\tilde{N_k}$ becomes

$$\tilde{N_k} = -iq_y\delta\langle v_x\rangle \frac{k_x}{-i(\Omega_{\boldsymbol{q}} - q_y v_{gy}) + \delta\omega_k} \frac{\partial N_0}{\partial k_y}, \tag{1.18}$$

so the turbulent PV flux, equivalent to the modulation of Reynolds force, is given by

$$\langle \tilde{v_y}\nabla^2\tilde{\psi}\rangle = -q_y^2\delta\langle v_x\rangle \int d^2k \frac{k_x^2 k_y}{k^4} \frac{|\delta\omega_k|}{(\Omega_{\boldsymbol{q}} - q_y v_{gy})^2 + \delta\omega_k^2} \left(\frac{\partial N_0}{\partial k_y}\right), \tag{1.19}$$

and the growth rate of the seed zonal flow is given by

$$Im(\Omega_q) = -q_y^2 \int d^2k \frac{k_x^2 k_y}{k^4} \frac{|\delta\omega_k|}{(\Omega_{\boldsymbol{q}} - q_y v_{gy})^2 + \delta\omega_k^2} \left(\frac{\partial N_0}{\partial k_y}\right). \tag{1.20}$$

The condition to have instability ($k_y\partial_{k_y}N_0 < 0$) is satisfied for most realistic equilibrium spectra for Rossby wave and drift wave turbulence. The fundamental mechanism of zonal flow generation includes not only local wave-wave interactions (in wavenumber space) but also non-local couplings between waves and flows. Therefore, zonal flow growth rate should depend on both the spectral structure of turbulence and properties of zonal flow itself. Equation (1.20) shows that the growth rate is indeed a function of wave spectrum $N_0(\boldsymbol{k})$ and zonal flow wave number q_y. We can relate the PV flux derived in perturbation theory to that defined in the mixing length model.

$$\frac{\partial}{\partial t}\delta\langle v_x\rangle = \langle \tilde{v}_y\tilde{q}\rangle = -\frac{\langle \tilde{v}_y^2\rangle}{\delta\omega}\frac{\partial}{\partial y}\langle q\rangle = \frac{\langle \tilde{v}_y^2\rangle}{\delta\omega}\frac{\partial^2}{\partial y^2}\delta\langle v_x\rangle, \tag{1.21}$$

so the mixing rate is given by

$$\delta\omega^{-1} = \int d^2k \frac{k_y}{k^4|\tilde{\psi}_k|^2} \frac{|\delta\omega_k|}{(\Omega_{\boldsymbol{q}} - q_y v_{gy})^2 + \delta\omega_k^2} \left(\frac{\partial N_0}{\partial k_y}\right). \tag{1.22}$$

It is worth noting that the sum of turbulence energy and zonal flow energy is conserved in this system. The energy density and enstrophy density of wave packets are $k^2|\tilde{\psi}_k|^2$ and $k^4|\tilde{\psi}_k|^2$, so the energy density is related to N_k. We use wave kinetic equation to obtain the evolution of turbulence energy

$$\begin{aligned} \frac{\partial}{\partial t}E_w &= \frac{1}{2}\int \frac{1}{k^2}\left[-v_{gy}\frac{\partial}{\partial y} + \delta\omega_k + k_x\frac{\partial}{\partial y}\delta V_x\frac{\partial}{\partial k_y}\right](N_0 + \tilde{N_k})d^2xd^2k \\ &= \int \frac{k_x k_y}{k^4}\frac{\partial}{\partial y}\delta\langle v_x\rangle\tilde{N_k}d^2xd^2k \end{aligned} \tag{1.23}$$

Some terms vanish because the seed zonal flow is random ($\int \delta\langle v_x\rangle d^2x = 0$) and the equilibrium wave action satisfies $\partial_y N_0 = 0$. On the other hand, the evolution of zonal flow energy is given by

$$\begin{aligned} \frac{\partial}{\partial t} E_{\rm ZF} = \frac{\partial}{\partial t} \int \frac{1}{2} \delta\langle v\rangle_x^2 d^2x &= \delta\langle v_x\rangle \frac{\partial}{\partial y} \int \frac{k_x k_y}{k^4} \tilde{N}_k d^2x d^2k \\ &= -\int \frac{\partial}{\partial y} \delta\langle v_x\rangle \frac{k_x k_y}{k^4} \tilde{N}_k d^2x d^2k \end{aligned} \tag{1.24}$$

Equations(1.23) and (1.24) show that the changes of turbulence energy and zonal flow energy cancel each other, and the total energy is conserved. The increase of zonal flow energy by modulational instability therefore indicates a loss of turbulence energy. The analogy between energy conservation theorems for wave-zonal flow systems and quasi-linear theory is shown in table 1.7.

Table 1.7: Analogy between energy balance theorems for quasi-linear theory and wave kinetic theory.

	quasi-linear	wave-kinetic
particles	resonant particles kinetic energy $E_{\rm res}$	Rossby/drift wave packets wave-packet energy E_w
fields	waves, collective modes total wave energy W	zonal flow shearing field zonal flow energy $E_{\rm ZF}$
energy conservation	$\frac{\partial}{\partial t}(E_{\rm res} + W) = 0$	$\frac{\partial}{\partial t}(E_w + E_{\rm ZF}) = 0$

We note that there are systems with little or no scale separation, and/or with strong nonlinearity. Even though the perturbation analyses become invalid in these systems, they are important because they allow us to derive the PV flux precisely and learn the micro-physics in more depth. Also, even if the quantitative results derived via perturbation theory are limited to weakly turbulent systems with scale separation, some of the underlying physics of modulational instability exist in other systems as well. We also note that the initial growth of a seed zonal flow is only part of the theoretical description of zonal flow formation.

1.4.3 Constrained relaxation models

The zonal flow problem is in general a problem of turbulence self organization, in which two classes of turbulence phenomena, of disparate scales, nonlinearly interact with each other. An integrated understanding of such problem requires studies of many elements, including excitation of zonal flows by turbulence, the back reaction of zonal flows on turbulence, linear, collisional damping of zonal flows, zonal flow instability or nonlinear saturation mechanism for zonal flows (especially in nearly collisionless regimes), and various feedback loops by which the system regulates and organizes itself.

It is extremely difficult to attack all these topics at the same time. A analytical model covers all possible mechanisms 'of the loop' in great detail is too complex to develop based on our current knowledge. Obviously, turbulence is much smarter than us. So one way to understand this complex system, in a bigger envelope, is to use general principles, without considering some details of the underlying microphysics. (We all know from high school that using energy conservation to solve many physics problems is often easier than using Newton's second law.) Since our goal here is to find a representation of anisotropic PV mixing, we seek for general perspective to derive the structure of the PV flux. Specifically, we use structure approach in constrained relaxation models. We ask *what forms must the PV flux have so as to satisfy the general principles governing turbulence relaxation to some relaxed or self-organized state?*

The minimum enstrophy principle by Bretherton and Haidvogel [29] is a plausible and demonstrably useful guide for turbulence relaxation. In their hypothesis, two-dimensional turbulence evolves toward a state of minimum potential enstrophy, for given conserved kinetic energy. Their variational argument is based on the concept of selective decay, which is in turn based on the dual cascade in two-dimensional turbulence. As we mentioned earlier, in two-dimensional turbulence, kinetic energy inverse cascades to large, weakly dissipated spatial scales, whereas enstrophy forward cascades to small spatial scales and there is damped by viscosity. In the presence of weak dissipation, total kinetic energy is thus approximately conserved relative to total enstrophy, which is dissipated. Based on the variational

argument, a linear relationship between vorticity and streamfunction is obtained. In the relaxed state, PV is constant along streamlines and so the nonlinear term $v \cdot \nabla q$ in the PV equation is annihilated. The theory predicts the structure of the flow in the end state. However, it does not address the dynamics of the relaxation. How the mean profiles evolve during the relaxation is an important question for zonal flow formation.

There are other selective decay principles used to derive turbulence relaxation equations; for example, minimized enstrophy subject to conserved magnitude of PV flux [30], maximized entropy subject to conserved total entrophy [31], minimized diffusion energy subject to a conserved rate of entropy production [32], and etc. These constrained relaxation models, with different conserving and dissipating functionals, all use variational principles to derive equations of the steady state. However, like the minimum enstrophy hypothesis, most of the variational analyses give no insight into the dynamics of the relaxation process. To understand the dynamics of zonal flow, in this thesis we study the PV flux during a selective decay toward a minimum enstrophy state using structural approach. In particular, we ask *what form must the mean field PV flux have so as to dissipate enstrophy while conserving energy?*

We note that the minimum enstrophy state is a subclass of statistical equilibrium states of quasi-geostrophic turbulence (Miller-Robert theory), and the statistical equilibrium states are a subclass of of stable stationary states. The theoretical study of the self-organization of quasi two-dimensional turbulence is also addressed based on statistical mechanics methods. Bouchet and Venaille in their review paper [33] summarize the important statistical mechanics and thermodynamics concepts used in the study of turbulence self-organization. Statistical equilibria are predicted as the final state (after long time evolution of complex turbulent flows). They compare quantitative models based on these statistical equilibria to observations. As statistical methods are outside the scope of this thesis, I do not give a further introduction here, but rather refers the interested readers to the review paper.

We also note that the minimum enstrophy state may not be precisely the

same as the self-organized state, on account of the dissipation, external drive, and boundary conditions of the system. Therefore, we also approach the problem using symmetry principles of some self-organized state. Self-organization is often found in dissipative nonlinear systems, in which instability can occur to dissipate the free energy source, and sometimes triggers an avalanche-like dissipation event above some threshold level. Nonlinear energy dissipation processes are observed in diverse fields: from geophysics, plasma physics, astrophysics, to sociology and neurobiology, even to natural events like earthquakes and snow avalanches. One common property of nonlinear energy dissipation processes is evolution toward complexity, characterized by a combination of feedback loops (positive and negative), self-production, self-reference, recycling of matter, and etc. A theory which explains the nonlinear energy dissipation processes is the self-organized criticality (SOC) theory. It was first developed by Bak et al. [34, 35] for cellular automaton models, and has been applied to tokamak plasma self-organization (see e.g., [36]). In this thesis, we study the general form of PV flux near a SOC state. When the PV profile deviates from that of the SOC state, the system tends to regulate itself and relax back to the SOC state. The deviation drives the PV flux. The dynamics of self-organization is complex. However, the underlying symmetries of the problem allows us to construct a possible general form for the PV flux.

SOC is often described in terms of sand pile dynamics, because the robustness of SOC is similar to a critical slope of a sandpile, which is maintained when new sand grains are dropped to the pile. Avalanches occur when the local slope exceeds certain criticality. The SOC dynamics is a subject of intensive theoretical and computational investigation, but is beyond the scope of this thesis. We simply consider a SOC state, or a state very close to SOC state, as the output of the long time evolution of a complex turbulence-zonal flow system. Then we can can use simple symmetry principles to constrain the form of fluxes, employing ideas from SOC in models of running sand piles [37]. We derive a form of PV flux by asking *what form must the form of the PV flux in a "PV-sandpile" have so as to satisfy the joint reflection symmetry principle?*

1.5 Organization of the thesis

In this thesis, we describe the general theory of anisotropic flow formation in quasi two-dimensional turbulence from the perspective of PV transport in real space. The aim is to calculate the spatial PV flux, and so to develop a vorticity or momentum transport operator, for use in modelling codes. Chapter 2 and Chapter 3 form a complete study of calculating PV Flux. The general structure of the PV flux is deduced non-perturbatively in Chapter 2 and then the transport coefficients are calculated perturbatively in Chapter 3. Chapter 4 is a separate work considering the effect of mean shear flows on zonal flow generation. An overview of each chapter follows:

In Chapter 2, the general structure of PV flux is deduced non-perturbatively using two relaxation models: the first is a mean field theory for the dynamics of minimum enstrophy relaxation based on the requirement that the mean flux of PV dissipates total potential enstrophy but conserves total fluid kinetic energy. The analyses show that the structure of the PV flux has the form of a sum of a positive definite hyper-viscous and a viscous flux of PV. Turbulence spreading is shown to be related to PV mixing via the link of turbulence energy flux to PV flux. In the relaxed state, the ratio of the PV gradient to zonal flow velocity is homogenized. This structure of the relaxed state is consistent with PV staircases. The homogenized quantity sets a constraint on the amplitudes of PV and zonal flow in the relaxed state. The second relaxation model is derived from a joint reflection symmetry principle, which constrains the PV flux driven by the deviation from the self-organized state. The form of PV flux contains a nonlinear convective term in addition to the viscous and hyper-viscous terms. The nonlinear convective term, however, can be viewed as a generalized diffusion, on account of the gradient-dependent ballistic transport in avalanche-like systems.

In Chapter 3, the detailed transport coefficients are calculated using perturbation theory. For a broad turbulence spectrum, a modulational calculation of the PV flux gives both a negative viscosity and a positive hyper-viscosity. For a narrow turbulence spectrum, the result of a parametric instability analysis shows that PV transport is also convective.

In Chapter 4, the effect of mean shear flows on zonal flow formation is considered. The generation of zonal flows by modulational instability in the presence of large-scale mean shear flows is studied using the method of characteristics as applied to the wave kinetic equation. It is shown that mean shear flows reduce the modulational instability growth rate by shortening the coherency time of the wave spectrum with the zonal shear. The scalings of zonal flow growth rate and turbulent vorticity flux with mean shear are determined in the strong shear limit.

Chapter 5 summarized the results of the thesis and gives future directions.

Chapter 2

Mean Field Theory of Turbulent Relaxation and Vorticity Transport

2.1 Introduction

The formation of large-scale shearing structures due to momentum transport–i.e., zonal flow formation–is a common feature of both geostrophic fluids and magnetically confined plasmas (e.g., [38, 1, 14, 39, 40]). We study the dynamics of structure formation from the perspective of potential vorticity (PV) transport in real space. The reason that PV mixing is the key element of zonal flow formation is that PV conservation is the fundamental freezing-in law constraint on zonal flow generation by inhomogeneous PV mixing. Note that since zonal flows are elongated, asymmetric vortex modes, translation symmetry in the direction of the flow and inhomogeneity across the direction of the flow are essential to zonal flow formation. The importance of PV mixing to the zonal flow problem is clearly seen via the Taylor identity, which states that the cross-flow flux of PV equals the along-flow component of the Reynolds force, which drives the flow. PV mixing is related to disparate-scale interaction between two classes of fluctuations, namely turbulence and waves, and zonal flows. Most of the theoretical calculations of PV

flux for zonal flow generation are perturbative analyses and focus on the stability of ambient wave spectrum to a seed zonal flow [41, 42]. These types of analyses are, however, valid only in the initial stage of zonal flow formation. Therefore, there is a need to develop a mean field theory based on general, structural principles, and not limited by perturbative methods. Here, we examine and compare two approaches to the question of how to obtain the general form of the PV flux: the selective decay hypothesis and the joint reflection symmetry principle.

In the first approach, we study the dynamics of the PV flux during a selective decay process toward a minimum enstrophy state. The relaxed state of a high Reynolds number, turbulent, two-dimensional fluid is thought to be one of minimum potential enstrophy, for given conserved kinetic energy. This hypothesis constitutes the minimum enstrophy principle of Bretherton and Haidvogel [29]. Their variational argument is based on the concept of selective decay, which is in turn based on the dual cascade in two-dimensional turbulence. In two-dimensional turbulence, kinetic energy inverse cascades to large, weakly dissipated spatial scales, whereas enstrophy forward cascades to small spatial scales and there is viscously damped. In the presence of weak dissipation, total kinetic energy is thus approximately conserved relative to total enstrophy, which is dissipated. In this scenario, the system evolves toward a state of a minimum enstrophy. Interestingly, the theory does not specify that the minimum enstrophy is actually achieved in the relaxed state. The theory predicts the structure of the flow in the end state; however, it gives no insight into the all-important question of how the mean profiles evolve during the relaxation process. Here, we discuss the *dynamics* of minimum enstrophy relaxation, which leads to zonal flow formation. In particular, since inhomogeneous potential vorticity (PV) mixing is the fundamental mechanism of zonal flow formation, we ask *what form must the mean field PV flux have so as to dissipate enstrophy while conserving energy*?

We derive a mean field theory for the PV flux during minimum enstrophy relaxation. We show that the structure of the PV flux which dissipates enstrophy is not Fickian diffusion of PV; rather it is $\Gamma_q = \langle v_x \rangle^{-1} \nabla \left[\mu \nabla \left(\nabla \langle q \rangle / \langle v_x \rangle \right) \right]$ where the proportionality coefficient μ is a function of zonal velocity. In other words,

PV flux is a form involving viscosity and hyper-viscosity, with flow-dependent transport coefficients. Among the possible forms of PV flux which can minimize enstrophy while conserving energy, we consider the simplest, smoothest solution in this thesis. *We show that in the relaxed state, the ratio between PV gradient and zonal flow is homogenized.* Interestingly, this proportionality relationship between PV gradient and zonal flow is observed in PV staircases.

Turbulence spreading [43, 44, 45] is closely related to PV mixing because the transport of turbulence intensity, namely fluctuation energy or potential enstrophy, has influence on Reynolds stresses and flow dynamics. The momentum theorems for the zonal flow in Rossby/drift wave turbulence [46] link turbulent flux of potential enstrophy density to zonal flow momentum and turbulence pseudomomentum, along with the driving flux and dissipation. Here, note that the pseudomomentum, or wave momentum density, is defined as $-\langle\tilde{q}^2\rangle/2(\partial_y\langle q\rangle)$ for a quasi-geostrophic system, and so is proportional to the wave action density in the weakly nonlinear limit. In this work, turbulence spreading is linked to PV mixing via the relation of energy flux to PV flux. The turbulent flux of kinetic energy density during minimum enstrophy relaxation is shown to be proportional to the gradient of the (ultimately homogenized) quantity, which is the ratio of PV gradient to the zonal flow. A possible explanation of up-gradient transport of PV due to turbulence spreading–which is based on the connection between PV mixing and turbulence spreading–is discussed in the last section.

The structural approach of the minimum enstrophy relaxation model exploits ideas from the study of relaxation dynamics in three-dimensional magnetohydrodynamic (MHD), given the analogy between minimum enstrophy relaxation in two-dimensional turbulence and Taylor relaxation [47] in three-dimensional MHD turbulence. In Taylor relaxation, magnetic energy is minimized subject to the constraint of conservation of global magnetic helicity. Taylor's conjecture is based on the concept of selective decay and the assumption of magnetic field line stochasticity during turbulent relaxation. In 3D MHD turbulence, energy forward cascades to small scales, while magnetic helicity inverse cascades to large scales. Thus, energy is dissipated, while magnetic helicity is rugged. The flux tube which is

most rugged on the longest time scales is the tube which contains the entire system, resulting from the stochasticity of field lines. The relaxed state of the Taylor process is a force free magnetic field configuration. The parallel current profile in the Taylor state is homogenized, so there is no available free energy in the current gradient. The related criteria for stability of the magnetostatic equilibrium of an arbitrarily prescribed topology during magnetic relaxation in a perfectly conducting fluid are further discussed by Moffatt [48]. The Taylor hypothesis is successful in predicting the magnetic field configuration of some laboratory plasmas and astrophysical plasmas. However, as for the minimum enstrophy principle, Taylor relaxation theory does not address the dynamics of the relaxation, which is characterized by the helicity density flux. Boozer [49] argues that the simplest form of helicity density flux which dissipates magnetic energy is that of diffusion of current or 'hyper-resistivity'–hyper-diffusion of magnetic helicity. The dynamical model of Taylor relaxation and helicity transport was developed further by Diamond & Malkov [50] using more general symmetry considerations than Boozer's. In particular, they use the joint reflection symmetry principle [37] to show that the current profile on mesoscales evolves according to a Burgers equation, suggesting that the helicity transport is non-diffusive and intermittent during Taylor relaxation. In particular, a $1/f$ spectrum of helicity 'transport events' or 'avalanches', is predicted.

In the second approach, we follow Diamond and Malkov and derive a simple 'PV-avalanche' model of the dynamics of turbulent relaxation of the excursion from the self-organized profile using symmetry principles alone. We ask *what form must the form of the PV flux have so as to satisfy the joint reflection symmetry principle?* The result is a sum of a viscous, a hyper-viscous, and a convective transport of PV. The PV equation has the same structure as the Kuramoto-Sivashinsky equation, which is known for its negative diffusion (large-scale instability) and higher-order stabilizing diffusion (small-scale damping). Comparing the minimum enstrophy model and the PV-avalanche model, we find that the structure of viscous and hyper-viscous transport of PV appears in both models, while the convective transport of PV, which suggests intermittent PV transport during turbulence self-

organization, is only found in the PV-avalanche analysis. Nevertheless, we note that the nonlinear convective term of the PV flux can be viewed as a generalized diffusion, on account of the gradient-dependent ballistic transport in avalanche-like systems.

We note that the minimum enstrophy state may not be precisely the same as the self-organized state, on account of the dissipation, external drive, and boundary conditions of the system. We also note that selective decay is a *hypothesis* based on the observation of the dual cascade in two-dimensional turbulence, and is not derived from first physical principles. There are relaxed states derived from more fundamental principles, namely, statistical equilibrium states and stable stationary states (see, e.g., Ref. [51] and [33]). However, the minimum enstrophy principle is a plausible and demonstrably useful guide, which gives us predictions of the structure of PV and flows, and the enstrophy level in the relaxed state. The selective decay principles can and have been applied in a number of areas of physics, such as MHD and geophysics. Selective decay hypotheses have been supported by a number of computational studies (e.g., Ref. [52] and [53]) and experimental studies (e.g., successful prediction of the magnetic configuration of reversed field pinch plasmas). The minimum enstrophy state is a subclass of stable states. When there is no external forcing and dissipation, the minimum enstrophy state is one of the possible attractors. In the presence of viscous damping, the minimum enstrophy state is the attractor of the system. However, when the viscosity approaches zero, the system may be trapped in long-lived quasistationary states while relaxing to equilibrium, like many other long-range interacting systems. Thus, the time scale of convergence needs to be considered carefully to determine the relevancy of the minimum enstrophy model to inertial time scales. The final state is determined by the balance between free relaxation and forcing. Determining the exact ultimate state for any particular system is an extremely difficult question and is beyond the scope of this work.

The rest of the chapter is organized as follows. Section 2.2 presents the non-perturbative analyses of PV flux, including the use of the minimum enstrophy principle in 2.2.1, and the joint reflection symmetry principle in 2.2.2. The

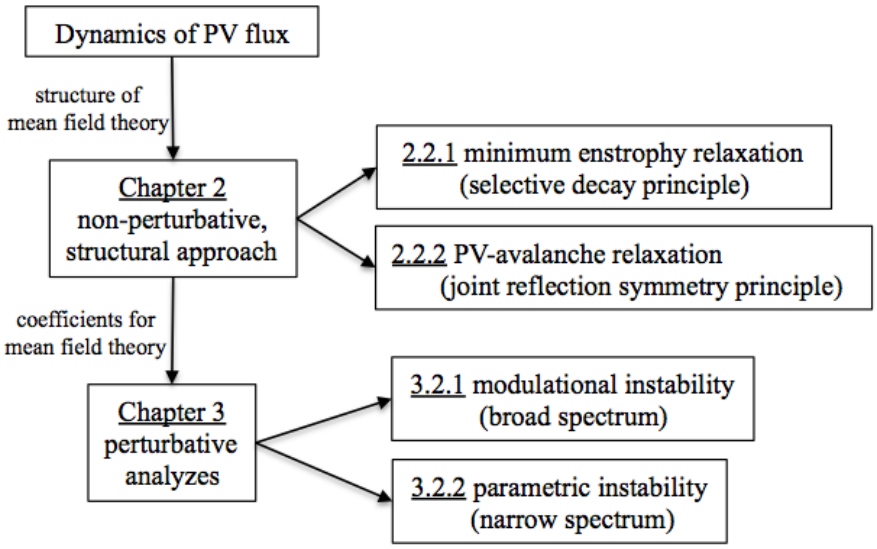

Figure 2.1: Flowchart for the paper.

discussion, synthesis and conclusions are given in section 2.3. In the next chapter, momentum transport coefficients are derived via perturbation theory, including modulational instability in 3.2.1 and parametric instability in 3.2.2. The structure of Chapter 2 and Chapter 3 is illustrated in the flowchart of Fig (2.1).

2.2 Deducing the form of the potential vorticity flux from non-perturbative analyses

2.2.1 Minimum enstrophy principle

We approach the question of the dynamics of momentum transport in 2D turbulence by asking what the form of PV flux must be to dissipate enstrophy but conserve energy. We start with the conservative PV evolution equation

$$\partial_t q + v \cdot \nabla q = \nu_0 \nabla^2 q, \tag{2.1}$$

where ν_0 is molecular viscosity. Equation (2.1) states PV as a material invariant and so applies to many quasi-2D systems, including, but not limited to, the following two systems. In 2D quasigeostrophic turbulence [1], the PV and velocity fields

are $q = \nabla^2\psi + \beta y$ and $(v_x, v_y) = (-\partial\psi/\partial y, \partial\psi/\partial x)$, where ψ is the streamfunction and β is the latitudinal gradient of the Coriolis parameter. In drift wave turbulence [**?**], the PV is $q = n - \nabla^2\phi$, where n is the ion density and the Laplacian of the electrostatic potential ϕ is the ion vorticity due to $\boldsymbol{E} \times \boldsymbol{B}$ drift. In this paper we use the coordinates of a 2D geostrophic system; the x-axis is in the zonal direction, the direction of symmetry (the poloidal direction in tokamaks), and the y-axis is in the meridional direction, the direction of anisotropy (the radial direction in tokamaks). Periodic boundary conditions in the $\hat{x}$ direction are imposed. Writing the nonlinear term, which is the divergence of the PV flux, as N,

$$N \equiv -\nabla \cdot (\boldsymbol{v}q), \tag{2.2}$$

we average equation (2.1) over the zonal direction to get the mean field equation for PV

$$\partial_t \langle q \rangle = \langle N \rangle + \nu_0 \partial_y^2 \langle q \rangle. \tag{2.3}$$

The selective decay hypothesis states that 2D turbulence relaxes to a minimum enstrophy state. During relaxation, the enstrophy forward cascades to smaller and smaller scales until it is dissipated by viscosity. Thus the total potential enstrophy

$$\Omega = \frac{1}{2} \int q^2 \, dxdy \tag{2.4}$$

must decrease with time. On the other hand, the kinetic energy inverse cascades to large scales and sees negligible or weak coupling to viscous dissipation, as compared to the enstrophy. Only scale invariant frictional drag can damp flow energy at large scales. The rate of large scale energy drag is much slower than the rate of small scale enstrophy dissipation. Thus the total kinetic energy

$$E = \frac{1}{2} \int (\nabla\psi)^2 \, dxdy \tag{2.5}$$

should remain invariant on the characteristic enstrophy dissipation time. Note that the total energy of some systems consists of kinetic, potential, and internal energies, but only the kinetic energy is conserved in the minimum enstrophy hypothesis. This is because the nonadiabatic internal energy (i.e. $\sim \langle (\tilde{n}/n - e\tilde{\phi}/T)^2 \rangle$ for drift

wave turbulence) forward cascades to dissipation [54]. The evolution of the total kinetic energy is given by

$$\partial_t E = -\int \psi \partial_t (\partial_x^2 + \partial_y^2)\psi \; dxdy + \int \partial_x \left(\psi \partial_t \partial_x \psi\right) dxdy + \int \partial_y \left(\psi \partial_t \partial_y \psi\right) dxdy. \quad (2.6)$$

The second term of equation (2.6) vanishes because of the periodic boundary condition in $\hat{x}$ direction, and the third term is dropped due to the condition of zero stream function or zero zonal flow at the $\pm y_0$ boundaries, $\langle \psi \partial_y \psi \rangle|_{\pm y_0} = 0$. Therefore, conservation of the total kinetic energy (apart from feeble collisional dissipation) in mean field theory gives

$$\partial_t E = -\int \langle \psi \rangle \partial_t \langle q \rangle \; dxdy = -\int \langle \psi \rangle \langle N \rangle \; dxdy = -\int \partial_y \Gamma_E dxdy, \quad (2.7)$$

where $\langle \, \rangle$ is the zonal average, and the energy density flux Γ_E is defined as $\langle v_y \frac{(\nabla \psi)^2}{2} \rangle$. Thus, the nonlinear term is necessarily tied to the energy flux by

$$\langle N \rangle = \langle \psi \rangle^{-1} \partial_y \Gamma_E. \quad (2.8)$$

The form of the energy density flux is constrained by the requirement of decay of total potential enstrophy, i.e., by the demand that

$$\partial_t \Omega = \int \langle q \rangle \langle N \rangle dxdy = \int \langle q \rangle \langle \psi \rangle^{-1} \partial_y \Gamma_E \; dxdy < 0. \quad (2.9)$$

Noting that the energy flux vanishes at the $\pm y_0$ boundaries, (i.e. $\Gamma_E|_{\pm y_0}$=0), and so equation (2.9) becomes

$$\partial_t \Omega = -\int \Gamma_E \; \partial_y \left(\langle q \rangle \langle \psi \rangle^{-1} \right) dxdy < 0, \quad (2.10)$$

which in turn forces

$$\Gamma_E = \nu \partial_y \left(\langle q \rangle \langle \psi \rangle^{-1} \right). \quad (2.11)$$

It is worthwhile mentioning here that a finite flux at the boundary would contribute a surface integral term to the total enstrophy evolution. PV relaxation at the point y would then become explicitly dependent upon fluxes at the boundary, thus rendering the mean field theory manifestly non-local. We therefore see this as an important topic for future research. The simplest solution for Γ_E is for it to be directly proportional to $\partial_y \left(\langle q \rangle \langle \psi \rangle^{-1} \right)$, with a positive proportionality parameter

ν. The obvious requisite dependence on turbulence intensity is contained in ν. In this mean field theory, ν is not determined. Note that any odd derivate of $\langle q\rangle\langle\psi\rangle^{-1}$ or any combination of an odd derivative of $\langle q\rangle\langle\psi\rangle^{-1}$ and an even power of $\langle q\rangle$ or $\langle v_x\rangle$ will contribute a term which dissipates enstrophy. For example, $\Gamma_E = \nu\langle q\rangle^2\partial_y\left(\langle q\rangle\langle\psi\rangle^{-1}\right) + \partial_y^5\left(\langle q\rangle\langle\psi\rangle^{-1}\right)$ also gives $\partial_t\Omega < 0$. Thus, the solution we present here is the smoothest (i.e., dominant in long wavelength limit), and lowest order (i.e., not combined with any higher power of $\langle q\rangle^2$ or $\langle v_x\rangle^2$). The reasons we study the simplest solution are: 1) the smoothest solution reveals the leading behavior of the PV flux on large scale. This is relevant to our concern with the large-scale flow dynamics. The higher order derivatives should be included to study the relaxation dynamics at smaller scales and the finer scale structure of the shear flow. 2) The dependence of PV flux on the higher order powers of the shear flow intensity can be absorbed into ν. The nonlinear term and the PV equation are then given by the simplest, leading form of Γ_E:

$$\langle N\rangle = \langle\psi\rangle^{-1}\partial_y\left[\nu\partial_y\left(\langle q\rangle\langle\psi\rangle^{-1}\right)\right] \tag{2.12}$$

and

$$\partial_t\langle q\rangle = \nu_0\partial_y^2\langle q\rangle + \langle\psi\rangle^{-1}\partial_y\left[\nu\partial_y\left(\langle q\rangle\langle\psi\rangle^{-1}\right)\right]. \tag{2.13}$$

The system evolves to the relaxed state, $\partial_t\langle q\rangle = 0$, when $\langle q\rangle\langle\psi\rangle^{-1}$ approaches a constant, i.e. $\partial_y(\langle q\rangle\langle\psi\rangle^{-1}) = 0$, where the nonlinear term is annihilated and the mean PV flux vanishes. This is consistent with the results from calculus of variations, in which the enstrophy is minimized at constant energy, so

$$\begin{aligned}\delta\Omega + \lambda\delta E &= \int q\delta(\nabla^2\psi)\; dxdy + \lambda\int\nabla\psi\cdot\nabla\delta\psi\; dxdy \\ &= \int(q-\lambda\psi)\nabla^2\delta\psi\; dxdy\end{aligned} \tag{2.14}$$

is required to vanish. Here $\langle q\rangle\langle\psi\rangle^{-1}$ is equal to the Lagrange multiplier λ. In the relaxed state, PV is constant along streamlines and so the nonlinear term $v\cdot\nabla q$ is annihilated.

Since what we seek is the structure of the PV flux, we prefer to maintain the form of the nonlinear term in the mean PV evolution as an explicit divergence of a PV flux, i.e., now take

$$\langle N\rangle = \langle-\nabla\cdot(\boldsymbol{v}q)\rangle = -\partial_y\Gamma_q, \tag{2.15}$$

where Γ_q is the PV flux in the direction of inhomogeneity, $\hat{y}$. We repeat the minimum enstrophy analysis as before. Starting with mean field PV equation:

$$\partial_t \langle q \rangle = -\partial_y \Gamma_q + \nu_0 \partial_y^2 \langle q \rangle, \tag{2.16}$$

conservation of total kinetic energy (with the boundary condition of $\Gamma_q|_{\pm y_0} = 0$),

$$\partial_t E = \int \langle \psi \rangle \partial_y \Gamma_q dx dy = -\int \partial_y \langle \psi \rangle \Gamma_q dx dy = -\int \partial_y \Gamma_E dx dy, \tag{2.17}$$

relates PV flux to energy flux by

$$\Gamma_q = (\partial_y \langle \psi \rangle)^{-1} \partial_y \Gamma_E. \tag{2.18}$$

The connection between PV flux and energy flux has direct implication for turbulence spreading, which we discuss later in this paper. We then derive the energy flux from the constraint of the dissipation of potential enstrophy (with the boundary condition of $\Gamma_E|_{\pm y_0} = 0$),

$$\partial_t \Omega = -\int \langle q \rangle \partial_y \Gamma_q dx dy = -\int \partial_y \left[(\partial_y \langle \psi \rangle)^{-1} \partial_y \langle q \rangle \right] \Gamma_E \; dx dy < 0, \tag{2.19}$$

so the simplest, smoothest solution of Γ_E is directly proportional to $\partial_y \left[(\partial_y \langle \psi \rangle)^{-1} \partial_y \langle q \rangle \right]$, with a positive proportionality parameter μ. We therefore find the form of PV flux to be:

$$\begin{aligned} \Gamma_q &= (\partial_y \langle \psi \rangle)^{-1} \partial_y \left[\mu \partial_y \left((\partial_y \langle \psi \rangle)^{-1} \partial_y \langle q \rangle \right) \right] \\ &= \langle v_x \rangle^{-1} \partial_y \left[\mu \left(\langle v_x \rangle^{-2} \langle q \rangle \partial_y \langle q \rangle + \langle v_x \rangle^{-1} \partial_y^2 \langle q \rangle \right) \right]. \end{aligned} \tag{2.20}$$

The relaxed state is achieved when $(\partial_y \langle \psi \rangle)^{-1} \partial_y \langle q \rangle$ is constant. The difference between the results of N and $\partial_y \Gamma_q$ formulations comes from the treatment of derivatives in the nonlinear term, i.e. taking $N = -\partial_y \Gamma_q$, as we can see clearly from the homogenized quantities in the two approaches, $\langle \psi \rangle^{-1} \langle q \rangle$ and $(\partial_y \langle \psi \rangle)^{-1} \partial_y \langle q \rangle$. The derivative of equation $\langle q \rangle = \lambda \langle \psi \rangle$, from the N approach, gives the equation $\partial_y \langle q \rangle = \lambda \partial_y \langle \psi \rangle$, obtained from the Γ_q approach. Thus, the two solutions are consistent. The $\partial_y \Gamma_q$ formulation is more accurate, since it starts with a more precise form of the nonlinear term in PV equation. Γ_q is smoother than N, and hence better satisfies the conditions of the mean-field approximation that the fluctuations

around the average value be small, so that terms quadratic in the fluctuations can be neglected. Moreover, while the stream function ψ is unique up to an arbitrary constant, the absolute value of its derivative $\partial_y\psi = -v_x$ has a clear physical meaning. Therefore, we consider the outcome from the $\partial_y\Gamma_q$ approach to be the primary result. The following discussion is based primarily on equation (2.20).

The structure of the PV flux in equation (2.20) contains both hyper-diffusive and diffusive terms. The mean PV evolution,

$$\partial_t\langle q\rangle = -\partial_y\left[\frac{1}{\partial_y\langle\psi\rangle}\partial_y\left[\mu\partial_y\left(\frac{\partial_y\langle q\rangle}{\partial_y\langle\psi\rangle}\right)\right]\right] + \nu_0\partial_y^2\langle q\rangle, \tag{2.21}$$

shows that hyper-viscosity is the leading high k_y dependence and so it controls the small scales. From equation (2.21) we can also prove that hyper-viscosity term damps the energy of the mean zonal flow:

$$\partial_t(\partial_y\langle v_x\rangle)^2 = \partial_t\langle q\rangle^2 = -\frac{2\mu}{\partial_y\langle\psi\rangle}\left(\frac{\langle q\rangle\partial_y^4\langle q\rangle}{\partial_y\langle\psi\rangle}\right) + \text{ non hyper-viscosity terms}, \tag{2.22}$$

and

$$-\int\frac{\mu}{\partial_y\langle\psi\rangle}\left(\frac{\langle q\rangle\partial_y^4\langle q\rangle}{\partial_y\langle\psi\rangle}\right)dxdy = -\int\mu\left(\frac{\partial_y^2\langle q\rangle}{\partial_y\langle\psi\rangle}\right)^2 dxdy < 0. \tag{2.23}$$

Therefore, the hyper-viscosity represents the nonlinear saturation mechanism of zonal flow growth and partially defines the scale dependence of turbulent momentum flux. The other important implication of equation (2.20) is that the PV flux is explicitly zonal flow-dependent. The zonal velocity appears in the denominators of hyper-viscosity and viscosity terms, as well as the diffusion coefficient; this is not seen in perturbative analyses (e.g., Ref. [41, 42]). We emphasize that within the mean field approach, the selective decay analysis for the PV flux in this work is entirely non-perturbative and contains no assumption about turbulence magnitude.

The prediction of the homogenization of $(\partial_y\langle\psi\rangle)^{-1}\partial_y\langle q\rangle$ in minimum enstrophy relaxation is a new result. It states explicitly that zonal flows track the PV gradient in the relaxed state, i.e., strong zonal flows are localized to the regions of larger PV gradient. The trend is realized in the PV staircase, where strong jets produced by inhomogeneous PV mixing peak at PV jump discontinuities [24]. The jet pattern of the $\boldsymbol{E}\times\boldsymbol{B}$ staircase is also observed in plasma simulations [3].

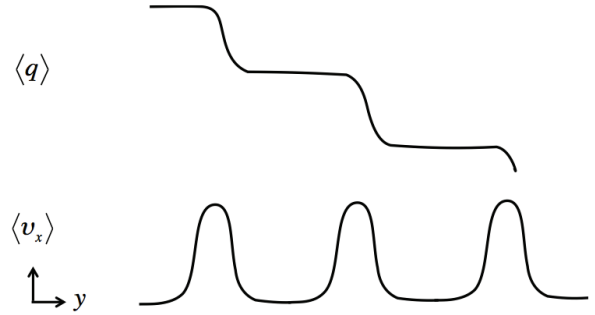

Figure 2.2: PV staircase.

Figure (2.2) shows a cartoon of the PV staircase. Strong zonal flows are located around 'the edges of PV steps.' We can write the PV gradient as

$$\partial_y \langle q \rangle = \sum_i a_i f(y - y_i), \tag{2.24}$$

where a_i are constants and f is a function peaked at y_i. f can be approximated as a delta function in the limit of a step profile. Since $\partial_y \langle q \rangle / \langle v_x \rangle$ is a constant, the zonal flow must have the same spatial profile as the PV gradient, i.e.

$$\langle v_x \rangle = \sum_i b_i f(y - y_i), \tag{2.25}$$

where $b_i = -\lambda a_i$. While the prediction of the form of the function $f(y - y_i)$ is beyond the scope of this work, the constant proportionality between a_i and b_i reconciles the highly structured profiles of the staircase with the homogenization or mixing process required to produce it. In a related vein, both $\partial_y \langle q \rangle$ and $\partial_y \langle \psi \rangle$ can each be large and variable, though the ratio is constrained. The observation that the structural analysis of selective decay can lead to an end state with a PV staircase-like structure suggests that the staircase may arise naturally as a consequence of minimum enstrophy relaxation. The result also demonstrates the impact of inhomogeneous PV mixing in minimum enstrophy relaxation.

One can define a characteristic scale from the proportionality between PV gradient and zonal flow velocity, i.e.

$$l_c = \left| \frac{\partial_y \langle q \rangle}{\langle v_x \rangle} \right|^{-1/2}. \tag{2.26}$$

In minimum enstrophy state, $l_c = |\lambda|^{-1/2}$ and PV flux can vanish on scale l_c. As a result, l_c characterizes the scale at which the terms in the PV flux can compete and cancel. For scales smaller than l_c, hyper-viscosity dominates and damping wins. For scales larger than l_c, effective viscosity dominates. Since effective viscosity can be negative, growth can occur for $l > l_c$. It is interesting to compare l_c with the Rhines scale [55] $l_R \sim (\partial_y \langle q \rangle / \tilde{v}_{rms})^{-1/2}$, where $\tilde{v}_{rms}$ is the root-mean-square velocity at the energy containing scales. The question of which velocity should really be used to calculate the Rhines Scale is still being debated (see, e.g. Ref. [56] and [57]). l_c and l_R both depend on the gradient of the mean field PV; what distinguishes them is that l_c is determined by mean zonal velocity while l_R is set by fluctuation velocity. The characteristic scale and Rhines scale become indistinguishable when $\tilde{v}_{rms}$ reaches the level of zonal flow velocity.

PV mixing in minimum enstrophy relaxation is also related to turbulence spreading, since we can see from equation (2.18) that Γ_E and Γ_q are related. Γ_E and Γ_q are the spatial flux of kinetic energy density and PV in the direction of inhomogeneity. Since there is no mean flow in the direction of inhomogeneity, Γ_E represents the effective spreading flux of turbulence kinetic energy and is given by

$$\Gamma_E = -\int \Gamma_q \langle v_x \rangle dy = -\int \frac{1}{\langle v_x \rangle} \partial_y \left[\mu \partial_y \left(\frac{\partial_y \langle q \rangle}{\langle v_x \rangle} \right) \right] \langle v_x \rangle dy = \mu \partial_y \left(\frac{\partial_y \langle q \rangle}{\langle v_x \rangle} \right). \quad (2.27)$$

Equation (2.27) shows that the gradient of the homogenized quantity, $\partial_y \left(\partial_y \langle q \rangle / \langle v_x \rangle \right)$, drives spreading, too. Indeed, we see that the spreading flux vanishes when $\partial_y \langle q \rangle / \langle v_x \rangle$ is homogenized. It is known that inhomogeneous turbulence has tendency to relax its intensity gradients through turbulent transport in space. We show that inhomogeneous turbulence during minimum enstrophy relaxation tends to homogenize the gradient of $\partial_y \langle q \rangle / \langle v_x \rangle$ through turbulent transport of momentum (PV mixing) and energy (turbulence spreading). The dependence of Γ_E on zonal flow follows from the fact that turbulence spreading is a mesoscale transport process. Note that the step size of the PV staircase, which corresponds to the distance between zonal flow layers, is also mesoscale. Both observations suggest that the relaxation process is a non-local phenomena. This is a necessary consequence of PV inversion, i.e. the relation $\nabla^2 \psi + \beta y = q$, so that $\langle v_x \rangle$ is an integral of the $q(y)$ profile. Thus Γ_E and Γ_q are in fact non-local in $q(y)$.

An expression for the relaxation rate can be derived by linear perturbation theory about the minimum enstrophy state. We write $\langle q\rangle = q_m(y)+\delta q(y,t), \langle\psi\rangle = \psi_m(y) + \delta\psi(y,t)$ and use the homogenization condition in relaxed state $\partial_y q_m = \lambda\partial_y\psi_m$. Assuming $\delta q(y,t) = \delta q_0 \exp(-\gamma_{rel}t - i\omega t + iky)$, the relaxation rate is found to be

$$\begin{aligned} \gamma_{rel} &= \mu\left(\frac{k^4+4\lambda k^2+3\lambda^2}{\langle v_x\rangle^2} - \frac{8q_m^2(k^2+\lambda)}{\langle v_x\rangle^4}\right) \\ \omega &= \mu\left(-\frac{4q_m k^3+10q_m k\lambda}{\langle v_x\rangle^3} + \frac{8q_m^3 k}{\langle v_x\rangle^5}\right). \end{aligned} \tag{2.28}$$

The condition of relaxation–i.e., that modes are damped–requires positive γ_{rel}:

$$k^2 > \frac{8q_m^2}{\langle v_x\rangle^2} - 3\lambda, \tag{2.29}$$

i.e., perturbation scales smaller than $(8q_m^2/\langle v_x\rangle^2 + 3\ \partial_y q_m/\langle v_x\rangle)^{-1/2}$. $k^2 > 0$ relates q_m to λ and $\langle v_x\rangle$ by

$$\frac{8q_m^2}{\langle v_x\rangle^2} > 3\lambda. \tag{2.30}$$

Equation (2.30) shows that zonal flow cannot grow arbitrarily large, and is constrained by the potential enstrophy density and scale parameter λ. It also shows that a critical residual enstrophy density q_m^2 is needed in the minimum enstrophy state, so as to sustain a zonal flow of a certain level. Equation (2.30) specifies the 'minimum enstrophy' of relaxation. Therefore, we not only obtain the structure of the end state, which is expressed in terms of λ, the constant of proportionality between PV gradient and zonal flow velocity, but we also observe that potential enstrophy intensity and zonal flow strength are ultimately related in the relaxed state. It is interesting to note that the PV evolves like a damped oscillator near the relaxed state.

2.2.2 Symmetry principles

We have derived the form of PV flux using the minimum enstrophy principle. In this subsection, we look at the problem using more general considerations–namely flux symmetry principles. We discuss the general form of PV flux near a self-organized state, which is not specified. When the PV profile $q(y)$ deviates

from that of the self-organized state $q_0(y)$, the system tends to regulate itself and relax to the self-organized state. Note that the self-organized state may not be precisely the same as the minimum enstrophy state, taking account of the dissipation, external drive, and boundary conditions of the system. We view the relaxation to a self-organized state as similar to relaxation of a running sandpile [37] and consider local PV as analogous to the local sand grain density. Then the deviation of the local PV profile from the self-organized state $\delta q(y) = q(y) - q_0(y)$ drives the PV flux. The dynamics of self-organization is complex. However, the underlying symmetries of the problem allows us to construct a possible general form for the PV flux.

Due to the conservation of PV, δq evolves according to

$$\partial_t \delta q + \partial_y \Gamma[\delta q] = \nu_0 \partial_y^2 \delta q + s, \tag{2.31}$$

where $\Gamma[\delta q]$ is the flux of δq and s represents the external sources and sinks. We assume that the dynamics of the relaxation process to the self-organized state is similar to the running sandpile models of Hwa & Kardar [37], Diamond & Hahm [36], and Diamond & Malkov [50], i.e., the excesses beyond the self-organized profile ($\delta q > 0$) move down the local PV gradient while voids ($\delta q < 0$) move up the gradient as illustrated in Fig. 2.3. Therefore, the form of $\Gamma[\delta q]$ is invariant under $y \to -y$ and $\delta q \to -\delta q$. The general form of $\Gamma[\delta q]$ which satisfies this symmetry constraint is given by

$$\Gamma[\delta q] = \sum_l \alpha_l (\delta q)^{2l} + \sum_m \beta_m \left(\partial_y \delta q\right)^m + \sum_n \gamma_n \left(\partial_y^3 \delta q\right)^n + ... \tag{2.32}$$

We are interested in the large-scale properties of the system, so higher-order spatial derivatives are neglected. Assuming the deviations to be small, we also drop the higher-order terms in δq. Thus, the simplest approximation becomes

$$\Gamma[\delta q] = \frac{\alpha}{2}(\delta q)^2 + \beta \partial_y \delta q + \gamma \partial_y^3 \delta q, \tag{2.33}$$

and δq evolves according to

$$\partial_t \delta q + \alpha \delta q \partial_y \delta q + \beta \partial_y^2 \delta q + \gamma \partial_y^4 \delta q = 0. \tag{2.34}$$

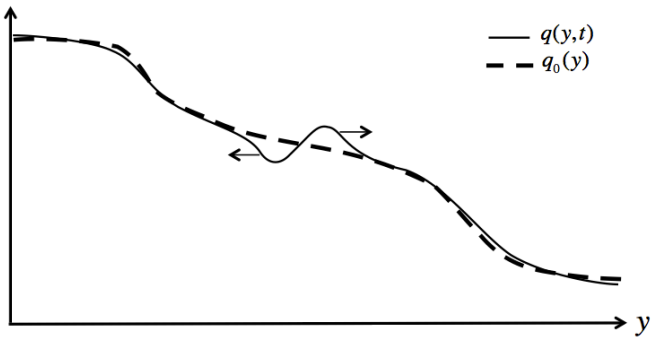

Figure 2.3: Positive deviation of the local PV from the self-organized profile q_0 moves down the slope while negative deviation moves up the gradient.

The transport parameters α, β, γ are not determined by this analysis. Similar to the PV flux derived from the minimum enstrophy analysis, the structure of the PV flux in equation (2.33) contains a diffusive term and a hyper-diffusive term. However, equation (2.33) has another piece–a nonlinear convective term. Since the symmetry principle is more general than the minimum enstrophy principle, it is reasonable that the PV flux derived from the former includes but is not limited to term of the PV flux derived from the latter. Note that the avalanche-like transport is in fact triggered by the deviation of the local gradient from the critical gradient. In the absence of a mean gradient, the deviation from the mean profile (δq) will spread out, but its center remains in the same place. Thus, δq implicitly contains information about the local PV gradient. The transport coefficients, which can be functions of δq (while consistent with the symmetry constraints), are related to the mean PV gradient as well. The ballistic propagation of the self-organized turbulent structures is strongly related to a gradient-dependent effective diffusivity ($\Gamma_q \sim -D(\partial_y q)\partial_y q \rightarrow -D(\delta q)\delta q$), which is, in turn, related to the convective component of the PV flux in the PV-avalanche model ($\Gamma[\delta q] \sim \delta q^2 \rightarrow -D(\delta q)\delta q$, with $D(\delta q) \rightarrow D_0 \delta q$).

Equation (2.34) is very similar to the Kuramoto-Sivashinsky (K-S) equation in one dimension. In K-S equation, α, β, γ are positive constant; as a result, the second-order spatial derivative term is responsible for an instability at large scales (i.e., negative diffusion), the fourth-order derivative term provides damping at small scales, and the non-linear term stabilizes by transferring energy between

large and small scales. Since the competitive roles of large-scale flow growth and saturation by diffusive and hyper-diffusive terms have been shown in the minimum enstrophy model, it is plausible to assume that the parameters β and γ are positive in equation (2.34). The nonlinear term has the same form as that in the Burgers equation, suggesting intermittent PV transport during turbulence self-organization. The numerical studies of K-S equation with fixed boundary conditions has shown various types of 'shock' patterns (e.g., Ref. [58]).

The key issue of the 'negative viscosity phenomena' in quasi-geostrophic systems is: what is the form of the momentum/PV flux? While the conventional approaches (e.g., perturbation theory) explore the large scale instabilities, it is interesting to ask whether the diffusion-type flux leading to instabilities is sufficient to describe the whole dynamics. The PV-avalanche model based on general, non-perturbative principles indicates ballistic events, namely avalanches. A generalized transport coefficient with the dependence on local PV and PV gradient can characterize the negative viscosity phenomena, as well as the ballistic propagation of distortions or 'defects' of the PV profiles [59], which are likely induced by nonlinear wave interactions or external perturbations. Therefore, we suggest that the profile-dependent transport coefficient is, in some sense, a more general representation than the well-known 'negative viscosity' for the PV flux associated with jet/structure formation, since PV transport behavior is generically linked to PV profile and its gradient.

2.3 Conclusion and Discussion

In this chapter, we have explored non-perturbative approaches to the calculation of the PV flux in quasi-2D turbulent systems which conserve PV. We deduced the general forms of PV flux from two relaxation models: 1) the minimum enstrophy relaxation model using selective decay principle and 2) the PV-avalanche model using the joint reflection symmetry principle. The structure of PV flux derived from both relaxation models consists of a viscous and a hyperviscous transport of PV. The PV flux deduced from the PV-avalanche model has

another convective term, which is, however, dependent on the gradient of the mean PV profile.

In the minimum enstrophy relaxation model, we asked what form must the mean field PV flux have so as to dissipate enstrophy while conserving kinetic energy. The nonlinear term is annihilated in the end state of selective decay. We derived PV flux by writing the nonlinear term as N and $\partial_y \Gamma_q$. We showed that the results of these two formulations are consistent. The finding from the $\partial_y \Gamma_q$ approach is considered the primary result because the $\partial_y \Gamma_q$ formation is more accurate and better satisfies the mean field approximation. The PV flux is shown to be $\Gamma_q = \langle v_x \rangle^{-1} \partial_y \left[\mu \partial_y \left(\langle v_x \rangle^{-1} \partial_y \langle q \rangle \right) \right]$; it consists of diffusive and hyper-diffusive terms. We noted that there are other forms of PV flux which can minimize enstrophy while conserving energy. In this work, we studied only the simplest, smoothest form of the PV flux. We showed that the hyper-viscosity is positive and that the hyper-viscous term damps the energy of the mean zonal flow. Thus, the hyper-viscosity reflects the saturation mechanism of zonal flows and the scale dependence of the momentum flux. The results are pragmatically useful in the context of transport modeling, where the problems of zonal flow scale and saturation are important.

We found the homogenized quantity in the relaxed state to be the ratio of PV gradient to zonal flow velocity, implying that strong zonal flows are located at sharp PV gradients. The observation that the structure of the relaxed state is consistent with the structure of the PV staircase suggests that the staircase arises naturally as a consequence of minimum enstrophy relaxation and links inhomogeneous PV mixing to minimum enstrophy relaxation. We demonstrated that turbulence spreading is linked to PV mixing by showing the dependence of energy flux on PV flux: $\Gamma_E = -\int \Gamma_q \langle v_x \rangle dy = \mu \partial_y \left(\langle v_x \rangle^{-1} \partial_y \langle q \rangle \right)$. Since the spreading flux is driven by the gradient of the quantity which ultimately is homogenized, it vanishes in the relaxed state. A relaxation rate was derived using linear perturbation theory. We found the 'minimum enstrophy' required to sustain a zonal flow of a certain level in the relaxed state satisfies: $q_m^2 > 3\lambda \langle v_x \rangle^2 / 8$. A characteristic scale l_c was defined from the homogenized quantity, $l_c = |\partial_y \langle q \rangle / \langle v_x \rangle|^{-1/2}$, so that positive hyper-viscosity dominates at scales smaller than l_c, while effective viscosity

dominates at scales larger than l_c. We noted that l_c is similar to the Rhines scale. Rhines scale and l_c become indistinguishable when $\tilde{v}_{rms}$ and $\langle v_x \rangle$ are comparable.

In the PV-avalanche model, the form of the PV flux, which is driven by the deviation from the self-organized state, is constrained by the joint reflection symmetry condition. We found that one of the simplest forms of the PV flux contains a diffusive term, a hyper-diffusive term, and a nonlinear convective term. The PV equation has the same structure as the Kuramoto-Sivashinsky equation, which is known for its negative diffusion and higher-order stabilizing dissipation. The structure of viscous and hyper-viscous transport of PV was shown previously in the minimum enstrophy model, while the coefficients of viscosity and hyper-viscosity were derived later for the modulational instability calculation. The convective transport of PV, which suggests intermittent PV transport during turbulence self-organization, was not explicitly shown in the selective decay analysis. Nevertheless, we noted that for the case of avalanche-like transport, δq is counted as the deviation of the local gradient from the mean (critical) gradient, and the transport coefficients, constrained by the presence of the mean gradient, will depend on δq. Thus, a nonlinear convective component of PV flux ($\Gamma[\delta q] \sim \delta q^2$) is equivalent to a generalized diffusive transport (i.e., $\Gamma_q \sim -D(\nabla q - \nabla q_{\rm crit})\nabla q \to -D(\delta q)\delta q$, with $D(\delta q) \to D_0 \delta q$). These may represent similar transport processes.

To sum up, we compare the structures of PV flux derived via two relaxation models: the transport flux-oriented mean field theory (based on the minimum enstrophy principle) and the generalized Fickian mean field theory (based on the joint reflection symmetry principle); the PV flux of the later includes the terms of the former together with a convective term. We proposed that a profile-dependent transport coefficient gives a more general form of the PV flux of systems where negative viscosity phenomena take place, since the relative dependence on the instant PV profile, especially the profile gradient, is crucial to the ballistic propagation of PV defects–avalanches. While noting that the profile gradient dependence of the transport coefficients has potential effects on transport behavior, the detail of the dependency is beyond the scope of this work.

PV mixing, the fundamental process for zonal flow generation, is directly

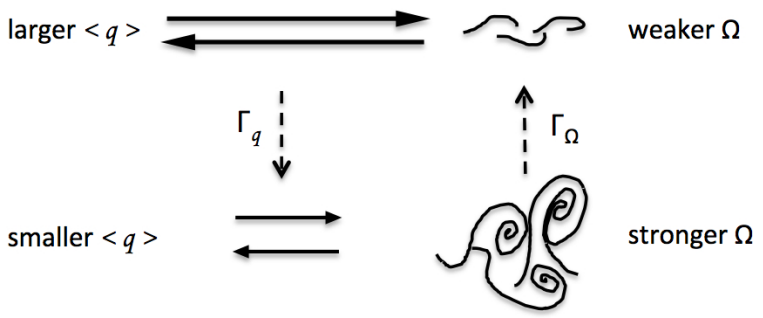

Figure 2.4: PV mixing tends to transport PV from the region of larger mean PV (i.e., stronger zonal shears) to the region of smaller mean PV, while turbulence spreading tends to transport turbulence from the region of stronger turbulent intensity turbulent potential enstrophy $\Omega \equiv \langle \tilde{\boldsymbol{q}}^2 \rangle$ or turbulent energy $\langle \tilde{\boldsymbol{v}}^2 \rangle$) to the region of weaker turbulent intensity.

linked to the forward enstrophy cascade in wave-number space. The importance of such small scale mixing processes is seen from the appearance of hyper-viscosity in the PV flux, which contributes to zonal flow energy damping. The terms in the PV flux which contribute to zonal flow energy growth (i.e., effective negative viscosity,) however, are not well reconciled with the picture of diffusive mixing of PV in real space. Here we offer a possible explanation, based on the connection between PV mixing and turbulence spreading derived from the minimum enstrophy analyses. We may consider turbulence spreading as a process which contributes to up-gradient, or 'anti-diffusive', mixing of PV. The argument is as follows: it is reasonable to assume that PV mixing in real space tends to transport PV from the region of larger mean PV to the region of smaller mean PV. Because a stronger mean vorticity corresponds to a stronger shearing field which suppresses turbulence, the PV mixing process tends to transport PV away from the region of weak (turbulence) excitation toward the region of stronger excitation. In contrast, the spreading of turbulent enstrophy tends to transport enstrophy from the strongly turbulent region to the weakly turbulent region (Figure 2.4). When the tendency of turbulence spreading is greater, the net transport of PV appears up-gradient, and so the apparent effective viscosity becomes negative. The relaxed state is reached when PV mixing and turbulent enstrophy spreading are balanced. The total PV fluxes we calculated in the relaxation model and the modulational insta-

bility analysis include both trends.

We conclude by noting that, the dynamics of PV flux derived analytically in this work has not been confirmed by numerical tests. Therefore, an important topic for future research would be developing a numerical simulation test and comparing its results with the analytical predictions.

Chapter 2 is a reprint of material appearing in Pei-Chun Hsu and P. H. Diamond, Phys. Plasmas, **22**, 032314 (2015) and Pei-Chun Hsu, P. H. Diamond, and S. M. Tobias *Phys. Rev. E* (accepted). The dissertation author was the primary investigator and author of this article.

Chapter 3

Perturbation Theory of Potential Vorticity Flux

3.1 Introduction

In Chapter 2, we have explored non-perturbative approaches to derive the general structure of PV flux. In this chapter, to systematically study the dynamics of PV flux, we calculate the transport coefficients using perturbation theory in two cases: 1) modulational instability for a broad turbulence spectrum and 2) parametric instability for a narrow turbulence spectrum. The results of modulational calculation shows that the PV flux contains a negative viscosity and a positive hyper-viscosity. The viscous and the hyper-viscous transport of PV are found in both the minimum enstrophy relaxation model and the PV-avalanche model. For parametric instability, the linear growth rate shows that turbulent vorticity transport is convective. *The results of both relaxation principles and perturbative analyses show that PV flux is not well represented by Fickian diffusion.* While considerable progress has been made in the wave-mean interaction theory of zonal flow generation and the flow structure in the end relaxed state, here we present a study of the dynamics of PV transport which links these two questions.

The rest of the chapter is organized as follows. Section 3.2 derives momentum transport coefficients via perturbation theory, including modulational insta-

bility in 3.2.1 and parametric instability in 3.2.2. The discussion and conclusions are given in section 3.3. The structure of Chapter 3, together with Chapter 2, is illustrated in the flowchart of Fig (2.1).

3.2 Deducing the transport coefficients from perturbative analyses

In this section, the structure of the PV flux is further analyzed using perturbation theory. The aim is to obtain the turbulent transport coefficients and to study the underlying physics. We study both the modulational instability of a broad fluctuation spectrum and the parametric instability of a narrow fluctuation spectrum, both to a large-scale seed zonal flow. Wave action (population) density conservation is used to evaluate the response of the wave spectrum to the test shear. We consider 2D quasi-geostrophic turbulence ($q = \nabla^2\psi + \beta y$), in which the wave action density $N_k = \varepsilon_k/\omega_k = -k^4|\psi_k|^2/(\beta k_x)$ can be renormalized to the enstrophy density $k^4|\psi_k|^2$, since β is a constant and k_x is unchanged by zonal flow shearing ($dk_x/dt = -\partial(k_x\langle v_x\rangle)/\partial x$=0). Thus, we see that the wave action density represents the intensity field of PV and its evolution has a direct connection with PV mixing. The Reynolds force, i.e., PV flux, which drives mean zonal flow is linked to the enstrophy density as $-\partial_y\langle\tilde{v}_y\tilde{v}_x\rangle = \partial_y \int d^2k \frac{k_x k_y}{k^2}(k^4|\tilde{\psi}_k|^2)$.

3.2.1 Modulational instability

We first study the modulational instability of a wave spectrum to a seed zonal flow $\delta\langle v_x\rangle$ (with wave number $\boldsymbol{q}$ and eigen-frequency $\Omega_{\boldsymbol{q}}$). For a slowly varying, large scale shear flow, N_k changes adiabatically with the shear flow perturbation, and the modulational response of Rossby waves by the seed flow is determined by the linearized wave kinetic equation:

$$\frac{\partial \tilde{N}_k}{\partial t} + v_{gy}\frac{\partial}{\partial y}\tilde{N}_k + \delta\omega_k \tilde{N}_k = \frac{\partial(k_x\delta\langle v_x\rangle)}{\partial y}\frac{\partial N_0}{\partial k_y}, \tag{3.1}$$

where v_g is the group velocity of wave-packets and $\delta\omega_k$ represents nonlinear self-decorrelation rate via wave-wave interaction. For small perturbations $(\tilde{N}_k, \delta\langle v_x\rangle) \sim$

$e^{-i\Omega_{\boldsymbol{q}}t+iq_y y}$, the modulation of $\tilde{N}_k$ becomes

$$\tilde{N_k} = -iq\delta\langle v_x\rangle \frac{k_x}{-i(\Omega_{\boldsymbol{q}} - q_y v_{gy}) + \delta\omega_k} \frac{\partial N_0}{\partial k_y}, \tag{3.2}$$

so the growth rate of the seed zonal flow is given by

$$\gamma_q = -q^2 \int d^2k \frac{k_x^2 k_y}{k^4} \frac{|\delta\omega_k|}{(\Omega_{\boldsymbol{q}} - q_y v_{gy})^2 + \delta\omega_k^2} \left(\frac{\partial N_0}{\partial k_y}\right), \tag{3.3}$$

where N_0 is normalized to the mean enstrophy density. The condition to have instability ($k_y \partial_{k_y} N_0 < 0$) is satisfied for most realistic equilibrium spectra for Rossby wave and drift wave turbulence. The fundamental mechanism of zonal flow generation includes not only local wave-wave interactions (in wavenumber space) but also non-local couplings between waves and flows. Therefore, zonal flow growth rate should depend on both the spectral structure of turbulence and properties of zonal flow itself. Equation (3.3) shows that the growth rate is indeed a function of wave spectrum $N_0(\boldsymbol{k})$ and zonal flow width q_y.

In the limit of $q_y v_{gy} << \delta\omega_k$, the response function is expanded as

$$\frac{|\delta\omega_k|}{(\Omega_{\boldsymbol{q}} - q_y v_{gy})^2 + \delta\omega_k^2} \approx \frac{1}{|\delta\omega|}(1 - \frac{q_y^2}{q_c^2}), \tag{3.4}$$

where the critical excursion length of wave-packets q_c^{-1} is defined as

$$q_c \equiv \frac{|\delta\omega_k|}{v_{gy}}. \tag{3.5}$$

The critical length can be understood as the mean free path of the wave-packets, considering wave-packets as quasi-particles. Thus, the $q_y v_{gy} << |\delta\omega_k|$ limit means that the width of the zonal flow is larger than the (cross-flow) mean free path of the wave-packets. This corresponds to the scale separation criterion of the wave kinetic equation. This expansion finally implies that the shear flow evolution consists of two parts and so equation (3.3) becomes

$$\gamma_{\boldsymbol{q}} = -q_y^2 D_t - q_y^4 H_t, \tag{3.6}$$

where the turbulent viscosity D_t and hyper-viscosity H_t are given by

$$D_t = \int d^2k \frac{k_x^2}{|\delta\omega_k| k^4} \frac{k_y \partial N_0}{\partial k_y}, \tag{3.7}$$

and

$$H_t = -\int d^2k \left(\frac{v_{gy}}{\delta\omega_k}\right)^2 \frac{k_x^2}{|\delta\omega_k|k^4} \frac{k_y \partial N_0}{\partial k_y}. \tag{3.8}$$

Given that $k_y \partial_{k_y} N_0 < 0$, the modulational calculation yields both a negative turbulent viscosity, which contributes to zonal flow growth, and a positive turbulent hyper-viscosity, which accounts for the saturation mechanism of zonal flow growth. Note that the large-scale instability due to negative diffusivity and small-scale damping due to higher-order diffusion are like what we observe in the K-S equation. The negative viscosity follows from the zeroth order term in the expansion of the response function. Thus, the resonance interaction between zonal flow and wave-packets results in the growth of zonal flow at the expense of the wave energy. Figure 3.1 shows a cartoon of a wave-packet traveling through a zonal flow. When the width of the zonal flow is larger than critical wave excursion length (the criterion for the expansion), the negative viscosity dominates, i.e., there is a net transfer of energy from the wave-packet to the zonal flow, and so the energy of the wave-packet decreases (right panel of Fig. 3.1). In the limit when zonal flow scale approaches the critical scale, the negative viscosity and positive hyper-viscosity balance each other, i.e., the net exchange of energy between the wave-packet and zonal flow goes to zero, and so the energy of the wave-packet remains the same (left panel of Fig. 3.1). The PV flux consisting of an effective viscosity and a positive

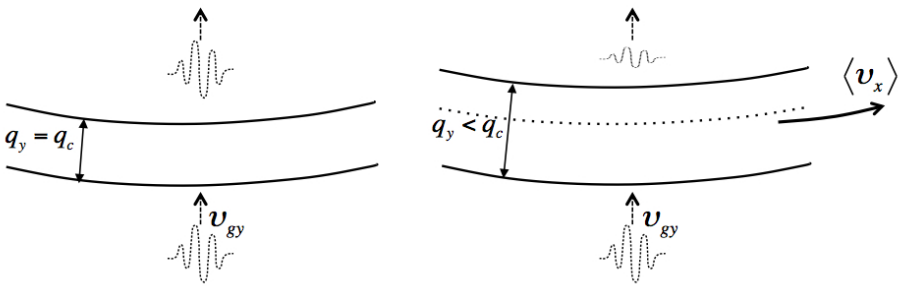

Figure 3.1: Schematic illustration of a wave-packet traveling across a zonal flow. The intensity/energy of the wave-packet becomes weaker after crossing through a zonal flow with its width larger than the critical excursion length of the wave-packet (right). When the width of the zonal flow is equal to (or smaller than) the critical length, the energy of the wave-packet does not change (left).

hyper-viscoschemasity is consistent with the structure of PV flux derived using the non-perturbative minimum enstrophy relaxation model. The critical length q_c^{-1} is similar to the characteristic scale l_c defined in the minimum enstrophy model because both of them characterize some scale at which viscous and hyper-viscous terms balance each other. At larger scales, negative viscosity dominates so zonal flows can grow; at smaller scales, positive hyper-viscosity dominates so zonal flows are damped. The difference of q_c^{-1} and l_c is that q_c^{-1} is defined in the context of wave dynamics, while l_c is defined by mean profiles.

3.2.2 Parametric instability

The modulational instability discussed in the preceding subsection is developed for the wave kinetic limit, i.e., it applies to a broad wave spectrum, or, more specifically, the condition of $\delta\omega_k > \gamma_q$. In this subsection we consider the case of a narrow turbulence spectrum. The instability of a gas of drift/Rossby waves to a seed zonal flow becomes the coherent hydrodynamic type (called parametric instability [42]), when the frequency spread of the wave spectrum is small compared to the growth rate of the zonal flow ($\delta\omega_k < \gamma_q$). Note that modulational instability and parametric instability are two regimes of the same process, namely, that small scale wave-packets are unstable with respect to a large scale perturbation. The dispersal of the wave-packets is what differentiates the regimes. The wave-packets which disperse slower than the growth rate of the perturbation react coherently to the perturbation, and so the instability belongs to the hydrodynamic regime, while the wave-packets which disperse faster than the growth rate of the perturbation belong to the kinetic regime.

A narrow spectrum of wave-packets in wave kinetic theory act like pseudo-particles by analogy with charged particles in plasma fluids. The analogy between the pseudo-fluid and the plasma fluid is summarized in table 3.1. Note that one distinction between them is that there is no direct proportionality between the velocity $\boldsymbol{V}^w$ and momentum $\boldsymbol{P}^w$ of pseudo-fluid. The dynamics of the pseudo-fluid is derived from multiplying the wave kinetic equation, by v_{gy} and integrating

Table 3.1: Analogy between pseudo-fluid and plasma fluid.

	pseudo-fluid	plasma fluid
elements	wave-packets	charged particles (species α)
distribution function	$N_{\boldsymbol{k}}(\boldsymbol{k}, \omega_{\boldsymbol{k}})$	$f_\alpha(\boldsymbol{r}, \boldsymbol{v}, t)$
mean free path	$\lvert\boldsymbol{v}_g\rvert/\delta\omega_{\boldsymbol{k}}$	$1/n_\alpha\sigma$
density	$n^w = \int N_{\boldsymbol{k}} d\boldsymbol{k}$	$n_\alpha = \int f_\alpha d\boldsymbol{v}$
momentum	$\boldsymbol{P}^w = \int \boldsymbol{k} N_{\boldsymbol{k}} d\boldsymbol{k}$	$\boldsymbol{p}_\alpha = \int m_\alpha \boldsymbol{v} f_\alpha d\boldsymbol{v}$
velocity	$\boldsymbol{V}^w = \frac{\int \boldsymbol{v}_g N_{\boldsymbol{k}} d\boldsymbol{k}}{\int N_{\boldsymbol{k}} d\boldsymbol{k}}$	$\boldsymbol{u}_\alpha = \frac{\int \boldsymbol{v} f_\alpha d\boldsymbol{v}}{\int f_\alpha d\boldsymbol{v}} = \frac{\boldsymbol{p_\alpha}}{m_\alpha n_\alpha}$

over k.

$$\frac{\partial}{\partial t}\int v_{gy} N_k dk + \int v_{gy}\frac{\partial}{\partial y} v_{gy} N_k dk - \int k_x \delta\langle v_x\rangle' \frac{\partial}{\partial k_y} v_{gy} N_k = -\int v_{gy}\delta\omega_k N_k dk, \quad (3.9)$$

where $\delta\langle v_x\rangle' \equiv \partial_y \delta\langle v_x\rangle$. Normalizing equation(3.9) by the pseudo-density n^w, the first term on the left hand side gives $\partial_t V^w$, the velocity evolution of the pesudo-fluid. The second term can be decomposed into two parts:

$$\frac{\int v_{gy}\frac{\partial}{\partial y} v_{gy} N_k dk}{\int N_k dk} = \int V_y^w \frac{\partial}{\partial y} V_y^w N_k dk + \frac{\int (v_{gy} - V_y^w)\frac{\partial}{\partial y}(v_{gy} - V_y^w) N_k dk}{\int N_k dk}. \quad (3.10)$$

The second part can be viewed as the 'pressure' gradient of the pseudo-fluid. When the spectrum of wave-packets is narrow, the effective 'temperature' is low because of weak dispersion. Thus, we can neglect this pressure term and consider a pure fluid type instability. The third term on the left hand side of equation (3.9) normalized by n^w is given by

$$\frac{-\int k_x \delta\langle v_x\rangle' \frac{\partial}{\partial k_y} v_{gy} N_k}{\int N_k dk} = -a\delta\langle v_x\rangle', \quad (3.11)$$

where

$$a = \frac{\int \left(\frac{2\beta k_x^2}{k^4} - \frac{8\beta k_x^2 k_y^2}{k^6}\right) N_k dk}{\int N_k dk}. \quad (3.12)$$

The term on the right hand side of equation (3.9) is related to the dispersal of wave-packets due to wave-wave interaction, and so is neglected in the hydrodynamic regime for simplicity. Finally, putting the four terms together, we obtain the dynamic equation for the pseudo-fluid

$$\frac{\partial}{\partial t} V_y^w + V_y^w \frac{\partial}{\partial y} V_y^w = -a\delta\langle v_x\rangle'. \quad (3.13)$$

This equation is equivalent to the inviscid Burgers' equation with a source term on the right hand side contributed by the zonal shear. Given that the development of discontinuities (shock waves) is a crucial phenomenon that arises with the Burgers' equation, we speculate that coherent structures/shocks composed of wave-packets may form due to zonal shear stirring. It is worth noting that while the shock structure is the result of the nonlinear term, the zonal flow is what triggers it. Interestingly, shock formation in spectral-space, on account of zonal flow shearing, has been found in the study of intermittency in drift wave-zonal flow turbulence by Diamond & Malkov [60]. Using basic conservation and symmetry properties, they derive a generalized Burgers' equation for the wave action density in the radial wave number (i.e., k_y in this paper) space, in that damping and spatial propagation terms are present. The shock solutions to the generalized Burgers' equation are events of spectral pulses, which correspond to wave-packets, propagate ballistically to higher k_y. The transport in k_y results from shearing-induced refraction.

To relate the dynamics of the pseudo-fluid dynamics to zonal flow generation, we write the Reynolds stress in terms of the wave action density and the Rossby wave group velocity: $\langle \tilde{v}_y \tilde{v}_x \rangle = \int v_{gy} k_x N_k d^2k$. In the fluid limit, the right hand side is approximated as $V_y^w P_x^w$, which is the pseudo-momentum flux carried by the pseudo-fluid. The evolution of the zonal flow then becomes

$$\frac{\partial}{\partial t}\delta\langle v_x \rangle = -\frac{\partial}{\partial y} V_y^w P_x^w. \tag{3.14}$$

Next, we consider the instability to small perturbations by taking $V_y^w = V_{y,0}^w + \widetilde{V_y^w}$; $P_x^w = P_{x,0}^w + \widetilde{P_x^w}$ with the perturbations linearly proportional to the zonal shear $\delta\langle v_x \rangle'$. We can derive two coupled equations for the perturbations from equations (3.13) and (3.14)

$$\frac{\partial}{\partial t}\widetilde{V_y^w} + V_{y,0}^w \frac{\partial}{\partial y}\widetilde{V_y^w} = -a\delta\langle v_x \rangle'. \tag{3.15}$$

$$\frac{\partial}{\partial t}\delta\langle v_x \rangle = -V_{y,0}^w \frac{\partial}{\partial y}\widetilde{P_x^w} - P_{x,0}^w \frac{\partial}{\partial y}\widetilde{V_y^w}. \tag{3.16}$$

The pseudo-momentum P_x^w evolves in the same way as the zonal flow, that is shown from multiplying the wave kinetic equation by k_x and integrating over $\boldsymbol{k}$

$$\frac{\partial}{\partial t}\int k_x N_x d^2k = -\frac{\partial}{\partial y}\int v_{gy} k_x N_k d^2k. \tag{3.17}$$

Because only $\widetilde{P_x^w}$ contributes to the time derivative term, we substitute $\widetilde{P_x^w}$ with $\delta\langle v_x\rangle$ in equation (3.16) and rewrite the coupled equations in the Fourier form

$$(-i\Omega_q + iqV_{y,0}^w)\widetilde{V_y^w} = -iqa\delta\langle v_x\rangle, \tag{3.18}$$

$$(-i\Omega_q + iqV_{y,0}^w)\delta\langle v_x\rangle = -iqP_{x,0}^w\widetilde{V_y^w}, \tag{3.19}$$

so that we obtain the dispersion relation:

$$(\Omega_q - qV_{y,0}^w)^2 = q^2aP_{x,0}^w. \tag{3.20}$$

In monochromatic limit, a and $P_{x,0}^w$ are simply

$$a = \frac{2\beta k_x^2}{k^4}\left(1 - \frac{4k_y^2}{k^2}\right); P_{x,0}^w = -\frac{k^4|\psi_k|^2}{2\beta}, \tag{3.21}$$

and the reduced dispersion relation,

$$(\Omega_q - qV_{y,0}^w)^2 = -q^2k_x^2|\psi_k|^2\left(1 - \frac{4k_y^2}{k^2}\right), \tag{3.22}$$

is consistent with the result obtained by Smolyakov et. al.[42]. The coherent instability requires the condition of $k_x^2 - 3k_y^2 > 0$, i.e., radially extended, anisotropic turbulence. In other words, the wave structure set the marginality of the coherent secondary instability. Note that the criterion required for modulational instability does not depend on the wave spatial structure.

The growth rate of the zonal flow in equation (3.22) is proportional to the zonal flow wave number $|q|$, showing that PV transport in parametric instability is convective. This type of momentum transport may be faster than turbulent momentum diffusion. However, the saturation mechanism of this instability needs to be investigated further. The structure of the PV flux in the PV-avalanche relaxation (relaxation of a PV deviation back to a self-organized state) model contains a convective transport of PV. Here we derive the transport coefficient for the convective PV transport in weak turbulence and narrow turbulence spectrum limit. From equations (3.12) and (3.20), we can see that the transport coefficient depends on the fluctuation spectrum.

3.3 Conclusion and Discussion

In this Chapter, to derive the transport coefficients rigorously, we used perturbation theory to study the instability of an ensemble of wave packets to a large scale seed perturbation. Instabilities of two regimes were considered: 1) modulational instability for a broad turbulence spectrum and 2) parametric instability for a narrow turbulence spectrum. In the modulational instability analysis of the wave kinetic equation, we found that to the lowest order, PV flux is composed of a negative viscous and a positive hyper-viscous terms. The viscous and hyper-viscous transport of PV are shown in the minimum enstrophy relaxation model and the PV-avalanche model as well. The negative viscosity from the resonance interaction between zonal flow and wave-packets contributes to the growth of the zonal flow. The positive hyper-viscosity reflects the saturation mechanism of zonal flows and the scale dependence of the PV flux. A critical scale q_c^{-1} was defined so that negative viscosity term is dominant at scales larger than q_c^{-1} while positive hyper-viscosity term is dominant at scales smaller than q_c^{-1}. In the parametric instability analysis, we derived a model of a pseudo-fluid composed of wave-packets. The dynamic equation for the pseudo-fluid is the inviscid Burgers' equation, with a source term contributed by the zonal flow. This suggests that coherent structures–wave-packets–may form due to zonal shear stirring. The PV transport associated with the pseudo-fluid is a convective process, since the growth rate of the zonal flow in the parametric instability is proportional to the zonal flow wave number. The PV transport coefficients were shown to depend on the fluctuation spectrum.

The zonal flow growth rates of madulational instability and parametric instability are summarized in table 4.1. The proportionality of growth rate to zonal flow wave number reveals the diffusive nature of madulational instability and convective property of parametric instability.

Table 3.2: Zonal flow growth rate in two models.

modulational instability	$\gamma_q \simeq q^2 k_x^2 \lvert\psi_k\rvert^2 \frac{1}{\delta\omega(1-\frac{q^2}{q_c^2})}$
parametric instability	$\gamma_q = \sqrt{q^2 k_x^2 \lvert\psi_k\rvert^2 \left(1 - \frac{4k_y^2}{k^2}\right)}$

To sum up the studies in Chapter 2 and Chapter 3, we have explored different approaches to the calculation of the PV flux in quasi-2D turbulent systems which conserve PV. In Chapter 2, we non-perturbatively deduced the general forms of PV flux from two relaxation models. In this chapter, we calculated the transport coefficients using perturbation theory. A negative viscosity and a positive hyper-viscosity are derived from the broad-band modulational analysis, while a coefficient associated with the convective term is obtained from the narrow-band parametric analysis. The results of Chapter and Chapter 3 are summarized in table 3.3.

Table 3.3: Elements of the PV flux from structural, non-perturbative approaches and perturbative analyses.

	PV flux	conv.	visc.	hyper-visc.	coefficients
(non-pert.)	min. enstrophy relaxation		•	•	
	PV-avalanche relaxation	•	•	•	
(perturb.)	modulational instability		•	•	$D_t < 0, H_t > 0$
	parametric instability	•			$\gamma_q \sim \lvert q \rvert$

Chapter 3 is a reprint of material appearing in Pei-Chun Hsu and P. H. Diamond, *Phys. Plasmas*, **22**, 032314 (2015). The dissertation author was the primary investigator and author of this article.

Chapter 4

Zonal Flow Formation in the Presence of Ambient Mean Shear

4.1 Introduction

Shearing structures are commonly observed in laboratory plasmas, planetary atmospheres, and the solar interior. In many of the systems two kinds of shear flows co-exist: 1) zonal flows which are generated by and coupled to turbulence [14, 39] and 2) mean shear flows which are driven by background gradients or external stresses [61]. Turbulence, zonal flows and mean shears, all have effects on one another. The role of shearing in de-correlating turbulent eddies and regulating turbulent transport [14, 39, 61, 62, 63] is well known. Besides the shearing effects on turbulence, mean shear flows also affect the formation of zonal flows. In this paper, we study the effect of mean shear flows on modulational instability generation of zonal flows. In particular, we use wave kinetics to investigate quantitatively how a mean shear affects the correlation between turbulent wave packets and the zonal flow shearing field during modulational instability. Zonal flows are generated by modulational instability, in which the modulations due to a seed zonal flow induce variation in the fluctuation wave spectrum, and the Reynolds stress driven by this modulated (i.e. tilted) wave spectrum amplifies the initial perturbation. By de-correlating the modulated wave packet and the zonal shear, mean shears

inhibit the growth of zonal flows.

Magnetically confined plasma is one of the systems in which mean shear flows, zonal flows, and drift wave turbulence co-exist and interact with one another. In tokamaks, the reduction of turbulence by flow shearing is believed to be a key mechanism for the low to high (L-H) plasma confinement mode transition, in which plasmas organize themselves into a high confinement state (H mode) by the formation of transport barriers. Of critical importance to the research of the L-H transition is the understanding of the interplay among mean and zonal shearing fields and drift wave packets. Zonal flows and mean shears play different roles in the L-H transition, because they differ in their generation mechanism, temporal behavior, and spatial structure. Zonal flows are generated by turbulence via the Reynolds stress while mean $E \times B$ flows are driven by the pressure gradient. Therefore, zonal flows must eventually decay when the underlying turbulence drive is extinguished, while mean shear flows can be sustained in the absence of turbulence. The shearing of zonal flows has a complex spatial structure and is of limited coherency in time while the shearing by mean flows is coherent over longer times. With respect to their spatial scales, the scale of mean shears is macroscopic, comparable to the characteristic scale lengths of the system profiles, while the scale of zonal flows is mesoscopic, between the micro-scale turbulence correlation length and macro-scale system size. The zonal flow and drift wave packet both have a mesoscale character: L_P^{-1} <meso wavenumber< k, where L_P is the profile scale and k is the turbulence wave number. An illustration of the multi-scale system with macro-scale mean shears, meso-scale zonal flows and drift wave packets is shown in Fig. 4.1. In the predator-prey model for the L-H transition [16, 18], the transition is triggered by zonal flows regulating turbulence and lowering the power threshold. By extracting kinetic energy from drift wave turbulence, zonal flows regulate the turbulence level and associated transport, allowing the buildup of a steep pressure gradient. During the transition, the self-regulation of turbulence by zonal flows causes an oscillatory temporal behavior. Then, as the mean shear grows sufficiently strong, both turbulence and zonal flows are damped at the final stage of the L-H transition. Thus, the role of mean shear flows in the L-H

transition is not only to de-correlate turbulence but also to regulate zonal flows. The comprehension of the L-H transition requires an understanding of the coupled dynamics of a system of turbulence, zonal flows, and mean shears. In this paper we present a quantitative study of one of the key issues: the effect of a mean shear flow on the modulational instability of zonal flows.

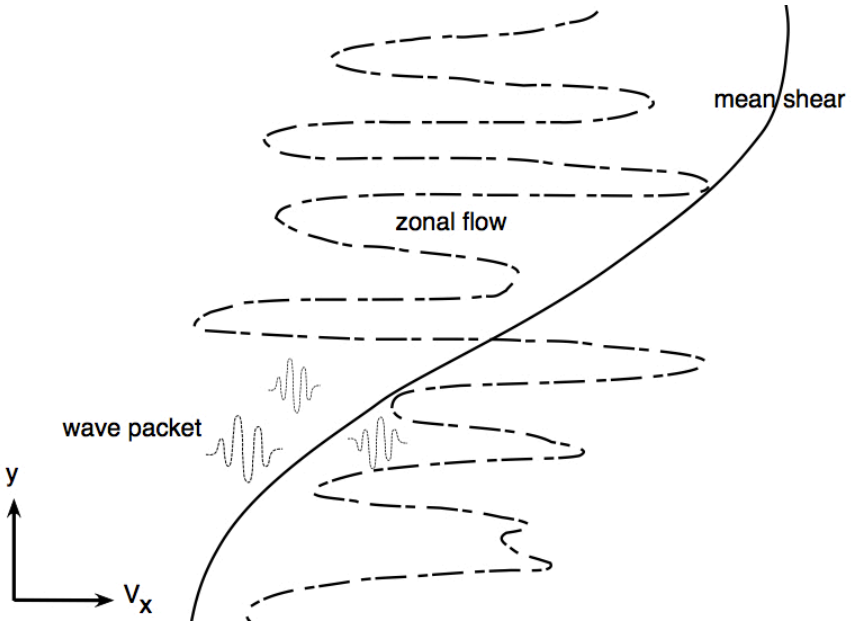

Figure 4.1: Multi-scale system.

Another system where mean shears may have significant effect on turbulent momentum transport associated with zonal flows is the solar tachocline. Helioseismology reveals that the angular velocity varies with latitude in the convection zone while the rotation in the radiation zone is nearly uniform. Between the convective envelope and radiative interior there exists a thin transition layer (less than 5 % of the solar radius,) known as the tachocline. It is still unclear how the tachocline remains thin under the force of the overlying differential rotation of the convection zone. Spiegel and Zahn [64] attribute the thin tachocline to anisotropic turbulence. They argue that turbulence in the stably stratified tachocline has negligible vertical motion and hence acts like a large constant horizontal viscosity producing mixing on spherical surfaces. The anisotropic turbulent viscosity in their model diffuses the latitudinal differential rotation, prevents the spreading of differential

rotation into the radiative interior, and keeps the tachocline thin. However, the effect of the large scale differential rotation on turbulent momentum transport is not considered in the Spiegel-Zahn model. Moreover, turbulent momentum transport coefficients should probably depend on shearing flows, since turbulence in the tachocline is coupled to both turbulence-generated flows and large scale rotation shears. Therefore, models for momentum transport in the tachocline should consider the interplay between solar differential rotation, zonal flows, and turbulence and waves. Similar to the mean $E \times B$ shears in tokamaks, differential rotation in the solar tachocline can be treated as a stable, imposed macro-scale mean shear because it is maintained by large-scale stresses from the convective zone above and its evolution timescale is much longer than that of turbulence and turbulence-driven zonal flows. We study the influence of the meridional differential rotation on turbulent momentum transport in a 2D quasi-geostrophic fluid. The effect of the radial differential rotation on turbulent transport in the solar tachocline is investigated by Kim [65]. Note that the model in this paper is purely hydrodynamic. Magnetic fields may exist and have important effects on the formation of the tachocline and transport in the tachocline. There also are MHD models of the tachocline. Gough and McIntyre [66] argue that a fossil magnetic field in the radiative interior is required to prevent the spreading of the shear, since turbulence in the tachocline would mix potential vorticity (PV) and drive shear flows. Therefore, the key problem remains to be how turbulence in the tachocline acts to redistribute angular momentum, i.e., what the form of turbulent momentum (or PV) flux is in the tachocline. In the β-plane MHD model by Tobias et. al [67], magnetic field is found to suppress turbulent momentum transport and the generation of mean flows in the tachocline. An MHD model of the mean shear-zonal flow-turbulence coupling system will be considered in future work.

In this paper, we examine the effect of mean shear flows on the modulational instability and growth of zonal flows. We consider systems in which macro-scale mean shear and meso-scale zonal shear coexist and discuss the effects of fixed zonal mean shears on turbulent momentum transport and the coupling between different scale shearing fields. We show that mean shear flows reduce the turbulent

momentum transport which forms zonal flows by decorrelating wave packets and the zonal flow shearing field during the process of modulation. The de-correlation by mean shear during the modulation also reduces the growth rate of the zonal flow. The scalings of turbulent momentum flux and zonal flow growth rate with a strong mean shear Ω are both $\Omega^{-2/3}$.

Previous work has explored the effect of mean shears on reducing the growth of the modulational instability (see, e.g. Ref. [68, 69]), following the initial work by Kim & Diamond [16]. However, this paper makes a significant advance. Specifically, this paper includes 1) an analysis of the effect of a mean shear on modulational wave action density $\tilde{N}_k$, zonal flow growth rate γ_q, and turbulent viscosity ν_t; 2) a study of zonal/mean flow shearing, potential vorticity (PV) mixing and their interaction in modulational instabiliy; 3) a calculation of the spatial flux of PV. Of course, a lot more needs to be done to completely unravel the physics of drift/Rossby wave-zonal flow turbulence in tokamaks and the tachocline.

The organization of the remainder of this paper is as follows. Section 3.2.1 gives an introduction to zonal flow formation via modulational instability without the presence of mean shearing field. The effect of ambient mean shear flows on zonal flow generation is studied in section 4.3. Section 4.4 presents our conclusion and discussions.

4.2 Zonal flow generation via modulational instability

Before considering the effect of mean shears on the generation of zonal flows, we first briefly review the modulational instability of the zonal flow formation [14, 70]. The systems we are interested in are drift wave turbulence in magnetically confined plasmas and quasi-geostrophic turbulence in geophysical fluid dynamics (GFD). Both systems are approximately two dimensional because of the strong guiding field applied to magnetized plasmas and the rapid planetary rotation and strong density stratification in the quasi-geostrophic limit. The model equations of these two systems are the Hasegawa-Mima (HM) equation [9] and the quasi-

geostrophic equation [5]. The Hasegawa-Mima equation for drift wave turbulence is given by

$$\frac{1}{\omega_{ci}}\frac{\partial}{\partial t}(\nabla^2\psi - \rho_s^{-2}\phi) - \frac{1}{L_n}\frac{\partial}{\partial y}\phi + \frac{1}{\rho_s L_n}J(\phi, \nabla^2\phi) = 0, \tag{4.1}$$

where ω_{ci} is the ion cyclotron frequency, ϕ is the normalized electrostatic potential, ρ_s is the ion gyroradius at electron temperature, L_n is the density gradient scale length, y-axis is in the poloidal direction, and J is the Jacobian operator. The 2D quasi-geostrophic equation is given by

$$\frac{\partial}{\partial t}(\nabla^2\psi - L^{-2}\psi) + \beta\frac{\partial}{\partial x}\psi + J(\psi, \nabla^2\psi) = 0, \tag{4.2}$$

where ψ is the stream function, L is the Rossby deformation radius, β represents the latitudinal variation of the Coriolis parameter, and x-axis is in the zonal direction. The Hasegawa-Mima equation and the quasi-geostrophic equation have the same structure. Both equations express material conservation of potential vorticity (PV) in the inviscid limit. We use the GFD notation and equation (1.5) for the rest of this paper, so the y-axis is in the direction of inhomogeneity: the radial direction in plasma or the meridional direction in GFD, and the x-axis is in the direction of symmetry, i.e., the direction of the zonal flows. Here, we consider the turbulence scales which are much smaller than L or ρ_s. In this limit, PV is $\nabla^2\psi + \beta y$ ($\beta = \frac{\partial}{\partial y}\ln n_0$ for drift wave turbulence). The flux of PV is simply the flux of vorticity, and the dispersion relation of the linear waves (drift waves in plasma or Rossby waves in GFD) is $\omega_k = -\beta k_x/k^2$, where $k^2 = k_x^2 + k_y^2$. Note that planetary vorticity βy varies in $\hat{y}$. As a consequence, the relative vorticity $\nabla^2\psi$ of a fluid parcel must change accordingly as it moves along the meridional direction in order to conserve PV, resulting in the propagation of a Rossby wave.

The physics of zonal flow generation by drift wave modulational instability is contained in the Hasegawa-Mima equation. However, it is recognized that there are many more complex dynamical models in magnetically confined fusion plasmas (e.g., ion temperature gradient (ITG), electron temperature gradient (ETG), and trapped electron mode (TEM) [71, 72, 73]). We note that all of ITGs, TEMs, ETGs etc are drift waves, in which ion (or electron, for ETG) polarization and finite Larmor radius (FLR) effects act as inertia which increases the dielectric, i.e.,

$\epsilon = 1 + k_\perp^2 \rho_s^2 + ...$, which then modifies (lowers) the wave frequency. In all cases the frequency is in the range of the drift wave frequency, and therefore can be written as $\omega \simeq \omega_{*e,i} f(k_\perp \rho_s)$ (or $f(k_\perp \rho_e)$, for ETG), where function $f(k_\perp \rho_s) < 1$. As $k_\perp \rho_s \to 0$, $\epsilon = 1 + k_\perp^2 \rho_s^2 + ... \to 1 + ...$, and so $f(k_\perp \rho_s) \to 1$. For example, the generic drift wave frequency is given as $\omega = \omega_{*i}/(1 + k_\perp^2 \rho_s^2)$. For the collisionless trapped electron mode (CTEM), the frequency is reduced as $\omega = \omega_{*e}/(1 + k_\perp^2 k_M^{-2})$ where $k_M^{-2} = \rho_s^2[1 + \tau^{-1}(1 + \eta_i)], \tau = \frac{T_e}{T_i}$, and $\eta_i = \frac{\partial_r \ln T_i}{\partial_r \ln n_i}$. In the case of the ion temperature gradient (ITG) mode, the influence of the ion temperature gradient is coupled with parallel ion motion, and the dispersion relation, taking account of the ion Larmor radius, is given as $\omega^2 - \omega\omega_{*e}/(1 + k_\perp^2 \rho_s^2(1 - \tau^{-1})) - k_{||}^2 c_s^2(1 + \tau^{-1}\eta_i \frac{\omega_{*e}}{\omega}) = 0$. The ETG mode is similar to the ITG mode, but with the roles of the electrons and ions reversed. In the ITG and TEM modes, we have the Boltzmann electron response for both waves and zonal mode, while the ion response to zonal flow perturbations is adiabatic in the ETG mode. Thus, the simplified model discussed in our paper captures the basic trends of the dependence of the dielectric and wave frequency on the polarization and FLR effects, which are common to all models, however more complicated.

In all cases one can understand the energy transfer between drift waves and zonal flows by exploiting the mean field evolution equation of the wave action density [14]:

$$\frac{d\langle N \rangle}{dt} = \frac{\partial}{\partial k_r} D_{k_r} \frac{\partial \langle N \rangle}{\partial k_r}. \tag{4.3}$$

Multiplying Eq(1) by ω_k and proceeding to integrate by parts gives the evolution of the wave energy:

$$\frac{d\varepsilon_{wave}}{dt} = -\int D_{k_r} \frac{\partial \omega_k}{\partial k_r} \frac{\partial \langle N \rangle}{\partial k_r} = -\int D_{k_r} v_{gr} \frac{\partial \langle N \rangle}{\partial k_r}, \tag{4.4}$$

where the group velocity $v_{gr} = \partial \omega_k / \partial k_r$ can be derived from the dielectric function $\epsilon(\omega, \boldsymbol{k})$, since $d\epsilon = \frac{\partial \epsilon}{\partial \omega} d\omega + \frac{\partial \epsilon}{\partial \boldsymbol{k}} \cdot d\boldsymbol{k} = 0$ along the wave path. Therefore the wave energy evolves (in terms of ϵ):

$$\frac{d\varepsilon_{wave}}{dt} = \int D_{k_r} \frac{\partial \epsilon / \partial k_r}{\partial \epsilon / \partial \omega}\bigg|_{\boldsymbol{k}, \omega_{\boldsymbol{k}}} \frac{\partial \langle N \rangle}{\partial k_r}. \tag{4.5}$$

For drift wave turbulence, $d\varepsilon_{wave}/dt < 0$ (i.e., the wave energy decreases and so the flow energy grows) since the conditions $k_r \partial \langle N \rangle / \partial k_r < 0$ and $v_{gr}/k_r < 0$

are virtually always satisfied. The condition $v_{gr}/k_r < 0$ results from the generic structure of ϵ: that the sign $k_r^{-1}(\partial\epsilon/\partial k_r)$ and $\partial\epsilon/\partial\omega$ are the same generically (e.g., $\epsilon(\omega, k_\perp\rho_s) = 1 - \frac{\omega_{*i}}{\omega(1+k_\perp^2\rho_s^2)}$). Thus, the growth of zonal flows at the expense of the wave energy is generic to all of the drift wave models and follows from the basic structure of ϵ. The simple model presented in this paper captures the basic physics of wave-flow energy transfer of the drift wave-zonal flow systems. While the details of $\epsilon(\omega, k_\perp\rho_s)$ or $f(k_\perp\rho_s)$ may change, or be more complicated, the trend that turbulence loses energy to the flows persists.

The modulational instability of a broad spectrum of Rossby or drift waves to a large-scale test zonal flow δV_x is given by:

$$\frac{\partial}{\partial t}\delta V_x = -\frac{\partial}{\partial y}\langle\tilde{v}_y\tilde{v}_x\rangle - \mu\delta V_x = \frac{\partial}{\partial y}\int d^2k k_x k_y |\tilde{\psi}_k(\delta V_x)|^2 - \mu\delta V_x, \qquad (4.6)$$

where μ is friction in GFD or collisional drag in plasma. Note that the Taylor identity relates the Reynolds force to the cross zonal stream flux of vorticity, indicating vorticity (or PV) transport and mixing in a system with one direction of symmetry as the fundamental mechanism of zonal flow formation in a quasi-2D fluid or plasma. We use wave action (population) density conservation to evaluate the modulational response of the wave spectrum to the test shear. The wave action density is given by $N_k = \varepsilon_k/\omega_k$, where ε_k is the wave energy density. In the case of drift wave turbulence, the wave energy density is given by $\varepsilon_k = (1+k_\perp^2\rho_s^2)|\psi_k|^2$ and so $N = (1+k_\perp^2\rho_s^2)^2|\psi_k|^2/\omega_*$. For zonal flow shears, ω_* is unchanged by flow shearing, so the wave action density and the potential enstrophy density $(1+k_\perp^2\rho_s^2)^2|\psi_k|^2$ are identical, up to a constant factor. In the systems considered in this work, we normalize the wave action density $N_k = -k^4|\psi_k|^2/(\beta k_x)$ to the enstrophy density $k^4|\psi_k|^2$, since β is a constant and k_x is unchanged by zonal flow shearing. Thus, we see that the wave action density represents the intensity field of PV and its evolution has a direct connection with PV mixing. The evolution of zonal flow is determined by the modulational response of enstrophy density $\tilde{N}_k$, as

$$\frac{\partial}{\partial t}\delta V_x = \frac{\partial}{\partial y}\int d^2k \frac{k_x k_y}{k^4}\tilde{N}_k - \mu\delta V_x = \frac{\partial}{\partial y}\int d^2k \frac{k_x k_y}{k^4}\left(\frac{\partial\tilde{N}_k}{\partial\delta V_x}\right)\delta V_x - \mu\delta V_x. \qquad (4.7)$$

N_k is determined by the linearized wave kinetic equation (WKE):

$$\frac{\partial \tilde{N}_k}{\partial t} + v_{gy}\frac{\partial}{\partial y}\tilde{N}_k + \delta\omega_k \tilde{N}_k = \frac{\partial (k_x \delta V_x)}{\partial y}\frac{\partial N_0}{\partial k_y}, \tag{4.8}$$

where N_0 is the mean enstrophy density. $\delta\omega_k$ represents nonlinear self-decorrelation rate via wave-wave interaction. The equilibrium balance has been used to relate linear growth rate and nonlinear damping rate. For small perturbations $(\tilde{N}_k, \delta V_x) \sim e^{-i\Omega_q t + iqy}$, the modulation of $\tilde{N}_k$ becomes

$$\tilde{N}_k = iq\delta V_x \frac{k_x}{-i(\Omega_q - qv_{gy}) + \delta\omega_k}\frac{\partial N_0}{\partial k_y}, \tag{4.9}$$

so the growth rate of the test zonal flow is given by

$$\gamma_q = -q^2 \int d^2k \frac{k_x^2 k_y}{k^4}\frac{|\delta\omega_k|}{(\Omega_q - qv_{gy})^2 + \delta\omega_k^2}\frac{\partial N_0}{\partial k_y}. \tag{4.10}$$

The condition to have instability ($k_y \partial N_0/\partial k_y < 0$) is satisfied for the equilibrium enstrophy spectrum for quasi-geostrophic turbulence and drift wave turbulence. The fundamental mechanism of zonal flow generation requires a synergy between local wave-wave interactions (in wavenumber space) and non-local couplings between waves and flows. Therefore, the zonal flow growth rate should depend on both the spectral structure of turbulence and properties of the zonal flow itself. From equation (4.10) we can see that the growth rate is indeed a function of wave spectrum $N_0(\boldsymbol{k})$ and zonal flow width q^{-1}. We will show in the next section that the growth rate also depends on ambient mean shear because mean shear de-correlates the couplings between wave and flows. The momentum transport associated with zonal flow modulational instability is given by

$$\frac{\partial}{\partial t}\delta V_x = \frac{\partial}{\partial y}\nu_t \frac{\partial}{\partial y}\delta V_x - \mu \delta V_x \simeq -q^2 \nu_t \delta V_x - \mu \delta V_x, \tag{4.11}$$

where the q dependence of turbulent viscosity ν_t is neglected. The leading behaviour of the zonal flow growth has the form of a negative viscosity instability:

$$\nu_t = \int d^2k \frac{k_x^2 k_y}{k^4}\frac{|\delta\omega_k|}{(\Omega_q - qv_{gy})^2 + \delta\omega_k^2}\frac{\partial N_0}{\partial k_y}. \tag{4.12}$$

On the other hand, there are several processes by which the growth of zonal flow is limited or saturated. A non-perturbative mean field theory for the dynamics

of minimum enstrophy relaxation shows that the PV flux consists of a positive hyper-viscosity term [74], which reflects the saturation mechanism of zonal flows. The nonlinear interaction between zonal flows and a wave packet scatters the wave packet and returns energy back to turbulence. Moreover, as a seed zonal flow grows, it saturates the modulational instability by deflecting the propagation of wave packets. This mechanism is similar to the decorrelation of wave packets' trajectory by mean flow shearing, which we will discuss in the next section. From a energetics viewpoint, since energy is conserved between zonal flow and turbulence waves, the growth of zonal flow energy must saturate as wave energy is depleted.

4.3 Effects of sheared mean flow

The shearing field of tokamaks and the solar tachocline often include both zonal flow shears and mean flow shears. One of the interesting problems regarding the interplay among Rossby/drift waves, zonal flows, and a mean shear flow is the effect of a mean shear flow on the generation of zonal flows. This interplay among turbulence, zonal flows, and mean shears is shown schematically in Fig. (4.2). In the previous session we have discussed how zonal flows grow by a long wave length modulation of wave turbulence. A mean flow shear can effectively decorrelate this modulation, thus inhibiting zonal flow growth. So as to address more realistic problems, in this section we study the modulational instability of test zonal flow in the presence of a sheared mean flow $V_0(y)\hat{x}$, focusing on calculating the suppression of zonal flow growth and PV transport.

In order to study the modulational instability in the ambient shearing field analytically, we use the method of characteristics to change coordinates to the shearing coordinates [75], in which the wave kinetic equation becomes an ordinary differential equation. The ray trajectory of a wave packet in the presence of a mean zonal shear $V_0\hat{x}$ can be determined by eikonal theory,

$$\begin{aligned} \frac{dk_y}{dt} &= -\frac{\partial \omega_k}{\partial y} = k_x \frac{\partial V_0}{\partial y}, \\ \frac{dy}{dt} &= \frac{\partial \omega_k}{\partial k_y} = v_{gy}, \end{aligned}$$

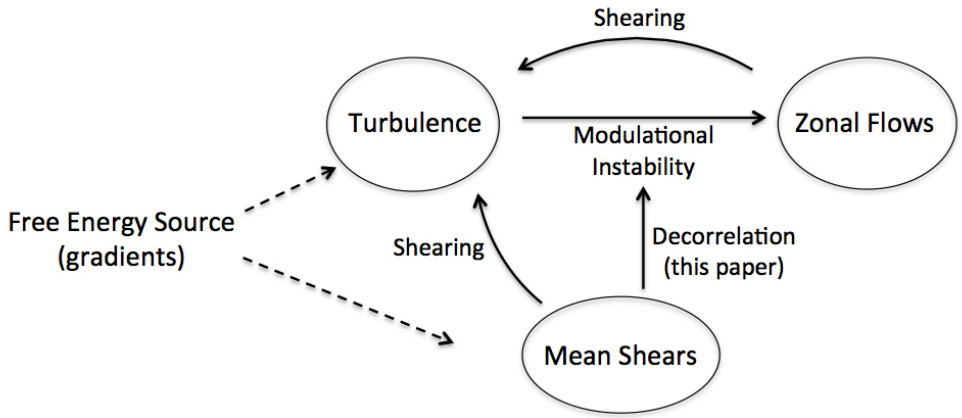

Figure 4.2: Interplay among turbulence, zonal flows and mean shears.

where the dispersion relation in the presence of mean shear is $\omega_k = k_x V_0 - \beta k_x/k^2$. For simplicity, a smooth mean shear $V_0(y) = -\Omega y$ is assumed, where Ω stands for the shearing rate. Therefore, the meridional wave number k_y of wave packets increases linearly in time:

$$k_y(t) = k_{y0} + k_x \Omega t. \tag{4.13}$$

The increase of k_y implies the increase of waves coupling to small scale dissipation. The increase of k_y also implies the decrease of meridional group velocity, which is given as $v_{gy} = 2\beta k_x k_y/k^4$. In other words, the growth of the effective wave inertia causes drift-Rossby wave packets to slow down, which in turn reduces the modulational response of waves. The meridional excursion of wave packets $e(t)$ is regulated by a mean shear as

$$\begin{aligned} y(t) &= y(0) + e(t), \\ e(t) &= \int_0^t \frac{2\beta k_x^2 (\frac{k_y(0)}{k_x} + \Omega t')}{k_x^4 \left[(1 + (\frac{k_y(0)}{k_x} + \Omega^2 t')^2)\right]^2} dt' \\ &= \frac{\beta}{k_x^2 \Omega} \left[\frac{1}{1 + \frac{k_y^2(0)}{k_x^2}} - \frac{1}{1 + (\frac{k_y(0)}{k_x} + \Omega t)^2} \right]. \end{aligned} \tag{4.14}$$

From equation (4.14) we can see that the excursion is reduced by the mean shear. In this limit of $\Omega \to \infty$, wave packets are trapped ($e(t) \to 0$), with limited excursion. The linearized wave kinetic equation for a test zonal shear $\delta V_x' = \partial_y \delta V_x$ in a sheared

mean flow is

$$\frac{\partial \tilde{N}}{\partial t} + v_{gy}\frac{\partial \tilde{N}}{\partial y} + k_x\Omega\frac{\partial \tilde{N}}{\partial k_y} + D(k_x^2 + k_y^2)\tilde{N} = k_x\delta V_x'\frac{\partial N_0}{\partial k_y}, \tag{4.15}$$

where turbulent diffusion Dk^2 is used as an estimate of $\delta\omega_k$. $\delta\omega_k$ represents a relaxation of the wave action density N to the equilibrium N_0, in the absence of modulation. As we discussed in the previous section, the wave action density and the potential enstrophy density are identical, up to a constant factor. We see that the wave action density represents the intensity field of PV and its evolution has a direct connection with PV mixing. Thus, $\delta\omega_k$ represents the decay due to forward enstrophy cascade and PV mixing. $\delta\omega_k$ is approximated as the characteristic time of PV mixing, which leads to the relaxation of N. Note that when we look at the phenomenon of zonal flow generation from the standpoint of PV mixing, it is the forward enstrophy cascade, not the inverse energy cascade, which is critical. The enstrophy forward cascade is analogous to induced diffusion to high wave number. The nonlinear coupling to small scale dissipation by the forward cascade effectively replaces the molecular viscosity by an eddy viscosity. The evolution of potential enstrophy by nonlinear interaction can be represented by a mixing process: $\langle \underline{v} \cdot \underline{\nabla}\, q^2 \rangle \sim \tau_k^{-1} \langle \tilde{q}^2 \rangle_k$, where τ_k is the characteristic mixing time. We use eddy viscosity to model the mixing related to forward enstrophy cascade, and so we have $\tau_k^{-1} \simeq \delta\omega_k \simeq k^2 D_k$.

We now use the method of characteristics to calculate the modulational response $\tilde{N}_k$. The first step is to perform a change of variables to shearing coordinates:

$$\zeta = k_y - k_x\Omega t,$$
$$\xi = y - e(t).$$

Transforming the partial derivatives to the new coordinate: $\partial_t \to \partial_t + \zeta_t\partial_\zeta + \xi_t\partial_\xi$, $\partial_{k_y} \to \partial_\zeta$, $\partial_y \to \partial_\xi$, the Green's function of equation (4.15) in the shearing coordinate, $G(\xi, \zeta, k_x, t; \xi_1, \zeta_1, k_{1x}, t_1)$, is determined by

$$\partial_t G + D(k_x^2 + k_y^2)G = \delta(t - t_1)\delta(\xi - \xi_1)\delta(k_x - k_{1x})\delta(\zeta - \zeta_1). \tag{4.16}$$

Defining α so that $\partial_t(\alpha t) = D(k_x^2 + k_y^2)$, the left hand side of equation (4.16) can be written as $e^{-\alpha t}\partial_t[e^{\alpha t}G]$. Solving for α:

$$\begin{aligned}
\alpha t &= \int_0^t dt'\, D[k_x^2 + (k_y(0) + k_x\Omega t')^2] \\
&= D\left[k_x^2 t + k_y^2(0)t + k_y(0)k_x\Omega t^2 + \frac{k_x^2\Omega^2 t^3}{3}\right] \\
&= D\left[k_x^2 t + \frac{k_y(t)^3}{3\Omega k_x} - \frac{k_y^3(0)}{3\Omega k_x}\right],
\end{aligned}$$

the Green's function is derived as

$$\begin{aligned}
G &= \delta(\xi - \xi_1)\delta(\zeta - \zeta_1)\delta(k_x - k_{1x}) \\
&\quad \times\exp\left\{-D\left[(k_x^2 + k_{y0}^2)t + k_x k_{y0}\Omega t^2 + \frac{k_x^2\Omega^2}{3}t^3\right]\right\} \\
&\quad \times\exp\left\{D\left[(k_{1x}^2 + k_{y0}^2)t_1 + k_{1x}k_{y0}\Omega t_1^2 + \frac{k_{1x}^2\Omega^2}{3}t_1^3\right]\right\}. \qquad (4.17)
\end{aligned}$$

Changing variables back to the original frame, the Green's function becomes

$$\begin{aligned}
g(y, k_y, k_x, t; y_1, k_{1y}, k_{1x}, t_1) &= \delta(y - y_1 - e(t) + e(t_1))\delta(k_y - k_{1y} - k_x\Omega(t - t_1)) \\
&\quad \delta(k_x - k_{1x}) \times \exp\left[D\left(k_x^2 t + \frac{k_y^3}{3\Omega k_x}\right)\right]\exp\left[D\left(k_{1x}^2 t_1 + \frac{k_{1y}^3}{3\Omega k_x}\right)\right] \qquad (4.18)
\end{aligned}$$

Thus, we can obtain the modulational enstrophy density induced by a test zonal shear in the presence of a mean shear as:

$$\begin{aligned}
\tilde{N_k} &= \int\int\int dt_1 dy_1 dk_1^2 g(y, k_y, k_x, t; y_1, k_{1y}, k_x, t_1)k_{1x}\delta V_x'(t_1, y_1)\frac{\partial N_0}{\partial k_y} \\
&= \int_0^\infty d\tau e^{-Dk^2Q\tau}\delta\hat{V_x'}e^{-i\Omega_q t_1 + iq(y - e(t) + e(t_1))}k_x\partial_{k_y}N_0, \qquad (4.19)
\end{aligned}$$

where

$$\begin{aligned}
\tau &= t - t_1, \\
Q &= 1 - \frac{k_x k_y}{k^2}\Omega\tau + \frac{k_x^2}{3k^2}\Omega^2\tau^2.
\end{aligned}$$

Note that when there is no mean shear, we have $Q = 1$ and $y = v_{gy}t$. Therefore, equation (4.19) reduces to equation (4.9). Considering the long time limit ($\Omega t >> 1$), the modulation of the enstrophy density $\tilde{N_k}$ becomes

$$\tilde{N_k} = \int_0^\infty d\tau e^{-\frac{\tau^3}{\tau_c^3} + i\Omega_q\tau + i\frac{q\beta}{k_0^2\Omega}}k_x\delta\hat{V_x'}\partial_{k_y}N_0, \qquad (4.20)$$

where the effective decorrelation rate of $\tilde{N}_k$ is defined as $\tau_c^{-1} \simeq \left(\frac{Dk_x^2\Omega^2}{3}\right)^{1/3}$. The decorrelation rate due to a random walk, (which is Dk^2 in the absence of shearing field), is enhanced by the coupling of shearing to turbulent decorrelation. In the limit of strong mean shear ($\Omega >> Dk^2$), the corresponding $\tilde{N}_k$ becomes

$$\begin{aligned}\tilde{N}_k &\simeq \left[\Gamma\left(\frac{4}{3}\right)\tau_c - \frac{\Omega_q^2}{6}\tau_c^3\right] e^{i\frac{q\beta}{k_0^2\Omega}} k_x \delta\hat{V}' \partial_{k_y} N_0 \\ &\simeq \left(\frac{3}{Dk_x^2\Omega^2}\right)^{1/3} e^{i\frac{q\beta}{k_0^2\Omega}} k_x \delta\hat{V}' \partial_{k_y} N_0 + O(\Omega^{-2}). \end{aligned} \tag{4.21}$$

The growth rate of zonal flow in strong mean shear limit is given as

$$\gamma_q \simeq -q^2 \int d^2k \frac{k_x^2 k_y}{k^4} \left(\frac{3}{Dk_x^2\Omega^2}\right)^{1/3} \frac{\partial N_0}{\partial k_y}. \tag{4.22}$$

Compared with the system without ambient mean shear in equation (4.10), a strong mean shear reduces the growth of zonal flow by $(\Omega/Dk_x^2)^{-2/3}$. Since vorticity flux is equal to Reynolds force, which drives zonal flow, vorticity flux is reduced by the mean shear as

$$\langle \tilde{v}_y \nabla^2 \tilde{\psi} \rangle \simeq -q^2 \delta V \int d^2k \frac{k_x^2 k_y}{k^4} \left(\frac{3}{Dk_x^2\Omega^2}\right)^{1/3} \frac{\partial N_0}{\partial k_y}. \tag{4.23}$$

As a consequence, the turbulent viscosity scales with the mean flow shearing rate to $\Omega^{-2/3}$ in strong shear limit,

$$\nu_t(\Omega) \simeq \int d^2k \frac{k_x^2 k_y}{k^4} \left(\frac{3}{Dk_x^2\Omega^2}\right)^{1/3} \frac{\partial N_0}{\partial k_y}. \tag{4.24}$$

Because the effective viscosity is negative, the decreasing magnitude of the viscosity corresponds to the suppression of zonal flow growth. In the theory of wave kinetics, wave packets mix PV and generating zonal flow. As the decorrelation rate of wave packets is enhanced by a mean shear, PV mixing by wave turbulence ultimately becomes less efficient. We can also see the inhibition of wave propagation by a strong mean shear from the excursion of the wave packets, which is suppressed, as shown in equation (4.14), and from the group velocity of Rossby wave $v_{gx} = 2\beta k_x k_y k^{-4}$, which is inversely proportional to shearing by the factor of Ω^{-3}.

It is worth proving that the rate of energy transfer from waves to zonal flows is reduced by a mean shear, while the sum of wave energy and zonal flow

energy is conserved in the presence of a mean shear. Since wave action density is conserved, wave energy density evolves according to

$$\frac{d}{dt}\varepsilon_k \simeq \frac{d\omega_k}{dt}\left(\frac{N_k}{-\beta k_x}\right) \simeq \frac{v_{gy}}{\beta}\langle \delta V_x' \tilde{N}_k \rangle, \tag{4.25}$$

where $N_k/(-\beta k_y)$ is the wave action density (N_k is renormalized to enstrophy density in this paper). We use the $\tilde{N}_k$ derived in limit of strong mean shear to obtain

$$\frac{d}{dt}\varepsilon_k \simeq \int dq\ q^2 \delta \hat{V}_x^2 \frac{2k_x^2 k_y}{k^4}\left(\frac{3}{Dk_x^2\Omega^2}\right)^{1/3}\frac{\partial N_0}{\partial k_y}. \tag{4.26}$$

On the other hand, the evolution of zonal flow energy in a strong mean shear is given by

$$\frac{\partial}{\partial t}\delta V_x^2 \simeq -2q^2\nu_t(\Omega)\delta V_x^2 \simeq -2q^2\delta V_x^2 \int d^2k \frac{k_x^2 k_y}{k^4}\left(\frac{3}{Dk_x^2\Omega^2}\right)^{1/3}\frac{\partial N_0}{\partial k_y}. \tag{4.27}$$

Equations (4.26) and (4.27) show that the total energy of wave packets and zonal flows is conserved in the presence of a strong mean shear,

$$\frac{d}{dt}\left(\sum_k \varepsilon_k + \sum_q \delta V_{xq}^2\right) = 0. \tag{4.28}$$

This is because the mean shear is assumed stable in this model ($d_t\Omega = 0$). However, the rate of energy transfer from turbulence to zonal flows is reduced by a mean shear with the scaling of $\Omega^{-2/3}$.

4.4 Conclusion

We have investigated the important issue of how mean shear flows affect the transport of PV and zonal flow generation. For the systems of interest (magnetized plasma and quasi-geostrophic fluids), the conservation of PV is an essential characteristic of drift-Rossby wave dynamics, and the spatial mixing of PV is a fundamental mechanism for large scale flow generation. In a system with no mean shears, modulational stability calculations show that small scale wave packets are unstable to long wavelength perturbations, i.e. seed zonal flows. The seed zonal flow enforces turbulent PV transport, which reinforces the growth of the seed zonal

flow. When a mean shear flow is introduced to the system, the growth rate of zonal flows is reduced because the correlation between wave packets and zonal flows is weakened. By inhibiting PV mixing or reducing the cross-phase of the Reynold stress, mean shear has a significant influence on zonal flow dynamics. We demonstrate that in the strong shear limit, the zonal flow growth rate as well as PV flux decreases as $\Omega^{-2/3}$.

The results allow an an improved interpretation of feedback of mean shear on modulational instability driving zonal flow in the L-H transition. Our model gives detailed dependence of the turbulent viscosity on mean shear and therefore gives a modification to the zonal flow evolution equation in the L-H transition models (e.g. Ref [16, 18]). Another application of the results would be to give a detailed prediction of the interplay between turbulence-driven shears and mean shears in I-phase. Here, I-phase refers to an intermediate, oscillatory phase between the L mode and the H mode, which occurs when the input power is near the H-mode power threshold. Understanding of the interaction between turbulence, zonal flows, and mean shears helps to elucidate the duration of I-phase. This is essential for the studies of nonlinear turbulent energy transfer (e.g. [76, 77]).

PV flux and turbulent viscosity are shown to be complex functions of turbulence spectrum (k, N_0), the structure of zonal flow (q), and nonlinear wave-wave self-decorrelation rate under modulation $(\delta\omega)$. The main effect of a strong mean shear flow $(\Omega >> \delta\omega)$ on turbulent momentum transport in our model is to enhance modulational decorrelation rate from $\delta\omega$ to $(\delta\omega\Omega^2)^{1/3}$ (Table 4.1). Based on

Table 4.1: Reduction of momentum transport by strong mean shear.

turbulent viscosity	$\nu_t \simeq \int d^2k \frac{k_x^2 k_y}{k^4} R \frac{\partial N_0}{\partial k_y}$
without mean shear	$R = \frac{\lvert Dk^2 \rvert}{(\Omega_q - q v_{gy})^2 + (Dk^2)^2}$
with strong mean shear	$R = \left(\frac{3}{Dk_x^2\Omega^2}\right)^{1/3}$

the results, we suggest that momentum transport in the solar tachocline is non-Fickian, and the effect of mean solar differential rotation needs to be considered. There are other mechanisms which may affect turbulent momentum transport in the tachocline, including, but not limited to: reduction of turbulence intensity by

mean and random shearing field, generation of turbulence by convective overshoot or shear, and reduction of turbulent transport by a magnetic field.

The effect of the magnetic field might possibly play a role in the tachocline. However, the plasma beta, defined as the ratio of the thermal pressure to the magnetic pressure, is expected to be very high ($\beta_p >> 1$) in the tachocline, so the effect of magnetic field is uncertain, and most importantly, there is no direct observation of magnetic field in the tachocline. Therefore, the hydrodynamic model is meaningful. As we discussed in the Introduction, it is still unclear how the tachocline evolves under the meridional circulation-driven burrowing. Different mechanisms which oppose the burrowing during solar evolution have been proposed. There are two principal mechanisms: 1) turbulent viscous mixing of horizontal velocity, as in the Spiegel-Zahn [64] scenario, and 2) a fossil magnetic field in the radiative interior, as in the Gough-McIntyre [66] scenario. Spiegel & Zahn [64] suggest that stably stratified turbulence efficiently diffuses angular momentum in the latitudinal direction (i.e., positive turbulent viscosity) and so prevents the spreading of the tachocline. However, Gough & McIntyre [66] point out that the turbulence in a stably stratified rotating layer does not act as to diffuse the latitudinal gradient of angular velocity. Instead the turbulence would mix PV and so drive mean flows. They propose a hypothetical fossil magnetic field in the radiation zone to oppose the burrowing of the tachocline. Because the fossil magnetic field is localized in the radiative interior, it does not directly influence the turbulent transport in the tachocline; it simply sets the boundary condition of the tachocline. In both the Spiegel-Zahn and Gough-McIntyre scenarios, turbulent transport in a stably stratified rotating layer plays a central role. This supports the need for a hydrodynamic analysis of turbulent mixing of PV in the tachocline.

One purpose of this work is to improve the hydrodynamic model of Spiegel-Zahn. The weak points of the Spiegel-Zahn model are the assumption of diffusion/mixing of horizontal momentum instead of PV, and the assumption of constant viscosity. Our model analyzes the inhomogeneous mixing of PV and includes the interaction between turbulence, turbulence-generated flows, and the background shear flows. We show that the turbulent viscosity is not constant; it

depends on turbulence spectrum and flow structures. Morover, the horizontal turbulent viscosity is found to be negative, i.e., tachocline burrowing is not balanced by horizontal turbulent momentum transport. Thus, the results suggest the need of other mechanisms to prevent tachocline penetration, and also point toward the (ultimately) critical role of jet frictional damping as dissipation. Our improved interpretation of the horizontal momentum transport could be used to develop a more accurate hydrodynamic tachocline model. While a 3D model for tachocline is beyond the scope of this work, we think it is worthwhile to couple the horizontal and the vertical fluxes of angular momentum related to Rossby wave turbulence. In other words, it would be interesting to revisit the Spiegel-Zahn model using the horizontal turbulent viscosity derived from this work. That, however, is a lengthy calculation which is beyond the scope of this paper.

In this work, we were concerned with the effects of mean shear on turbulence correlation times and thus turbulent fluxes and transport. However, mean shears can also reduce turbulent transport by altering the intensity of the turbulent fluctuations. Kim & Diamond [78] reconsider the effect of a strong mean shear flow on the transport of a passive scalar field. They show that the square amplitude of the turbulence scales with the mean shear as $\Omega^{-5/3}$ for a random flow with a localized frequency spectrum, while the flux of the passive scalar varies as Ω^{-1}. Their analytical results are confirmed by the calculations and numerical study by Leconte et. al. [79] In the study of interchange and ion temperature gradient turbulence models [80], it is shown that a strong reduction in transport of particles and heat results from a severe reduction in the amplitude of turbulent velocity. Those results indicate the importance of the turbulent transport suppression through the reduction in the turbulence intensity. Note that there is a fundamental difference between the mixing of passive scalars and active scalars. Back-reaction of mixed quantities on mixing carriers only occur for active scalars, like PV.

Like the majority of mean-field models, the scale separation in space and/or time is an underlying assumption of our perturbative analyses. The assumption simplifies the problem because it enables the use of the adiabatic invariant to calculate the modulational response of wave spectrum to a test zonal flow. The

scale separation clearly exists between meso-scale, low frequency zonal flows and micro-scale higher frequency drift waves in magnetized plasma systems. For solar tachocline, there is no observation from which to determine whether such scale separation is valid or not. It is nevertheless not an unreasonable assumption, considering that the scales of turbulence excited by penetrative convection are of the same order as solar granulation. For systems with no scale separation, it is more difficult to derive the momentum transport coefficients theoretically. One may approach the problem via the renormalization-group technique [81], but applying this method to analyze turbulent momentum transport is still in the developing stage and is beyond the scope of this paper.

Chapter 4 is a reprint of material appearing in Pei-Chun Hsu and P. H. Diamond, *Phys. Plasmas*, **22**, 022306, (2015). The dissertation author was the primary investigator and author of this article.

Chapter 5

Summary and future directions

In this thesis, the dynamics of inhomogeneous potential vorticity (PV) mixing was studied to describe the large-scale zonal flow formation in Rossby wave/drift wave turbulence. The study was set out to explore the non-perturbative dynamics in PV mixing and has developed two relaxation models to derive the general structure of PV flux. Perturbation theory was used to calculate the transport coefficients. The study has also sought to uncover how the background mean shear flows affect the dynamics of PV mixing and zonal flow generation. Thus, the study sought to answer three questions:

1. What is the general structure of the form of PV flux during turbulent relaxation processes? (Chapter 2)
2. What are the transport coefficients in the PV flux? (Chapter 3)
3. What are the effects of ambient mean shear flows on the generation of zonal flows and turbulent momentum transport? (Chapter 4)

Different approaches were explored to the calculation of the PV flux in quasi-2D turbulent systems which conserve PV. In Chapter 2, we non-perturbatively deduced the general forms of PV flux from two relaxation models: 1) the minimum enstrophy relaxation model using the selective decay principle and 2) the PV-avalanche model using the joint reflection symmetry principle. The process of PV mixing was shown to be non-Fickian. The structure of PV flux derived from both relaxation models consists of a viscous and a hyper-viscous transport of PV.

The PV flux deduced from the PV-avalanche model has another, convective, term, which is, however, dependent on the gradient of the mean PV profile.

In the selective decay model, we found that the ratio of PV gradient to zonal flow velocity is homogenized in the minimum enstrophy state, which implies strong zonal flows located at sharp PV gradients. This is consistent with the structure of the PV staircase, suggesting that the staircase arises naturally as a consequence of minimum enstrophy relaxation and also links inhomogeneous PV mixing to minimum enstrophy relaxation. Turbulence spreading is linked to PV mixing; the spreading flux is driven by the gradient of the homogenized quantity. The PV equation in the PV-avalanche model has the same structure as the Kuramoto-Sivashinsky equation, which is known for its negative diffusion and higher-order stabilizing dissipation. The convective transport of PV suggests intermittent PV transport during turbulence self-organization. Because a nonlinear convective component of avalanche-like flux can be counted as a generalized diffusive transport, the PV flux in the two relaxation models may represent similar transport processes.

To derive the transport coefficients rigorously, in Chapter 3 we then used perturbation theory to study the instability of a spectrum of wave packets to a large scale seed zonal flow. For a broad turbulence spectrum, the modulational instability analysis of the wave kinetic equation showed that to the lowest order, PV flux is composed of negative viscous and positive hyper-viscous terms. The viscous and hyper-viscous transport of PV are shown in the minimum enstrophy relaxation model and the PV-avalanche model as well. The negative viscosity from the resonance interaction between zonal flow and wave-packets contributes to the growth of the zonal flow, while the positive hyper-viscosity assures the saturation mechanism of zonal flows and the scale dependence of the PV flux. For a narrow turbulence spectrum, we derived a parametric instability model of a pseudo-fluid composed of wave-packets. The PV transport associated with the pseudo-fluid is a convective process, which is also shown in the PV-avalanche model.

The effects of a mean shear flow on zonal flow formation was studied in Chapter 4. In the presence of ambient mean shear, the growth rate of zonal flows is

reduced because the correlation between wave packets and zonal flows is weakened. By inhibiting PV mixing or reducing the cross-phase of the Reynold stress, mean shear has a significant influence on zonal flow dynamics. We demonstrated that in the strong shear limit, the zonal flow growth rate, as well as the PV flux, decreases with mean shearing rate as $\Omega^{-2/3}$. While previous work has explored the effect of mean shears on reducing the growth of the modulational instability (following the initial work by Kim and Diamond [78]), the study in this thesis gives a complete analysis, including 1) an analysis of the effect of a mean shear on modulational wave action density, zonal flow growth rate, and turbulent viscosity; 2) a study of zonal/mean flow shearing, PV mixing and their interaction in modulational instabiliy; 3) a calculation of the spatial flux of PV.

To sum up, this thesis has identified inhomogeneous PV mixing as the fundamental mechanism for zonal flow formation and has offered new perspectives and approaches to calculating spatial flux of PV. One important topic for future research is developing numerical simulation tests of the models discussed in this thesis and comparing the results to the analytical predictions. Some of the numerical tests we can do include: i) examining the form of the PV flux during relaxation and testing the hyper-viscous model derived in this thesis, ii) calculating the profile of the homogenized quantity predicted for the relaxed state, iii) calculating the minimum enstrophy in the relaxed state, iv) studying the PV flux spectrum–especially low frequency components–with avalanching in mind, v) studying the staircase formation during relaxation. Another topic for future research is including the magnetic field to the quasi-geostrophic equation, i.e., developing a β-plane MHD model of PV mixing processes, with particular emphasis on the effect of magnetic field on the cross phase of the Reynolds stress–PV flux.

Bibliography

[1] G. K. Vallis, *Atmospheric and Oceanic Fluid Dynamics*. Cambridge Univ. Press, 2006.

[2] F. Busse, "A simple model of convection in the jovian atmosphere," *Icarus*, vol. 29, pp. 255–260, 1976.

[3] G. Dif-Pradalier, P. H. Diamond, V. Grandgirard, Y. Sarazin, J. Abiteboul, X. Garbet, P. Ghendrih, A. Strugarek, S. Ku, and C. S. Chang, "On the validity of the local diffusive paradigm in turbulent plasma transport," *Phys. Rev. E*, vol. 82, p. 025401, 2010.

[4] P. H. Diamond, S.-I. Itoh, and K. Itoh, *Modern Plasma Physics, Volume I: Physical Kinetics of Turbulent Plasmas*. Cambridge University Press, 2010.

[5] J. G. Charney, "On the scale of atmospheric motions," *Geofysiske Publikasjoner Oslo*, vol. 17, pp. 1–17, 1948.

[6] M. F. Maury, *The physical geography of the sea*. New York, Harper & Brothers, 1st ed., 1855.

[7] W. Ferrel, "An essay on the winds and the currents of the ocean," *Nashville J. Medicine and Surgery*, vol. 11, pp. 287–301, 1856.

[8] A. Hasegawa and M. Wakatani, "Plasma edge turbulence," *Phys. Rev. Lett.*, vol. 50, pp. 682–686, 1983.

[9] A. Hasegawa and K. Mima, "Pseudo-three-dimensional turbulence in magnetized nonuniform plasma," *Physics of Fluids*, vol. 21, pp. 87–92, 1978.

[10] M. E. McIntyre, "Numerical weather prediction: a vision of the future," *Weather*, vol. 43, pp. 294–298, 1988.

[11] A. W. Brewer and A. W. Wilson, "The regions of formation of atmospheric ozone," *Q. J. R. Meteorol. Soc.*, vol. 94, pp. 249–265, 1968.

[12] R. Hook, "Some observations lately made at london concerning the planet jupiter," *Phil. Trans.*, vol. 1, no. 14, pp. 245–247, 1666.

[13] P. S. Marcus, T. Kundu, and C. Lee, "Vortex dynamics and zonal flows," *Phys. Plasmas*, vol. 7, no. 5, pp. 1630–1640, 2000.

[14] P. H. Diamond, S.-I. Itoh, K. Itoh, and T. S. Hahm, "Zonal flows in plasma-a review," *Plasma Phys. Control. Fusion*, vol. 47, pp. R35–R161, 2005.

[15] J. W. Connor and H. R. Wilson, "A review of theories of the l-h transition," *Plasma Phys. Control. Fusion*, vol. 42, no. 1, pp. R1–R74, 2000.

[16] E.-J. Kim and P. H. Diamond, "Zonal flows and transient dynamics of the L-H transition.," *Phys. Rev. Lett.*, vol. 90, no. 18, p. 185006(4), 2003.

[17] G. D. Conway, C. Angioni, F. Ryter, P. Sauter, J. Vicente, and A. U. Team, "Mean and oscillating plasma flows and turbulence interactions across the lh confinement transition," *Phys. Rev. Lett.*, vol. 106, no. 6, p. 065001, 2011.

[18] K. Miki, P. H. Diamond, Ö. D. Gürcan, G. R. Tynan, T. Estrada, L. Schmitz, and G. S. Xu, "Spatio-temporal evolution of the L-I-H transition," *Phys. Plasmas*, vol. 19, no. 9, p. 092306, 2012.

[19] G. Tynan, M. Xu, P. Diamond, J. Boedo, I. Cziegler, N. Fedorczak, P. Manz, K. Miki, S. Thakur, L. Schmitz, L. Zeng, E. Doyle, G. McKee, Z. Yan, G. Xu, B. Wan, H. Wang, H. Guo, J. Dong, K. Zhao, J. Cheng, W. Hong, and L. Yan, "Turbulent-driven low-frequency sheared e b flows as the trigger for the h-mode transition," *Nucl. Fusion*, vol. 53, no. 7, p. 073053, 2013.

[20] G. I. Taylor, "Eddy motion in the atmosphere," *Philos. Trans. Roy. Soc. London, A*, vol. 215, pp. 1–23, 1915.

[21] R. H. Kraichnan, "Inertial ranges in two-dimensional turbulence," *Phys. Fluids*, vol. 10, no. 7, pp. 1417–1423, 1967.

[22] P. B. Rhines, "Geostrophic turbulence," *Ann. Rev. Fluid Mech.*, vol. 11, pp. 401–441, 1979.

[23] P. H. Diamond and Y.-B. Kim, "Theory of mean poloidal flow generation by turbulence," *Phys. Fluids B*, vol. 3, no. 7, pp. 1626–1633, 1991.

[24] D. G. Dritschel and M. E. McIntyre, "Multiple jets as PV staircases: The phillips effect and the resilience of eddy-transport barriers," *J. Atmos. Sci.*, vol. 65, pp. 855–874, 2008.

[25] M. E. McIntyre, "How well do we understand the dynamics of stratospheric warmings?," *J. Meteor. Soc. Japan*, vol. 60, pp. 37–65, 1982.

[26] G. Dif-Pradalier, G. Hornung, P. Ghendrih, Y. Sarazin, F. Clairet, L. Vermare, P. H. Diamond, J. Abiteboul, T. Cartier-Michaud, C. Ehrlacher, D. Estève, X. Garbet, V. Grandgirard, Ö. D. Gürcan, P. Hennequin, Y. Kosuga, G. Latu, P. Maget, P. Morel, C. Norscini, R. Sabot, and A. Storelli, "Finding the elusive E x B staircase in magnetized plasmas," *Phys. Rev. Lett.*, vol. 114, p. 085004, 2015.

[27] P. H. Diamond, A. Hasegawa, and K. Mima, "Vorticity dynamics, drift wave turbulence, and zonal flows: a look back and a look ahead," *Plasma Phys. Control. Fusion*, vol. 53, no. 12, p. 124001, 2011.

[28] A. Smolyakov and P. Diamond, "Generalized action invariants for drift waves-zonal flow systems," *Phys. Plasmas*, vol. 6, no. 12, pp. 4410–4413, 1999.

[29] F. P. Bretherton and D. B. Haidogel, "Two-dimensional turbulence above topography," *J. Fluid Mech.*, vol. 78, pp. 129–154, 1976.

[30] S. T. Adcock and D. P. Marshall, "Interactions between geostrophic eddies and the mean circulation over large-scale bottom topography," *J. Phys. Oceanogr.*, vol. 30, pp. 3223–3238, 2000.

[31] G. Holloway, "Representing topographic stress for large-scale ocean models," *J. Phys. Oceanogr.*, vol. 22, pp. 1033–1046, 1992.

[32] R. Robert and J. Sommeria, "Relaxation towards a statistical equilibrium state in two-dimensional perfect fluid dynamics," *Phys. Rev. Lett.*, vol. 69, no. 19, pp. 2776–2779, 1992.

[33] F. Bouchet and A. Venaille, "Statistical mechanics of two-dimensional and geophysical flows," *Phys. Rep.*, vol. 515, pp. 227–295, 2012.

[34] P. Bak, C. Tang, and K. Wiesenfeld, "Self-organized criticality: An explanation of 1/f noise," *Phys. Rev. Lett.*, vol. 59, no. 4, pp. 381–384, 1987.

[35] P. Bak, C. Tang, and K. Wiesenfeld, "Self-organized criticality," *Phys. Rev. A*, vol. 38, no. 1, pp. 364–374, 1988.

[36] P. H. Diamond and T. S. Hahm, "On the dynamics of turbulent transport near marginal stability," *Phys. Plasmas*, vol. 2, no. 10, pp. 3640–3649, 1995.

[37] T. Hwa and M. Kardar, "Avalanches, hydrodynamics, and discharge events in models of sandpiles," *Phys. Rev. A*, vol. 45, no. 10, p. 7002, 1992.

[38] P. B. Rhines and W. R. Holland, "A theoretical discussion of eddy-driven mean flows," *Dyn. Atmos. Oceans*, vol. 3, pp. 289–325, 1979.

[39] K. Itoh, S.-I. Itoh, P. H. Diamond, T. S. Hahm, A. Fujisawa, G. R. Tynan, M. Yagi, and Y. Nagashima, "Physics of zonal flows," *Phys. Plasmas*, vol. 13, p. 055502(11), 2006.

[40] A. Fujisawa, K. Itoh, H. Iguchi, K. Matsuoka, S. Okamura, A. Shimizu, T. Minami, Y. Yoshimura, K. Nagaoka, C. Takahashi, M. Kojima, H. Nakano, S. Ohsima, S. Nishimura, M. Isobe, C. Suzuki, T. Akiyama, K. Ida, K. Toi, S.-I. Itoh, and P. H. Diamond, "Identification of zonal flows in a toroidal plasma," *Phys. Rev. Lett.*, vol. 93, p. 165002, 2004.

[41] C. P. Connaughton, B. T. Nadiga, S. V. Nazarenko, and B. E. Quinn, "Modulational instability of rossby and drift waves and generation of zonal jets," *J. Fluid Mech.*, vol. 654, pp. 207–231, 2010.

[42] A. I. Smolyakov, P. H. Diamond, and V. I. Shevchenko, "Zonal flow generation by parametric instability in magnetized plasmas and geostrophicfluids," *Phys. Plasmas*, vol. 7, no. 5, pp. 1349–1351, 2000.

[43] X. Garbet, L. Laurent, A. Samain, and J. Chinardet, "Radial propagation of turbulence in tokamaks," *Nuclear Fusion*, vol. 34, no. 7, p. 963, 1994.

[44] T. S. Hahm, P. H. Diamond, Z. Lin, K. Itoh, and S.-I. Itoh, "Turbulence spreading into the linearly stable zone and transport scaling," *Plasma Phys. Control. Fusion*, vol. 46, p. A323, 2004.

[45] Ö. D. Gürcan, P. H. Diamond, and T. S. Hahm, "Radial transport of fluctuation energy in a two-field model of drift-wave turbulence," *Phys. Plasmas*, vol. 13, p. 052306, 2006.

[46] P. H. Diamond, O. D. Gürcan, T. S. Hahm, K. Miki, Y. Kosuga, and X. Garbet, "Momentum theorems and the structure of atmospheric jets and zonal flows in plasmas," *Plasma Phys. Control. Fusion*, vol. 50, p. 124018, 2008.

[47] J. B. Taylor, "Relaxation of toroidal plasma and generation of reverse magnetic fields," *Phys. Rev. Lett.*, vol. 33, no. 19, pp. 1139–1141, 1974.

[48] H. K. Moffatt, "Magnetostatic equilibria and analogous euler flows of arbitrarily complex topology. part 2. stability considerations," *J. Fluid Mech.*, vol. 166, pp. 359–378, 1986.

[49] A. H. Boozer, "Ohm's law for mean magnetic fields," *J. Plasma Phys.*, vol. 35, pp. 133–139, 1986.

[50] P. H. Diamond and M. Malkov, "Dynamics of helicity transport and taylor relaxation," *Phys. Plasmas*, vol. 10, no. 6, pp. 2322–2329, 2003.

[51] G. F. CARNEVALE and J. S. FREDERIKSEN, "Nonlinear stability and statistical mechanics of flow over topography," *J. Fluid Mech.*, vol. 175, pp. 157–181, 1987.

[52] W. H. Matthaeus and D. Montgomery, "Selective decay hypothesis at high mechanical and magnetic reynolds numbers," *Ann. N. Y. Acad. Sci.*, vol. 357, pp. 203–222, 1980.

[53] J. P. Dahlburg, D. Montgomery, G. D. Doolen, and L. Turner, "Turbulent relaxation to a force-free field-reversed state," *Phys. Rev. Lett.*, vol. 57, no. 4, pp. 428–431, 1986.

[54] F. Y. Gang, P. H. Diamond, J. A. Crotinger, and A. E. Koniges, "Statistical dynamics of dissipative drift wave turbulence," *Phys. Fluid B*, vol. 3, no. 4, pp. 955–968, 1991.

[55] P. B. Rhines, "Waves and turbulence on a beta-plane," *J. Fluid Mech.*, vol. 69, pp. 417–443, 1975.

[56] S. Tobias and J. Marston, "Direct statistical simulation of out-of-equilibrium jets," *Phys. Rev. Lett.*, vol. 110, p. 104502, 2013.

[57] R. K. Scott and D. G. Dritschel, "The structure of zonal jets in geostrophic turbulence," *J. Fluid Mech.*, vol. 711, pp. 576–598, 2012.

[58] K. ADAMS, J. KING, and R. TEW, "Beyond-all-orders effects in multiple-scales asymptotics: travelling-wave solutions to the kuramoto-sivashinsky equation," *J. Eng. Math.*, vol. 45, pp. 197–226, 2003.

[59] A. E. Gill, "A mechanism for instability of plane couette flow and of poiseuille flow in a pipe," *J. Fluid Mech.*, vol. 2, pp. 503–511, 1965.

[60] P. H. Diamond and M. Malkov, "A simple model of intermittency in drift wave-zonal flow turbulence," *Physica Scripta.*, vol. T98, pp. 63–67, 2002.

[61] P. W. Terry, "Suppression of turbulence and transport by sheared flow," *Rev. Modern Phys.*, vol. 72, no. 1, pp. 109–165, 2000.

[62] H. Biglari, P. H. Diamond, and P. W. Terry, "Influence of sheared poloidal rotation on edge turbulence," *Phys. Fluids B*, vol. 2, no. 1, pp. 1–4, 1990.

[63] K. H. Burrell, "Effects of ExB velocity shear and magnetic shear on turbulence and transport in magnetic confinement devices," *Phys. Plasmas*, vol. 4, no. 5, pp. 1499–1518, 1997.

[64] E. A. Spiegel and J.-P. Zahn, "The solar tachocline," *A&A*, vol. 265, no. 1, pp. 106–114, 1992.

[65] E.-J. Kim, "Self-consistent theory of turbulent transport in the solar tachocline I. anisotropic turbulence," *A&A*, vol. 441, pp. 763–772, 2005.

[66] D. O. Gough and M. E. McIntyre, "Inevitability of a magnetic field in the sun's radiative interior," *Nature*, vol. 394, pp. 775–757, 1998.

[67] S. M. Tobias, D. W. Hughes, and P. H. Diamond, "Beta-plane magnetohydrodynamic turbulence in the solar tachocline," *ApJ*, vol. 667, no. 1, pp. L113–L116, 2007.

[68] J. Anderson and Y. Kishimoto, "Mean sheared flow and parallel ion motion effects on zonal flow generation in ion- temperature-gradient mode turbulence," *Phys. Plasmas*, vol. 13, p. 102304, 2006.

[69] D. Zhou, "The residual zonal flow in tokamak plasmas toroidally rotating at arbitrary velocity," *Phys. Plasmas*, vol. 21, p. 082508, 2014.

[70] A. Smolyakov, P. Diamond, and M. Malkov, "Coherent structure phenomena in drift wave - zonal flow turbulence," *Physical Review Letters*, vol. 84, pp. 491–494, 2000.

[71] W. M. Tang, "Microinstability theory in tokamaks," *nuclear fusion*, vol. 18, no. 8, pp. 1089–1160, 1978.

[72] M. N. Rosenbluth, "Microinstabilities," in *Plasma Physics*, (Vienna), pp. 485–513, International Atomic Energy Agency, 1965.

[73] B. B. Kadomtsev and O. P. Pogutse, "Turbulence in toroidal systems," in *Reviews of Plasma Physics* (M. A. Leontovich, ed.), vol. 5, p. 249, Consultants Bureau, New York, 1970.

[74] P.-C. Hsu and P. H. Diamond, "On calculating the potential vorticity flux," *Phys. Plasmas*, vol. 22, p. 032314, 2015.

[75] P. Goldreich and D. Lynden-Bell, "II. Spiral arms as sheared gravitational instabilities," *Mon. Not. R. Atron. Soc.*, vol. 130, pp. 125–158, 1965.

[76] M. Xu, G. R. Tynan, C. Holland, Z. Yan, S. H. Muller, and J. H. Yu, "Study of nonlinear spectral energy transfer in frequency domain," *Phys. Plasmas*, vol. 16, p. 042312, 2009.

[77] M. Xu, G. R. Tynan, P. H. Diamond, P. Manz, C. Holland, N. Fedorczak, S. C. Thakur, J. H. Yu, K. J. Zhao, J. Q. D. J. Cheng, W. Y. Hong, L. W. Yan, Q. W. Yang, X. M. Song, Y. H. L. Z. Cai, W. L. Zhong, Z. B. Shi, X. T. Ding, X. R. Duan, and Y. Liu, "Frequency-resolved nonlinear turbulent energy transfer into zonal flows in strongly heated L-mode plasmas in the HL-2A tokamak," *Phys. Rev. Lett.*, vol. 108, p. 245001, 2012.

[78] E.-J. Kim and P. H. Diamond, "Effect of mean flow shear on cross phase and transport reconsidered," *Phys. Rev. Lett.*, vol. 91, no. 7, p. 075001(4), 2003.

[79] M. Leconte, P. Beyer, S. Benkadda, and X. Garbet, "Effects of a fluctuating sheared flow on cross phase in passive-scalar turbulent diffusion," *Phys. Plasmas*, p. 112301, 2006.

[80] E.-J. Kim, P. H. Diamond, and T. S. Hahm, "Transport reduction by shear flows in dynamical models," *Phys. Plasmas*, vol. 11, no. 10, pp. 4554–4558, 2004.

[81] H. K. Moffatt, "Transport effects associated with turbulence with particular attention to the influence of helicity," *Rep. Prog. Phys.*, vol. 46, no. 5, pp. 621–664, 1983.